HYDROTHERMAL LIQUEFACTION OF MUNICIPAL WASTEWATER CULTIVATED ALGAE: INCREASING OVERALL SUSTAINABILITY AND VALUE STREAMS OF ALGAL BIOFUELS

By

Griffin William Roberts

Submitted to the graduate degree program in Chemical and Petroleum Engineering and the Graduate Faculty of the University of Kansas in partial fulfillment of the requirements for the degree of Doctor of Philosophy.

_____

Chairperson: Susan M. Stagg-Williams

_____

Belinda S.M. Sturm

_____

Laurence R. Weatherley

_____

Aaron M. Scurto

_____

Raghunath V. Chaudhari

Date Defended: April 27, 2015

The Thesis Committee for Griffin William Roberts

certifies that this is the approved version of the following thesis:

HYDROTHERMAL LIQUEFACTION OF MUNICIPAL WASTEWATER CULTIVATED ALGAE: INCREASING OVERALL SUSTAINABILITY AND VALUE STREAMS

_____

Chairperson: Susan M. Stagg-Williams

Date approved: May 11, 2015

Abstract

The forefront of the 21st century presents ongoing challenges in economics, energy, and environmental remediation, directly correlating with priorities for U.S. national security. Displacing petroleum-derived fuels with clean, affordable renewable fuels represents a solution to increase energy independence while stimulating economic growth and reducing carbon-based emissions. The U.S. government embodied this goal by passing the Energy Independence and Security Act (EISA) in 2007, mandating 36 billion gallons of annual biofuel production by 2022. Algae possess potential to support EISA goals and have been studied for the past 30-50 years as an energy source due to its fast growth rates, noncompetitive nature to food markets, and ability to grow using nutrient waste streams. Algae biofuels have been identified by the National Research Council to have significant sustainability concerns involving water, nutrient, and land use. Utilizing municipal wastewater to cultivate algae provides both water and nutrients needed for growth, partially alleviating these concerns.

This dissertation demonstrates a pathway for algae biofuels which increases both sustainability and production of high-value products. Algae are cultivated in pilot-scale open ponds located at the Lawrence Wastewater Treatment Plant (Lawrence, KS) using solely effluent from the secondary clarifier, prior to disinfection and discharge, as both water and nutrient sources. Open ponds were self-inoculated by wastewater effluent and produced a mixed-species culture of various microalgae and macroalgae. Algae cultivation provided further wastewater treatment, removing both nitrogen and phosphorus, which have devastating pollution effects when discharged to natural watersheds, especially in large draining watersheds like the Gulf Coast. Algae demonstrated significant removal of other trace metals such as iron, manganese,

barium, aluminum, and zinc. Calcium did not achieve high removal rate but did present a significant portion of algae biomass total weight; wastewater treatment using nitrification requires significant daily additions of buffers, most commonly lime or calcium hydroxide. Accumulation of these ions and metals in wastewater-cultivated algae results in a biomass with substantial amount of inorganic ash content. The cultivated biomass was converted to a carbon-rich biocrude, similar to petroleum crude oil, through a process called hydrothermal liquefaction (abbreviated as HTL), which uses subcritical water (water just below its supercritical point) as the chemical driving force for conversion. Biomass HTL produces four product fractions; liquid biocrude, solids (referred to as biochar), an aqueous product (referred to as aqueous co-product; abbreviated as ACP), and gasses. Many factors contribute to the overall viability of using algae HTL biocrude as a petroleum displacement, particularly yield and quality are important for overall economics and ability to utilize existing refining infrastructure, respectively.

The HTL product distribution and quality of wastewater-cultivated algae has been found to be extremely unique with significant advantageous over controlled fertilized growth strategies. Biocrude yields of were typically lower but substantially higher quality with lower oxygen content and higher amounts of direct fuel distillate fractions. This phenomenon is contributed to the fact that large amounts of pure-phase substituted hydroxyapatite (a calcium orthophosphate material) are synthesized *in-situ*, providing catalytically active sites. Hydroxyapatite (abbreviated HA) is a widely studied material for bone (and dental) tissue regeneration purposes and its acid-base catalytic properties. The specific HA produced during HTL of wastewater-cultivated algae presents unique characteristics for performance and tunability in each respective application, providing novel economic value streams for the production of algal biofuels. The

overall work of this dissertation concludes Lawrence Wastewater Treatment Plant could produce 10-18 barrels of crude oil and over 2 metric tons of refined hydroxyapatite per day for the creation of revenue sales.

The work within this dissertation encompasses novelty of characterization methods, HTL feedstocks, and identification of high-value products. Overall, efforts to demonstrate the feasibility of a sustainable biofuel strategy resulted in formulating hypotheses which led to novel discoveries in creating high-value heterogeneous catalysts and biomedical materials. The works presented have the potential to produce an overall process capable of selling significant quantities of biofuels as a by-product and not as the main economic generator, laying the foundation of breakthrough technology which can meet and potentially exceed the $3 per gal biofuel target.

Acknowledgements

I would like to thank the support of the Madison and Lila Self Graduate Fellowship for their financial support of my tenure at the University of Kansas. I thank my advisor(s) Susan Stagg-Williams and Belinda Sturm and their research groups. A special thanks to Marie-Odile Fortier for leading cultivation efforts and many conversations as well as Gabe Stanton, Umar Hamdeh, Tiffany Kinsella, and Alejandra Rocha for all their hard work. Also, I would like to acknowledge my undergraduate advisor(s) Paul Kenis and Sarah Perry and express a sincere gratitude for each of my additional committee members; Aaron Scurto, Lawrence Weatherley, and Raghunath Chaudhari.

I would like to thank the lifelong support of my friends and family. To my mother Barbara, thank you for showing me how to strive for the best and achieve my goals. To my father Hal, thank you for showing me the true nature of engineering and that you can build anything from everything. I also would like to express my extreme gratitude to Jennifer Melendez, whose steadfast support throughout the entire process was unprecedented. Thank you for your endearing friendship, loving compassion, and momentous wonder as a human being, mother, and partner.

Dedicated to my children

Barrett and Viviana

In memory of

Jesse Wayne Manning

Feb. 10, 1984 – Jan. 26, 2003

Preface

Significant portions of this dissertation have been previously published through the American Chemical Society and Royal Society of Chemistry which hold original copyrights for the content.

Reprinted with permission from Roberts, G. W.; Fortier, M.-O. P.; Sturm, B. S. M.; Stagg-Williams, S. M., Promising Pathway for Algal Biofuels through Wastewater Cultivation and Hydrothermal Conversion. *Energy & Fuels* **2013,** *27*, (2), 857-867. **DOI:** 10.1021/ef3020603. Copyright 2015 American Chemical Society.

Roberts, G. W.; Sturm, B. S.; Hamdeh, U.; Stanton, G. E.; Rocha, A.; Kinsella, T. L.; Fortier, M.-O. P.; Sazdar, S.; Detamore, M. S.; Stagg-Williams, S. M., Promoting catalysis and high-value product streams by in situ hydroxyapatite crystallization during hydrothermal liquefaction of microalgae cultivated with reclaimed nutrients. *Green Chemistry* **2015**, 17, 2560. **DOI:** 10.1039/C5GC00187K. Adapted with permission of the Royal Society of Chemistry.

Table of Contents

List of Figures

List of Tables

1 Introduction

1.1 Biofuels

A biofuel, as defined by Merriam-Webster, is a fuel composed of, or produced from, biological raw materials. Biofuels can be in any state of matter, solid, liquid, or gas, and used for various applications including transportation, heat, and even the base fuel for electricity production. Traditionally, society has used fossil fuel sources, such as petroleum crude, coal, and natural gas for both transportation needs and heating duties. However, factors such as but not limited to, market volatility, availability, environmental concerns, and socioeconomic control of these fossil sources has drastically increased the desire to create sustainable renewable fuels. The U.S. government has played a pivotal role by passing the Energy Independence and Security Act of 2007, mandating 36 billion gallons of annual transportation biofuel production by 2022.[1, 2]

Transportation biofuels are the primary focus for this dissertation, which typically include ethanol, biodiesel, and green gasoline/ diesel/ jet fuel (green-GDJ). Biodiesel is commonly confused with green-GDJ; however, the two are fundamentally and chemically different. Biodiesel is a generic name for fatty acid methyl esters (FAME) derived from the transesterification reaction of triglycerides and esterification of fatty acids. Green-GDJ are mixtures of hydrocarbons and aliphatics with similar compositions and boiling points of fuels produced from traditional petroleum refining which have been derived from a renewable source in place of a fossil source. In general, a biofuel's usability in the market place can be associated with three main factors; 1) What is the biological raw material to produce the fuel? Is that raw

material used in existing industries, and therefore compete in the market, i.e., is there a food for fuel debate? 2) Can that fuel be economically produced from the biological source; including both cultivating raw biomass and chemically transforming the biomass into fuel, and 3) Can the biofuel integrate seamlessly into the existing infrastructure, regarding both refining and end-use?

Each biological raw material(s), or feedstock, must undergo a chemical transformation and/or deconstruction chemistry to produce an end-use biofuel product. In general, feedstocks can dictate which transformation technology would be employed to produce a specific biofuel. Table 1-1 outlines transformation technologies that can be applied to various feedstocks to produce the three main biofuels indicated above.

Table 1-1. Feedstocks and corresponding transformation technologies for specific biofuels.

Biofuel	**Transformation Technology**	**Feedstock**
Ethanol	Fermentation	Corn Soybeans Sugar cane Switch grass Wood Agriculture residue
Biodiesel	Transesterification	Vegetable oil Waste cooking oil Animal tallow Jatropha Algae
Green-GDJ	Hydrodeoxygenation	Bio-oil(s)
	Fisher-Tropsch post gasification	All
	Upgrading post pyrolysis	All
	Upgrading post hydrothermal liquefaction	All

Cross referencing Table 1-1 to the three main factors of biofuel adoption will enable optimal choices for successful and sustainable biofuel production. Feedstocks such as corn, soybeans, sugar cane, and vegetable oil incorporate undesired food for fuel concerns. Ethanol produced from grasses, wood, and agriculture residues are commonly referred to as cellulosic ethanol.[3] Although cellulosic ethanol has promise, when evaluating factors 2 & 3, this biofuel has significant shortcomings in both economic transformation and end-use.[3] Deconstruction of the main components of biomass to fermentable sugars has proven inefficient and relies heavily on converting other components of the biomass, hemi-cellulose and lignin, into usable bi-products for an economic return.[4] Ethanol as a transportation fuel itself has significant shortcomings. Ethanol can only be combined with gasoline up to a certain blend because of its low energy density, solubility with water, and high oxygen content; commonly requiring engine modifications in order to burn significant concentrations within a fuel blend.[5, 6] Biodiesel has similar limitations; the transesterification of oils and fats requires initial separation of those oils from the base feedstock again requiring creation of separate value streams for both the residual biomass components and transformation side-products.[7-9] In addition, biodiesel is another oxygenated compound and depending upon the exact chemical fatty acid structure can have poor physical properties as a liquid fuel. For example, the cold point, or the temperature at which the fuel begins to solidify, is above typical ambient (winter) temperatures in the U.S. throughout a given year.[10] Therefore, biodiesel can require significant blending with conventional diesel in order to maintain proper engine performance. These factors tend to limit the quantity of biodiesel which is widely consumed. The feedstocks used for biodiesel production also require extensive pre-treatment to obtain a pure bio-oil, or triglycerides, which then can be converted to

FAMEs. This leaves significant portion the biomass requiring either separate transformation and/or incorporation into separate value streams for optimal economic return, further limiting the amount of biodiesel widely produced.[11]

Since the chemical compounds of Green-GDJ are no different than petrol fuels, it represents the main biofuel which can integrate optimally into existing infrastructure, specifically at the end-use.[12] Green-GDJ is also the most feedstock agnostic, allowing essentially any type of biomass to be converted to green-GDJ depending upon the transformation technology. The specific transformation technology employed for producing green-GDJ is where issues may arise. Hydrodeoxygenation of bio-oil(s) to green-GDJ suffers similar pre-treatment requirements as biodiesel.[13-15] Further, the main by-product of hydrodeoxygenation is carbon dioxide (CO_2) and/or carbon monoxide (CO). These products drastically reduce carbon efficiency; therefore, after pre-treatment and hydrodeoxygenation the overall carbon balance from initial biomass feedstock to green-GDJ can be very low. Fischer-Tropsch (FT) synthesis is the combination of hydrogen gas and CO to produce liquid fuels, thus, to produce green-GDJ from a particular feedstock the biomass must first be gasified into these components before synthesis.[15, 16] Both gasification and FT each require energy and produces CO_2, again, reducing the overall energy and carbon efficiencies. Pyrolysis is the thermal breakdown of biomass in the absence of water and oxygen producing a solid char and condensable gasses.[17] Once these gasses are condensed to pyrolysis oil, the oil can be upgraded to a viable green-GDJ fuel.[18] Upgrading generally consists of cracking, or reducing molecular weight distribution resulting in lower boiling point distillates, and heteroatom removal, i.e., removing oxygen, nitrogen, and sulfur. The main concerns with pyrolysis technologies are drying of the feedstock and the significant heteroatom

content (oxygen and nitrogen) of the condensed gasses. Pyrolysis oils from biomass can have upwards of 30 weight % (wt%) oxygen and higher with considerable acid contents.[17] This results in stability issues and must be extensively upgraded rather quickly to reduce the oxygen content. Oxygen can be removed via hydrodeoxygenation, requiring large amounts of hydrogen, to produce CO_2. Since pyrolysis is a dry process, wet biomass such as algae requires extensive drying negatively impacting the overall energy balance of the system.[19] Algae as a biofuel feedstock will be expanded in section 1.2: Algae. Producing green-GDJ from the upgrading of biocrude, or carbon-rich crude oil similar to petroleum, produced from hydrothermal liquefaction (HTL) of biomass serves as an extremely attractive process. HTL uses hot compressed water, below the supercritical point (374°C and 22 MPa), as the chemical driving force to decompose biomass resulting in the desired biocrude. The utilization of HTL to convert algal biomass into valuable products is the main focus of this thesis outlined in section 1.4: Hydrothermal Liquefaction (HTL) and a thorough review on HTL of algae is discussed in Chapter 2: Hydrothermal Liquefaction Review.

1.2 Algae

Algae represent one of the oldest, highly abundant sources of flora, typically representing the basis of the majority of food chains, on the planet.[20] Algae are highly prolific and predominately photosynthetic aquatic organisms which require certain essential components for growth, including nitrogen, phosphorus, carbon and trace elements. In addition, algae are extremely diverse and opportunistic organisms which can extract their essential components from a variety of sources, including wastewaters.[21-24] Therefore, algae can utilize non-potable

water, non-arable land, and waste streams making them attractive as a biofuel feedstock by eliminating any food for fuel concerns. Algae proliferation, in terms of biomass productivity, has been shown to exceed that of terrestrial flora normalized to the area of land use.[25] Algae also accumulate lipids and fats as triglycerides and free fatty acids in higher amounts than terrestrial flora seeds per unit area.[26] Table 1.2 indicates oil production of algae compared to terrestrial oil producing seed crops.[27] The range oil from algae given is based on a best case scenario and a theoretical maximum. Algal growth conditions, specifically nitrogen and phosphorus availabilities, greatly affect the lipid or oil productivity of any given algal species.[28] A simplified version of the well-known algal Redfield ratio[29] for carbon, nitrogen, and phosphorus is 106:16:1, respectively, representing a theoretical molecular formula for algae biomass. Deviations from the Redfield ratio for nitrogen and phosphorus (N:P) results in different algae assemblages; high lipid accumulation/ low proliferation or low lipid accumulation/ high proliferation for nitrogen limited and phosphorus limited, respectively.[30]

Table 1-2. Oil production of various biomass per unit area.[27, 31]

	Oil Production per Area (gal acre^{-1})
Algae	4,000 -38,000[27]
Oil Palm	635
Coconut	287
Jatropha	207
Rapeseed/Canola	127
Peanut	113
Sunflower	102
Safflower	83
Soybean	48
Hemp	39
Corn	18

The National Research Council (NRC) of the National Academies evaluated a wide array of algal cultivation strategies in conjunction with the various conversion technologies, with the exception of HTL, to understand the sustainability concerns for large scale implementation of algal biofuels.[32] The findings of the report concluded the major concerns were the availability of water and nutrients during algae cultivation. In other words, for long-term sustainability of algae biofuels it is necessary to exploit the opportunistic growth capabilities of algae, as previously described. This also implies there must be efficient material balances toward valuable products, post algal cultivation, in order to efficiently utilize the water and nutrients used during cultivation. An under-utilized source of both water and nutrients, viable for algal cultivation, is municipal wastewater. A of the primary goal of the work presented in this dissertation is to

demonstrate the sustainability of algal biofuels by utilizing municipal wastewater for algae cultivation.

1.3 Wastewater Cultivation of Algae

The objective of a wastewater treatment plant is to reclaim polluted waters for safe further use either by society or the environment.[33] The primary concern for a typical municipal wastewater treatment facility is to remove insoluble and soluble organic materials. This is achieved by various stages of solid separations/ settling processes in combination with activated sludge, or bacterial, digestions of the particulate and dissolved organics; commonly referred to as primary and secondary clarification, respectively. Not all wastewater plants are design equally. Each plant is designed and operated based off its respective governing body, i.e., each city and state may have different regulations, above that of the EPA, to achieve a particular maximum allowable lever of a particular "pollutant". Some commonly regulated pollutants are arsenic, atrazine, barium, chromium, fluoride, copper, lead, nitrate, selenium, chloramine, and total organic carbon (TOC). There also exists a class of unregulated components which have federal recommendation levels which are monitored to help in the development of future regulations, such as, calcium, magnesium, nickel, and total phosphorus to name a few. No current federal regulations exist for removing total nitrogen (TN) and total phosphorus (TP), however, there are future expectations. Therefore, a typical wastewater treatment plant discharges significant amounts of both nitrogen and phosphorus, providing a source of both water and nutrients in which the algal biofuel sector can take full advantage.

High levels of TN and TP in a treatment facilities discharge waters can result in negative effects when introduced to natural water bodies. This is particularly seen throughout the Mississippi delta area in the Gulf Coast.[34] These high levels of TN and TP cause algal blooms to occur where they normally would not; when an algal bloom dies the resultant organic matter is decomposed by a drastic increase in bacterial respiration. The increase in bacterial growth depletes the dissolved oxygen within the water body leading to anoxic conditions, which is highly detrimental to the natural ecosystem. Therefore, when algae is cultivated in a contained area around a wastewater treatment facility a win-win scenario is obtained by removing the TN and TP before water discharge, eliminating future devastation to ecosystems,[35] and producing substantial biomass for biofuels/ chemicals feedstock. This strategy has dual benefit; production of sustainable algae biomass and economically viable means to meet expected future regulations for nitrogen and phosphorus at wastewater treatment facilities.

1.4 Hydrothermal Liquefaction (HTL)

Hydrothermal liquefaction (HTL) utilizes subcritical water chemistry to convert biomass to a carbon-rich biocrude.[36, 37] Divergent from ambient water, subcritical water properties include a decreased dielectric constant, increased ionic product, and decreased density[38] which provide an acid-base reaction media capable to solubilize organic compounds.[39] HTL is particularly advantageous for algae conversion for multiple reasons. Algae biomass consists of macromolecules which include lipids and oils, carbohydrates, and proteins. Processes such as transesterification and hydrodeoxygenation solely utilize the lipid and oil content of the biomass where the remainder of the cell must be used elsewhere. Efficient use of the growth resources,

water and nutrients, dictates a whole cell conversion technology must be employed, and therefore, restricted to gasification, pyrolysis, and HTL. As stated earlier, gasification and pyrolysis are dry processes. Since algae are an aquatic biomass and cultivated in relatively low solids concentrations these conversion technologies will have limited energy efficiencies when processing as a dry biomass. HTL of algae typically proceeds as 5- 20 wt% solids concentration which represents the minimum of dewatering needed based on conversion technologies listed in Table 1-1 and also represents the only wet whole cell conversion technology. During HTL of algae, macromolecules are broken down and recovered as a biocrude with similar composition and properties to petroleum crude[37, 40, 41] and capable of refining similar to petroleum crude to produce end-use fuels and chemicals. A detailed overview and prior work review of algae HTL will be covered in Chapter 2: Hydrothermal Liquefaction Review.

1.5 Research Goals

The primary goals of the work presented in this dissertation are to establish a baseline study for the effectiveness of producing bio-based fuels and chemicals from algae cultivated with municipal wastewater as the sole nutrient and water source. Utilizing both reclaimed water and nutrients greatly increases the overall sustainability of algae cultivation while contributing to an increased environmental remediation effort. Algae cultivated in such a manner are shown to have significant differences from a controlled media growth, primarily in proximate and ultimate contents of the biomass. Once the algae were successfully cultivated, chemical transformation efforts are demonstrated through the use of HTL, representing the first study which was conducted using a mixed microalgae species and the first to utilize HTL on algae sultivated soley

from water and nutrients provided by a functioning wastewater treatment facility. Due to the cultivation strategy, algal variances carry downstream to HTL, which resulted in unexpected results, initially thought to be simply higher production rates of solid products. However, the work herein details the formulated hypotheses, experimental methods to confirm the hypotheses, and the discovery process of value-added components produced during the HTL of the algal biomass used. This work represents the foundation to achieve an overall process where algal biofuels are considered lower value by-product of producing higher-value catalysts and biomedical materials.

1.6 Research Work Overview and Outline

This dissertation is outlined in the following manner. A detailed review of algae HTL will be given in Chapter 2, to include previous works with the current literature detailing algae conversion with HTL. Chapter 3 outlines the materials used and methods performed for each subsequent chapter of the dissertation and will be used as reference within each chapter respectively; highlighting a novel method developed for achieving a full proximate analysis of biomass to overcome shortcoming identified in the current ASTM method for ash determination. The initial results of this dissertation will begin in Chapter 4 detailing the algae cultivation (from 2011) and its conversion via HTL. This chapter includes information from both a mixed-culture algae biomass, cited in *Energy & Fuels*, and macro-algae, work previously presented at a national conference (American Institute of Chemical Engineers Annual Meeting 2012), which were harvested from the same cultivation pond. The results and discussions from performing HTL on algae cultivated in 2013 are found in Chapter 5. Using knowledge gained and

hypotheses formulated from the previous chapter, this section details the discovery process of value-added product synthesis, and potential market places. Chapter 6 expands the discussion of *in-situ* synergies between the main HTL products and potential uses of the value-added products produced from the 2013 algae. Chapter 7 details future work that will need to be performed to answer the next round of questioning that pertains to the discoveries made and potential uses discussed in Chapter 5 & 6, respectively. Concluding remarks are made in Chapter 8.

1.7 References

1. Independence, E., Security Act of 2007. *Public law* **2007,** *110*, (140), 19.
2. Sissine, F. In *Energy Independence and Security Act of 2007: a summary of major provisions*, 2007; DTIC Document: 2007.
3. Brethauer, S.; Wyman, C. E., Review: continuous hydrolysis and fermentation for cellulosic ethanol production. *Bioresource Technology* **2010,** *101*, (13), 4862-4874.
4. Binder, J. B.; Raines, R. T., Fermentable sugars by chemical hydrolysis of biomass. *Proceedings of the National Academy of Sciences* **2010**.
5. Mužíková, Z.; Šimáček, P.; Pospíšil, M.; Šebor, G., Density, Viscosity and Water Phase Stability of 1-Butanol-Gasoline Blends. *Journal of Fuels* **2014,** *2014*.
6. Center, A. F. D., Fuel properties comparison. *Retrieved April* **2013,** *19*, 2013.
7. Meher, L.; Sagar, D. V.; Naik, S., Technical aspects of biodiesel production by transesterification—a review. *Renewable and sustainable energy reviews* **2006,** *10*, (3), 248-268.
8. Mata, T. M.; Martins, A. A.; Caetano, N. S., Microalgae for biodiesel production and other applications: a review. *Renewable and sustainable energy reviews* **2010,** *14*, (1), 217-232.
9. Singh, S.; Singh, D., Biodiesel production through the use of different sources and characterization of oils and their esters as the substitute of diesel: a review. *Renewable and Sustainable Energy Reviews* **2010,** *14*, (1), 200-216.
10. Hoekman, S. K.; Broch, A.; Robbins, C.; Ceniceros, E.; Natarajan, M., Review of biodiesel composition, properties, and specifications. *Renewable and Sustainable Energy Reviews* **2012,** *16*, (1), 143-169.
11. Haas, M. J., Improving the economics of biodiesel production through the use of low value lipids as feedstocks: vegetable oil soapstock. *Fuel Processing Technology* **2005,** *86*, (10), 1087-1096.
12. Kalnes, T.; Marker, T.; Shonnard, D. R., Green diesel: a second generation biofuel. *International Journal of Chemical Reactor Engineering* **2007,** *5*, (1).

13. Choudhary, T.; Phillips, C., Renewable fuels via catalytic hydrodeoxygenation. *Applied Catalysis A: General* **2011,** *397*, (1), 1-12.
14. Greenwell, H.; Laurens, L.; Shields, R.; Lovitt, R.; Flynn, K., Placing microalgae on the biofuels priority list: a review of the technological challenges. *Journal of the Royal Society Interface* **2009**, rsif20090322.
15. Naik, S.; Goud, V. V.; Rout, P. K.; Dalai, A. K., Production of first and second generation biofuels: a comprehensive review. *Renewable and Sustainable Energy Reviews* **2010,** *14*, (2), 578-597.
16. Tijmensen, M. J.; Faaij, A. P.; Hamelinck, C. N.; van Hardeveld, M. R., Exploration of the possibilities for production of Fischer Tropsch liquids and power via biomass gasification. *Biomass and Bioenergy* **2002,** *23*, (2), 129-152.
17. Mohan, D.; Pittman, C. U.; Steele, P. H., Pyrolysis of wood/biomass for bio-oil: a critical review. *Energy & Fuels* **2006,** *20*, (3), 848-889.
18. Bridgwater, A. V., Review of fast pyrolysis of biomass and product upgrading. *Biomass and bioenergy* **2012,** *38*, 68-94.
19. Demirbas, M. F., Biofuels from algae for sustainable development. *Applied Energy* **2011,** *88*, (10), 3473-3480.
20. Falkowski, P. G.; Katz, M. E.; Knoll, A. H.; Quigg, A.; Raven, J. A.; Schofield, O.; Taylor, F., The evolution of modern eukaryotic phytoplankton. *Science* **2004,** *305*, (5682), 354-360.
21. Sturm, B. S.; Peltier, E.; Smith, V.; deNoyelles, F., Controls of microalgal biomass and lipid production in municipal wastewater-fed bioreactors. *Environmental Progress & Sustainable Energy* **2012,** *31*, (1), 10-16.
22. Woertz, I.; Feffer, A.; Lundquist, T.; Nelson, Y., Algae Grown on Dairy and Municipal Wastewater for Simultaneous Nutrient Removal and Lipid Production for Biofuel Feedstock. *Journal of Environmental Engineering-Asce* **2009,** *135*, (11), 1115-1122.
23. Chinnasamy, S.; Bhatnagar, A.; Hunt, R. W.; Das, K. C., Microalgae cultivation in a wastewater dominated by carpet mill effluents for biofuel applications. *Bioresource Technology* **2010,** *101*, (9), 3097-3105.
24. Singh, M.; Reynolds, D. L.; Das, K. C., Microalgal system for treatment of effluent from poultry litter anaerobic digestion. *Bioresource Technology* **2011,** *102*, (23), 10841-10848.
25. Brennan, L.; Owende, P., Biofuels from microalgae—A review of technologies for production, processing, and extractions of biofuels and co-products. *Renewable and Sustainable Energy Reviews* **2010,** *14*, (2), 557-577.
26. Chisti, Y., Biodiesel from microalgae. *Biotechnology Advances* **2007,** *25*, (3), 294-306.
27. Weyer, K. M.; Bush, D. R.; Darzins, A.; Willson, B. D., Theoretical Maximum Algal Oil Production. *BioEnergy Research* **2009,** *3*, (2), 204-213.
28. Xin, L.; Hu, H. Y.; Ke, G.; Sun, Y. X., Effects of different nitrogen and phosphorus concentrations on the growth, nutrient uptake, and lipid accumulation of a freshwater microalga Scenedesmus sp. *Bioresour Technol* **2010,** *101*, (14), 5494-500.
29. Tett, P.; Droop, M.; Heaney, S., The Redfield ratio and phytoplankton growth rate. *Journal of the Marine Biological Association of the United Kingdom* **1985,** *65*, (02), 487-504.

30. Sturm, B. S. M.; Peltier, E.; Smith, V.; deNoyelles, F., Controls of microalgal biomass and lipid production in municipal wastewater-fed bioreactors. *Environmental Progress & Sustainable Energy* **2012,** *31*, (1), 10-16.
31. El Bassam, N., Handbook of bioenergy crops. *London, Earthscan* **2010**.
32. Council, N. R., Sustainable Development of Algal Biofuels in the United States. In Academies, N. R. C. o. t. N., Ed. National Academy Press: Committee on the Sustainable Development of Algal Biofuels, 2012.
33. Levine, A. D.; Asano, T., Peer reviewed: recovering sustainable water from wastewater. *Environmental science & technology* **2004,** *38*, (11), 201A-208A.
34. Rabalais, N. N.; Turner, R. E.; Díaz, R. J.; Justić, D., Global change and eutrophication of coastal waters. *ICES Journal of Marine Science: Journal du Conseil* **2009,** *66*, (7), 1528-1537.
35. Mitsch, W. J.; Day, J. W.; Gilliam, J. W.; Groffman, P. M.; Hey, D. L.; Randall, G. W.; Wang, N., Reducing Nitrogen Loading to the Gulf of Mexico from the Mississippi River Basin: Strategies to Counter a Persistent Ecological Problem Ecotechnology—the use of natural ecosystems to solve environmental problems—should be a part of efforts to shrink the zone of hypoxia in the Gulf of Mexico. *BioScience* **2001,** *51*, (5), 373-388.
36. López Barreiro, D.; Prins, W.; Ronsse, F.; Brilman, W., Hydrothermal liquefaction (HTL) of microalgae for biofuel production: State of the art review and future prospects. *Biomass and Bioenergy* **2013,** *53*, 113-127.
37. Roberts, G. W.; Fortier, M.-O. P.; Sturm, B. S. M.; Stagg-Williams, S. M., Promising Pathway for Algal Biofuels through Wastewater Cultivation and Hydrothermal Conversion. *Energy & Fuels* **2013,** *27*, (2), 857-867.
38. Möller , M.; Nilges , P.; Harnisch, F.; Schröder, U., Subcritical Water as Reaction Environment: Fundamentals of Hydrothermal Biomass Transformation. *ChemSusChem* **2011,** *4*, (5), 566-579.
39. Felício-Fernandes, G.; Laranjeira, M., Calcium phosphate biomaterials from marine algae. Hydrothermal synthesis and characterisation. *Quimica Nova* **2000,** *23*, (4), 441-446.
40. Elliott, D. C.; Hart, T. R.; Schmidt, A. J.; Neuenschwander, G. G.; Rotness, L. J.; Olarte, M. V.; Zacher, A. H.; Albrecht, K. O.; Hallen, R. T.; Holladay, J. E., Process development for hydrothermal liquefaction of algae feedstocks in a continuous-flow reactor. *Algal Research* **2013**.
41. Valdez, P. J.; Nelson, M. C.; Wang, H. Y.; Lin, X. N.; Savage, P. E., Hydrothermal liquefaction of Nannochloropsis sp.: Systematic study of process variables and analysis of the product fractions. *Biomass and Bioenergy* **2012,** *46*, 317-331.

2 Hydrothermal Liquefaction Review

2.1 Background

Properties of water such as dielectric constant, ionic product, viscosity, density, heat capacity, and compressibility are highly temperature dependent, especially at temperatures when approaching the supercritical point.[1] In this regime, water acts more as an organic solvent capable of both solubilizing traditionally insoluble components such as fats and oils and performing chemistries including acid-base reactions, hydrogen donation, free radicals, cracking, polymerization, hydrolysis, dehydration, and Maillard reactions.[2] Hydrothermal processing of biomass has been described via three steps; 1) depolymerization of biomass, 2) decompositions of monomers, and 3) recombination of reactive fragments,[2] where each mechanism and its extent are controlled by the compounds present and the reaction temperature. This greatly effects the product fraction distributions from hydrothermal processing, shown in Figure 2-1. Hydrothermal processing includes three main categories; hydrothermal carbonization (HTC), hydrothermal liquefaction (HTL), and hydrothermal gasification (HTG). Each category typically defined by the temperature ranges of 100-200 °C, 200- 350 °C, and 350-750 °C for HTC, HTL, and HTG, respectively.[1] As reaction temperature increases for each reaction class, the main products (desired) are solid biochar, biocrude, and gasses. Since each conversion temperature uses water as the reaction media, each process produces an aqueous co-product (ACP) comprised of soluble organics and inorganic ions. Beyond algae, hydrothermal processing has been used for conversion of various feedstocks including manure[3, 4], bacteria[5, 6] and cellulosic materials.[7-10]

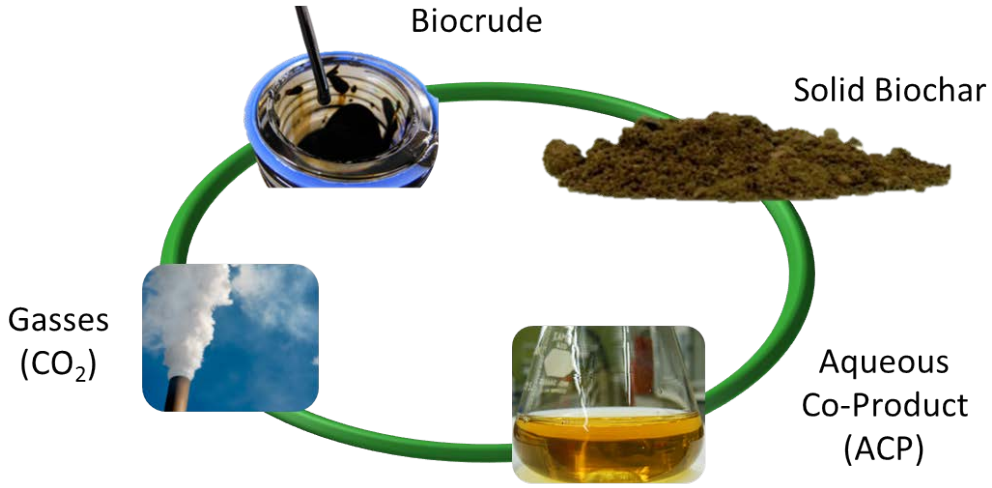

Figure 2-1. Product fractions for hydrothermal conversion of biomass. Main product for HTC, HTL, and HTG are solid biochar, biocrude, and gasses, respectively.

2.2 Literature Data

The majority of studies to date involving the HTL of algae are small scale batch systems from ranging from 5 mL to 1.8 L,[11, 12] however, recently a few continuous systems have been reported.[13-15] Although batch systems do not necessarily mimic commercial scale operation, they provide a platform in which reliable and rapid data collection can be performed in order to better understand product distribution and quality over a wide range of operating parameters and algal feedstocks. In addition, HTL studies have been performed in the presence of various heterogeneous and homogeneous catalysts.[16-22]

A typical batch operation of algae HTL includes a series of reaction, product removal/ separations, and product analysis stages. Reaction parameters of interest are typically percent solids (of algae), temperature, and time held at desired temperature. Ranges for these parameters have been studied from 5-20 wt%, 200- 350°C, and 5 min- 1 hr, respectively.[23] Product

separation techniques can, and generally do, include solvent extraction of the reaction products and reactor vessel, which results in a three phase system including organic liquid phase, aqueous liquid phase, and solid phase, representing the three main products described in Figure 2-1. The most common solvent used has been dichloromethane due to its volatility, solubility with biocrude components, and suitability for a gas chromatography analysis solvent. Other solvents, such as hexadecane, decane, hexane, cyclohexane, methoxycylopentane, and chloroform, have been studied to determine the effect of bulk yield and elemental recovery on extraction technique.[24] However, these solvents have been primarily studied solely for research purposes and if solvent extraction is deemed necessary at full commercial scale both choice of solvent and process design could contribute greatly to the overall sustainability and life cycle assessment of the process. Certain solvents, such as hydrocarbons, would represent molecules actually produced during HTL and could be separated and recycled to an extraction unit operation without the addition of new input streams.

Once the products are separated, various analytical tools are used to determine properties such as elemental content, particularly, carbon, hydrogen, nitrogen, and oxygen (CHNO or ultimate analysis), molecular profile through gas chromatography with mass spectrometry detection (GC-MS), and higher heating value (HHV) or energy content. Most data collected measures these parameters along with bulk yields of each product as a unit of measure for the reaction efficacy and are commonly used as comparison amongst data.

In general, the goal is to produce a biocrude with as similar properties to that of petroleum crude. Petroleum crude oil has reported ranges for CHNO and HHV presented in Table 2-1.[12, 25, 26]

Table 2-1. Properties of petroleum crude oil.

Petroleum CHNO (wt%) and HHV (MJ kg^{-1})	
C	83- 87
H	10- 14
N	0.1- 1.5
O	0.5- 6
HHV	41- 43

In contrast, the ultimate analysis of biocrude produced from the HTL of algae differs from that of petroleum, typically with lower C & H and higher N & O, requiring HTL biocrude to be upgraded to remove heteroatoms and increase the C & H content prior to end-use. Table 2-2 presents the average and standard deviations of bulk yields and biocrude properties reported in the literature from a number of different species of micro- and macro-algae processed under similar HTL conditions which are most relevant reaction conditions applicable to those presented in further chapters of this dissertation; average reaction temperature of 350 °C, 10 wt% biomass solids, and up to 1 hr reaction time. These conditions also represent a relative optimum for both biocrude production and quality.[12, 27-32] It has also been shown that shorter reaction time can promote increased productivity of biocrude with the expense of producing a lower quality crude, i.e., higher heteroatom content.[11] Table 2-3 comprises the individual data reviewed for obtaining the averages in Table 2-2. Interestingly, even under similar reaction conditions, similar algae species produce varying HTL results, and overall, the bulk yields present significant variance while still producing biocrude with relatively similar CHNO content, where

the individual C & O content of the biocrude has the highest degree of variance among the ultimate analysis.

Table 2-2. Average literature data on algae liquefaction at similar reaction conditions.

Average HTL Results			
Yields	wt%		
Biocrude	35.7	±	15.1
Solids	15.6	±	18.1
Aqueous	26.4	±	16.4
Biocrude	wt%		
C	72.3	±	3.4
H	8.9	±	0.7
N	5.6	±	1.2
O	11.8	±	4.6
HHV (MJ kg^{-1})	35.0	±	2.5

Table 2-3. Bulk yields and biocrude properties from published data on HTL of algae.

	Algal species	Product Yields (wt%)			Biocrude Properties (wt%)					Reference
		Oil	Solid	ACP	C	H	N	O	HHV (MJ/Kg)	
Micro										
1	*Spirulina platensis*	32	5	44	72.3	9.0	5.7	11.7	35.3	12
2	*Nannochloropsis Occulata*	35	2	60	68.1	8.8	4.1	18.9	34.5	33
3	*Porphyridium cruentum*	21	9	71	72.8	8.5	5.4	13.3	35.7	33
4	*Scenedesmus sp.*	45	7	17	72.6	9.0	6.5	10.5	35.5	34
5	*Spirulina sp*	31	11	23	72.2	9.1	8.1	9.2	35.8	34
6	*Nannochloropsis sp.*	30	5	29	75.8	10.6	4.5	9.1	N/A	24
7	*Chlorella sp.*	25	20*	50	70.7	8.6	5.9	14.8	35.1	35
8	*Nannochloropsis sp.*	10	75*	15	68.1	8.8	4.1	18.9	34.5	35
9	*Porphyridium sp.*	10	50*	40	72.8	8.5	5.4	13.3	35.7	35
10	*Spirulina sp.*	15	45*	35	73.3	9.2	7.0	10.4	36.8	35
11	*Tetraselmis sp.*	41	14	12	71.0	9.5	5.0	14.0	35.0	32
12	*Phaeodactylum tricornutum*	39	6	21	75	10	5	10	37	30
13	*Scenedesmus obliquus*	51	5	11	73.2	8.9	6.3	8.1	35.6	36
14	*Phaeodactylum tricornutum*	54	7	13	73.4	9.1	5.8	7.8	35.9	36
15	*Nannocholoropsis gaditana*	54	6	19	74.7	9.9	5.2	8.5	37.2	36
16	*Scenedesmus almeriensis*	58	3	13	74.3	9.1	6.1	8.4	36.2	36
17	*Tetraselmis suecica*	46	4	15	74.0	9.0	6.1	7.7	36.0	36
18	*Chlorella vulgaris*	55	4	17	72.5	8.7	7.1	8.6	35.0	36
19	*Porphyridium purpureum*	47	3	16	73.9	8.2	6.8	8.7	35.0	36
20	*Dunaliella tertiolecta*	55	6	18	72.0	8.8	6.2	9.9	34.9	36
Macro										
21	*Sargassum patens*	29	33	7	64.6	7.4	2.5	22.0	27.1	37
22	*Laminaria saccharina*	19	20	26	80.1	8.3	5.4	6.1	38.5	29
23	*Enteromorpha prolifera*	19	18	35	64.5	7.7	5.4	22.5	28.7	27

Typical reaction conditions are 320-370°C, 10 wt% algal solids, and 1 hr reaction time.

* Value includes solids and gas product yields

Even though the ultimate analysis of the biocrude is promising, there is still a significant gap between HTL biocrude and petroleum crude. This is easily seen within the Van Krevelen diagram presented in Figure 2-2. A Van Krevelen diagram shows the relationship between carbon, hydrogen, and oxygen, where a desirable fuel has large magnitude in the y-axis and small magnitude in the x-axis. This region would indicate a high energy density fuel with little upgrading needed to remove oxygen.

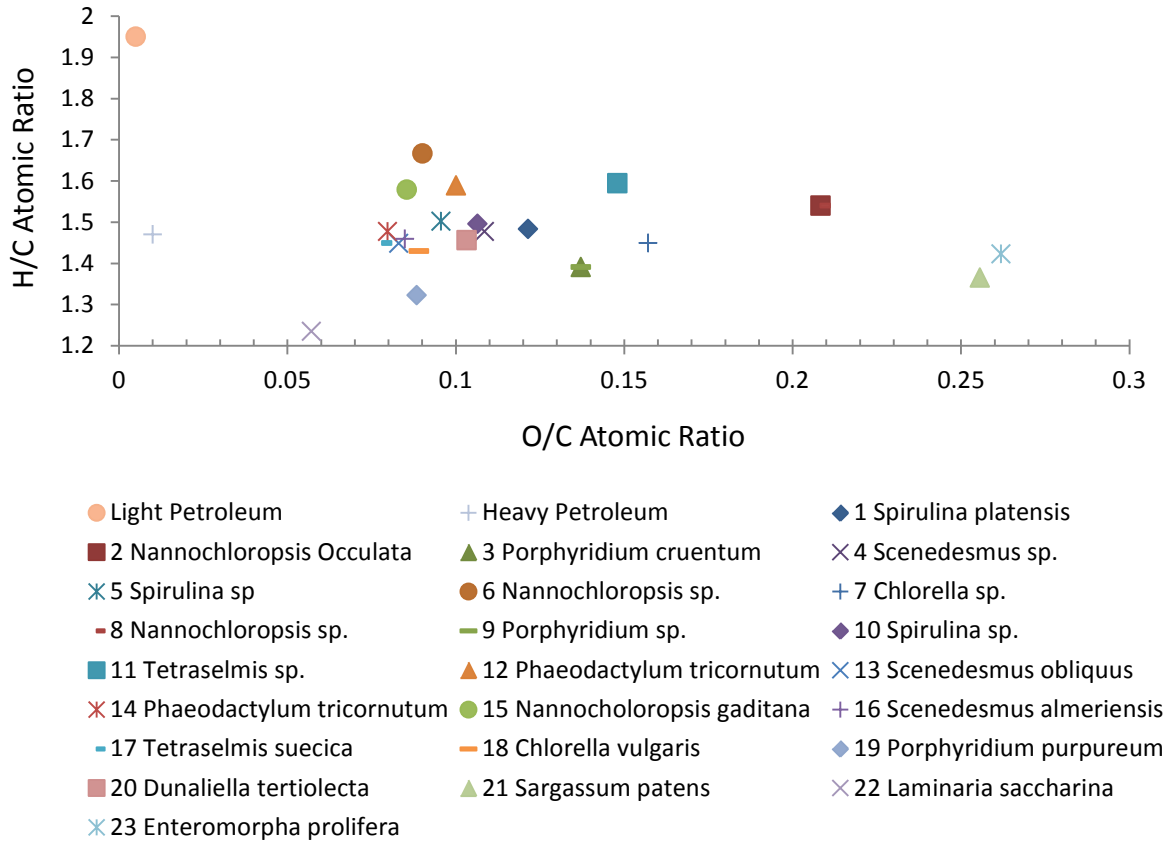

Figure 2-2. Van Krevelen diagram from literature HTL biocrude data contained in Table 2-1 and Table 2-2; identifying numbers correspond to the identifying numbers in Table 2-3.

In addition to the heteroatom content, the molecular profile of a biocrude is also important to understand in terms of upgrading to an end-use fuel. Typical biocrude from HTL of algae contain a wide array of chemical compounds with typical classes including straight chain and branched alkanes and alkenes, aromatics, keytones, fatty acids, fatty acid amides, alcohols, phenolics, indoles, pyridines, and nitriles.[22, 38] Identifying specific molecules within the HTL biocrude is important when deciding on particular upgrading strategy to remove the heteroatom content and increase the lower boiling point distillates. Cracking the higher boiling point distillates such as the vacuum gas oil and vacuum gas residual fractions will increase profitability of the biocrude by producing a larger fraction of useable fuels. Further detail of biocrude molecular profiles and distillate fractions from the literature will be discussed in relationship to the data collected for this dissertation and presented in Section 6.1: *In-situ* Catalytic Upgrading of the Biocrude from Hydroxyapatite Crystallization.

Other studies on the HTL of algae and related components have included the evaluation of algae with different biochemical components as compared to model compounds such as various proteins, sugars, and oils; which showed lipids and proteins are converted most readily into biocrude product with the carbohydrates more easily converted under alkali catalysts.[35] Converting the protein and carbohydrate portions of an algae cell into a viable biocrude (beyond lipids) makes HTL a highly suitable conversion route for low- lipid containing algae[39] or algae residuals which have gone through a lipid extraction process,[15, 34] where some cultivation strategies want to promote accumulation of omega-3 fatty acids for nutraceutical industry as a lucrative option to replace marine fatty fish.[40] Therefore, once these industries obtain their valuable lipids the remaining fraction of the algae biomass is a suitable biofuel feedstock. In

addition to lipids, HTL has also been used to extract polysaccharides prior to conversion to a biocrude.[41] Further fundamental studies have been reported in efforts to understand the complexity of reactive biomolecules in the presence of subcritical water and develop a reaction network to begin to understand kinetic parameters in regards to the formation of the bulk products formed shown in Figure 2-1.[42]

2.3 References

1. Möller , M.; Nilges , P.; Harnisch, F.; Schröder, U., Subcritical Water as Reaction Environment: Fundamentals of Hydrothermal Biomass Transformation. *ChemSusChem* **2011,** *4*, (5), 566-579.
2. Toor, S. S.; Rosendahl, L.; Rudolf, A., Hydrothermal liquefaction of biomass: A review of subcritical water technologies. *Energy* **2011,** *36*, (5), 2328-2342.
3. Yin, S.; Dolan, R.; Harris, M.; Tan, Z., Subcritical hydrothermal liquefaction of cattle manure to bio-oil: Effects of conversion parameters on bio-oil yield and characterization of bio-oil. *Bioresource Technology* **2010,** *101*, (10), 3657-3664.
4. Vardon, D. R.; Sharma, B. K.; Scott, J.; Yu, G.; Wang, Z.; Schideman, L.; Zhang, Y.; Strathmann, T. J., Chemical properties of biocrude oil from the hydrothermal liquefaction of Spirulina algae, swine manure, and digested anaerobic sludge. *Bioresource Technology* **2011,** *102*, (17), 8295-8303.
5. Valdez, P. J.; Nelson, M. C.; Faeth, J. L.; Wang, H. Y.; Lin, X. N.; Savage, P. E., Hydrothermal liquefaction of bacteria and yeast monocultures. *Energy & Fuels* **2013,** *28*, (1), 67-75.
6. Hammerschmidt, A.; Boukis, N.; Galla, U.; Dinjus, E.; Hitzmann, B., Conversion of yeast by hydrothermal treatment under reducing conditions. *Fuel* **2011,** *90*, (11), 3424-3432.
7. Jindal, M.; Jha, M., Catalytic Hydrothermal Liquefaction of Waste Furniture Sawdust to Bio-oil. *Indian Chemical Engineer* **2015**, (ahead-of-print), 1-15.
8. Zhu, Z.; Rosendahl, L.; Toor, S. S.; Yu, D.; Chen, G., Hydrothermal liquefaction of barley straw to bio-crude oil: Effects of reaction temperature and aqueous phase recirculation. *Applied Energy* **2015,** *137*, 183-192.
9. Karagöz, S.; Bhaskar, T.; Muto, A.; Sakata, Y.; Oshiki, T.; Kishimoto, T., Low-temperature catalytic hydrothermal treatment of wood biomass: analysis of liquid products. *Chemical Engineering Journal* **2005,** *108*, (1-2), 127-137.
10. Lu, W.; Yang, F.; Wang, C.; Yang, Z., Comparison of high-caloric fuel (HCF) from four different raw materials by deoxy-liquefaction. *Energy & Fuels* **2010,** *24*, (12), 6633-6643.

11. Faeth, J. L.; Valdez, P. J.; Savage, P. E., Fast Hydrothermal Liquefaction of Nannochloropsis sp. To Produce Biocrude. *Energy & Fuels* **2013,** *27*, (3), 1391-1398.
12. Jena, U.; Das, K. C.; Kastner, J. R., Effect of operating conditions of thermochemical liquefaction on biocrude production from Spirulina platensis. *Bioresource Technology* **2011,** *102*, (10), 6221-6229.
13. Jazrawi, C.; Biller, P.; Ross, A. B.; Montoya, A.; Maschmeyer, T.; Haynes, B. S., Pilot plant testing of continuous hydrothermal liquefaction of microalgae. *Algal Research* **2013,** *2*, (3), 268-277.
14. Elliott, D. C.; Biller, P.; Ross, A. B.; Schmidt, A. J.; Jones, S. B., Hydrothermal liquefaction of biomass: Developments from batch to continuous process. *Bioresource technology* **2015,** *178*, 147-156.
15. Elliott, D. C.; Hart, T. R.; Schmidt, A. J.; Neuenschwander, G. G.; Rotness, L. J.; Olarte, M. V.; Zacher, A. H.; Albrecht, K. O.; Hallen, R. T.; Holladay, J. E., Process development for hydrothermal liquefaction of algae feedstocks in a continuous-flow reactor. *Algal Research* **2013,** *2*, (4), 445-454.
16. Chen, Y.; Wu, Y.; Ding, R.; Zhang, P.; Liu, J.; Yang, M.; Zhang, P., Catalytic hydrothermal liquefaction ofD. tertiolectafor the production of bio-oil over different acid/base catalysts. *AIChE Journal* **2015,** *61*, (4), 1118-1128.
17. Duan, P.; Savage, P. E., Hydrothermal Liquefaction of a Microalga with Heterogeneous Catalysts. *Industrial & Engineering Chemistry Research* **2011**, (50), 52-61.
18. Li, H.; Hurley, S.; Xu, C., Liquefactions of peat in supercritical water with a novel iron catalyst. *Fuel* **2011,** *90*, (1), 412-420.
19. Yang, C.; Jia, L.; Chen, C.; Liu, G.; Fang, W., Bio-oil from hydro-liquefaction of Dunaliella salina over Ni/REHY catalyst. *Bioresource Technology* **2011,** *102*, (6), 4580-4584.
20. Jena, U.; Das, K. C.; Kastner, J. R., Comparison of the effects of Na2CO3, Ca3(PO4)2, and NiO catalysts on the thermochemical liquefaction of microalga Spirulina platensis. *Applied Energy* **2012,** *98*, 368-375.
21. Hammerschmidt, A.; Boukis, N.; Hauer, E.; Galla, U.; Dinjus, E.; Hitzmann, B.; Larsen, T.; Nygaard, S. D., Catalytic conversion of waste biomass by hydrothermal treatment. *Fuel* **2011,** *90*, (2), 555-562.
22. Bai, X.; Duan, P.; Xu, Y.; Zhang, A.; Savage, P. E., Hydrothermal catalytic processing of pretreated algal oil: A catalyst screening study. *Fuel* **2014,** *120*, 141-149.
23. Tian, C.; Li, B.; Liu, Z.; Zhang, Y.; Lu, H., Hydrothermal liquefaction for algal biorefinery: A critical review. *Renewable and Sustainable Energy Reviews* **2014,** *38*, 933-950.
24. Valdez, P. J.; Dickinson, J. G.; Savage, P. E., Characterization of Product Fractions from Hydrothermal Liquefaction ofNannochloropsissp. and the Influence of Solvents. *Energy & Fuels* **2011,** *25*, (7), 3235-3243.
25. Ross, A. B.; Biller, P.; Kubacki, M. L.; Li, H.; Lea-Langton, A.; Jones, J. M., Hydrothermal processing of microalgae using alkali and organic acids. *Fuel* **2010,** *89*, (9), 2234-2243.
26. Matar, S.; Hatch, L. F., *Chemistry of petrochemical processes*. Gulf Professional Publishing: 2001.

27. Zhou, D.; Zhang, L.; Zhang, S.; Fu, H.; Chen, J., Hydrothermal Liquefaction of Macroalgae Enteromorpha prolifera to Bio-oil. *Energy & Fuels* **2010,** *24*, (7), 4054-4061.
28. Brown, T. M.; Duan, P.; Savage, P. E., Hydrothermal Liquefaction and Gasification of Nannochloropsis sp. *Energy & Fuels* **2010,** *24*, (6), 3639-3646.
29. Anastasakis, K.; Ross, A. B., Hydrothermal liquefaction of the brown macro-alga Laminaria Saccharina: Effect of reaction conditions on product distribution and composition. *Bioresource Technology* **2011,** *102*, (7), 4876-4883.
30. Christensen, P. S.; Peng, G.; Vogel, F.; Iversen, B. B., Hydrothermal Liquefaction of the MicroalgaePhaeodactylum tricornutum: Impact of Reaction Conditions on Product and Elemental Distribution. *Energy & Fuels* **2014,** *28*, (9), 5792-5803.
31. Garcia Alba, L.; Torri, C.; Samorì, C.; van der Spek, J.; Fabbri, D.; Kersten, S. R. A.; Brilman, D. W. F., Hydrothermal Treatment (HTT) of Microalgae: Evaluation of the Process As Conversion Method in an Algae Biorefinery Concept. *Energy & Fuels* **2011**, 111201165948002.
32. Eboibi, B.; Lewis, D.; Ashman, P.; Chinnasamy, S., Effect of operating conditions on yield and quality of biocrude during hydrothermal liquefaction of halophytic microalga< i> Tetraselmis</i> sp. *Bioresource technology* **2014,** *170*, 20-29.
33. Biller, P.; Riley, R.; Ross, A. B., Catalytic hydrothermal processing of microalgae: Decomposition and upgrading of lipids. *Bioresource Technology* **2011,** *102*, (7), 4841-4848.
34. Vardon, D. R.; Sharma, B. K.; Blazina, G. V.; Rajagopalan, K.; Strathmann, T. J., Thermochemical conversion of raw and defatted algal biomass via hydrothermal liquefaction and slow pyrolysis. *Bioresource Technology* **2012,** *109*, 178-187.
35. Biller, P.; Ross, A. B., Potential yields and properties of oil from the hydrothermal liquefaction of microalgae with different biochemical content. *Bioresour Technol* **2011,** *102*, (1), 215-25.
36. Lopez Barreiro, D.; Zamalloa, C.; Boon, N.; Vyverman, W.; Ronsse, F.; Brilman, W.; Prins, W., Influence of strain-specific parameters on hydrothermal liquefaction of microalgae. *Bioresour Technol* **2013,** *146*, 463-71.
37. Li, D.; Chen, L.; Xu, D.; Zhang, X.; Ye, N.; Chen, F.; Chen, S., Preparation and characteristics of bio-oil from the marine brown alga Sargassum patens C. Agardh. *Bioresource Technology* **2012,** *104*, 737-742.
38. Roussis, S. G.; Cranford, R.; Sytkovetskiy, N., Thermal Treatment of Crude Algae Oils Prepared Under Hydrothermal Extraction Conditions. *Energy & Fuels* **2012,** *26*, (8), 5294-5299.
39. Yu, G.; Zhang, Y.; Schideman, L.; Funk, T.; Wang, Z., Distributions of carbon and nitrogen in the products from hydrothermal liquefaction of low-lipid microalgae. *Energy & Environmental Science* **2011,** *4*, (11), 4587.
40. Adarme-Vega, T. C.; Lim, D. K.; Timmins, M.; Vernen, F.; Li, Y.; Schenk, P. M., Microalgal biofactories: a promising approach towards sustainable omega-3 fatty acid production. *Microb Cell Fact* **2012,** *11*, (1), 96.
41. Miao, C.; Chakraborty, M.; Chen, S., Impact of reaction conditions on the simultaneous production of polysaccharides and bio-oil from heterotrophically grown Chlorella

sorokiniana by a unique sequential hydrothermal liquefaction process. *Bioresource Technology* **2012,** *110*, 617-627.
42. Valdez, P. J.; Savage, P. E., A reaction network for the hydrothermal liquefaction of Nannochloropsis sp. *Algal Research* **2013,** *2*, (4), 416-425.

3 Experimental Materials and Methods

Herein, the work represents the culmination of combined studies from two main lots of algae biomass cultivated and harvested in 2011 and 2013 from the Lawrence, KS Wastewater Treatment Plant. For identification purposes, the biomass, reaction parameters, and characterization techniques will be referred to by the corresponding year the algae was harvested; referred from here on as algae lot# 2011 and algae lot# 2013, respectively. Many procedures used in this work were taken from standard methods, adapted from those reported in the literature, or developed as novel methods. One particular novel method that was developed incorporated using thermogravimetric analysis to simultaneously obtain a full proximate analysis (moisture, volatile, fixed-carbon, and ash content) of either the algae biomass or HTL solid product. Significant limitations to the standard method of biomass ash determination (ASTM E1755) were identified; including being susceptible to inaccuracies during material handling and weighing procedures as well as be very time consuming (requiring multiple days). The development of the thermogravimetric method for proximate analysis overcame both of these limitations and provided additional characterizations beyond moisture and ash content which add valuable information in terms of volatile content and optimum burning temperatures of the samples.

3.1 Algae Cultivation

All algae cultivation used in this dissertation was grown and collected at the Lawrence, KS Wastewater Treatment Plant, in four 2500 gallon open pond reactors (height, 1.2 m;

diameter, 3.17 m). The open ponds operated continuously as stirred tanks fed by incoming water and nutrients supplied by effluent from the secondary clarifier before disinfection. Each reactor was held at a hydraulic residence time (HRT) of 10 days. Aeration and mixing was provided by fine-bubble air stones. No algae inoculum was used and native algae species were allowed to cultivate naturally. A representative mixed algae culture was identified and is presented in Table 3.1.

Table 3-1. Identified algae species.

Species Identified	
Scenedesmus quadricauda	*Cladophora sp.*
Navicula sp.	*Golenkinia radiata*
Scenedesmus bijuga	*Selenastrum sp.*
Oscillatoria sp.	*Cosmarium sp.*
Micractinium pusillum	*Pediastrum boryanum*
Merismopedia sp.	*Microcystis sp.*
Chlorella sp.	*Oedogonium sp.*
Cryptomonas sp.	*Cosmarium sp.*
Cyclotella sp.	*Spirogyra sp.*

Top-down ecological control was implemented through the addition of *Gambusia* fish which prey on zooplankton such as *Daphnia*. Operation of these pond reactors have been previously reported by Sturm and Lamer[1] and Sturm et al.[2] Effluent from the four reactors continuously flowed to four separate gravity sedimentation tanks each with a surface area of 1.56 ft^2 and an operating volume of 42.9 gal. Each system had an overflow velocity of 6.7 m day^{-1} at the operational flowrate. The concentrated microalgae samples (1-1.5% solids) were collected from the bottom of each sedimentation tank daily and were immediately processed. Algae harvested from the settling tanks were centrifuged at 3220 rcf for 10 minutes. The pellet was then freeze

dried, ground with a conventional coffee grinder, and stored at or below 4°C until processed for characterization(s) and HTL.

During the collection of algae lot# 2011 each settling tank was mixed together before centrifugation. Macroalgae (*Cladophora sp*.) grown on the tank walls were also collected and processed separately but in the same manner; furthermore identified as macro lot# 2011. The cultivation strategy for algae lot# 2013 deviated slightly from the above mentioned; each of the four reactors were set-up as duplicate sets of two reactors in series, in which the treatment plant's secondary effluent was sent to the first open pond, whose effluent was sent to a second open pond. Each pond had a hydraulic retention time (HRT) of 10 days resulting in a total of 20 day HRT for each set in the 2 X 2 system. Biomass grown in the second pond of one set was used as the algae lot# 2013. Figure 3-1 shows the process water/nutrient flow for each algae lot cultivated.

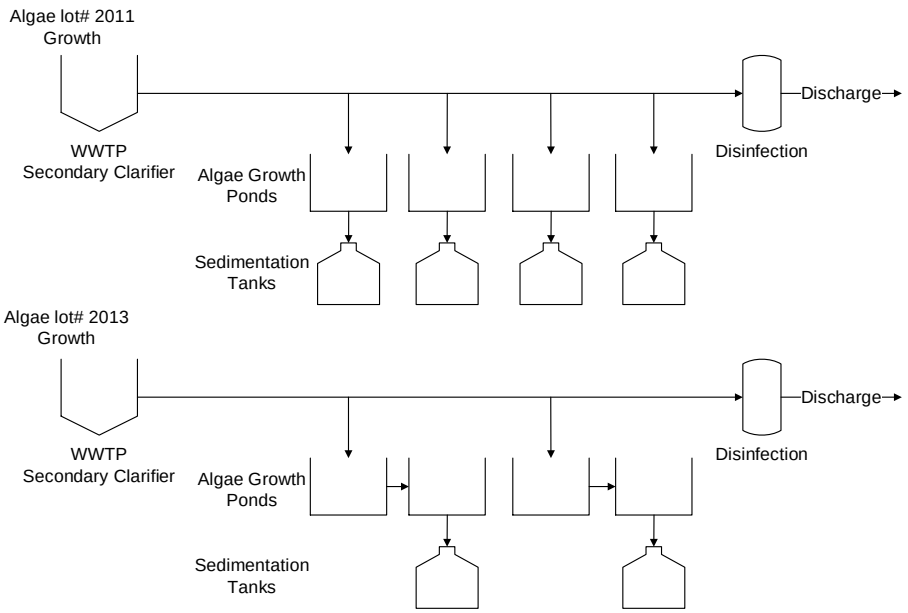

Figure 3-1. Algae cultivation schematic at the wastewater treatment plant (WWTP).

3.2 Algae Characterization

3.2.1 Proximate Analysis

Algae lot# 2011 was analyzed for moisture and ash in accordance with ASTM E1755 standard method using a Thermolyne 46100 high temperature furnace.[3] However, for algae lot# 2013 a method was developed using thermogravimetric analysis (TGA) on a TA Instruments SDT 600 to simultaneously obtain the full proximate analysis, including moisture, volatile, fixed-carbon, and ash contents. A description of the method used is as followed:

The full TGA proximate analysis uses a two stage thermo-degradation of the sample, including pyrolysis in nitrogen environment followed by combustion in air. The pyrolysis (Py) stage determines the moisture and volatile content and the post pyrolysis combustion (PPyC) determines the fixed-carbon and ash content of the biomass. During pyrolysis, the temperature is

increased to 90°C where it enters a stepwise function until 110 °C. During the stepwise function, the temperature was either isothermal or increasing at 1 °C min^{-1} depending upon criteria of the derivative weight change, i.e., the sample is isothermal when derivative weight change is >0.01 wt% min^{-1} and increasing temperature when the derivative weight change is <0.01 wt% min^{-1}. This allows accurate determination of a precise weight loss at a particular temperature. After the first stepwise function the temperature was ramped at a constant rate, 5-10°C min^{-1} to 800 °C and entered another stepwise function until 850 °C. Moisture and volatile matter was then determined at the point where weight changes were essentially zero at ~100 °C and 850 °C, respectively. The sample was then cooled to 120 °C and flow was switched from nitrogen to air commencing the PPyC phase for determination of the fixed-carbon and ash content. Under oxygen, the PPyC proceeded to 800 °C and enters another stepwise function to 850 °C. The calculations used for quantifying the proximate analysis are as followed, where %SR refers to mass percent of the sample remaining:

Moisture: 100% - %SR [after 1^{st} step-wise during Py]

Volatile: %SR [after 1^{st} step-wise during Py] – %SR [after 2^{nd} step-wise during Py]

Fixed Carbon: %SR [after 2^{nd} step-wise during Py] - %SR [after step-wise during PPyC]

Ash: %SR [after entire program]

3.2.2 Algae lot# 2013 Ash

Ash from algae lot# 2013 was obtained by placing a sample of freeze dried algae, ~100 mg, in a homemade quartz tube furnace with a programmable temperature controller. The sample was combusted under a flow of 100 mL min^{-1} of air during 2 °C min^{-1} ramp to 600 °C

and held for 8 h. The combustion procedure was performed three times to ensure all organic material was removed.

3.2.3 Ultimate analysis

The ultimate analysis or carbon, hydrogen, nitrogen, and oxygen (CHN & O) contents of algae lot# 2011 were determined by Micro Analysis Inc. (Wilmington, DE). Algae lot# 2013 was determined in house with a Perkin Elmer CHN Analyzer with O content determined by difference. Since algae cultivated for this thesis results in significant ash contents reporting the ultimate content on a ash free dry weight percent (afdw%) is important for comparing data throughout the literature. Samples are measured completely dry and therefore measured values are normalized to the ash for reporting afdw%. Typical procedure for measuring CHN contents include the following: after drying biomass samples in an oven overnight at 105 °C they are immediately placed in a desiccator. The analyzer is calibrated by running a series of black and k-factors (terminology used by the manufacturer) which include running a blank tin sample cup and a known amount of acetanilide (Perkin Elmer standard), respectively. Once stable readings are obtained for both k-factors and blanks, the acetanilide is analyzed as a sample to ensure that the proper CHN content is obtained by the instrument. Once the instrument is properly calibrated (performed during each day of analysis) each sample is repeated until at least three values within the instrument error (±0.03 wt%) is obtained. All samples (and k-factors) are weighed to the nearest 0.001 mg using a calibrated Perkin Elmer micro analytical balance.

3.2.4 Higher Heating Value (HHV)

Higher heating value (HHV), of algae lot# 2011, was obtained using a Parr 6200 calorimeter using decane (Fisher; 99+%) as a combustion agent. Utilization of a combustion agent first requires prior calibration within the instrument which is stored within the internal memory of the instrument. Decane was chosen to ensure reliable combustion and minimal evaporation during sample transfer from the balance to the calorimeter. All samples and combustion agents are measured to 0.1 mg using a Metler Toledo NewClassic MF analytical balance. HHV of algae lot# 2013 was not measured, however could be calculated by the following equation(s)

$$HHV = 14441.82(X) + 7018.311$$

Where, X = volatile matter / (volatile matter + fixed carbon + ash)

Or,

$$HHV = 343.08C + 424.92H + 261.98N + 27.76O$$

Where, CHNO = carbon, hydrogen, nitrogen, and oxygen on a dry-ash-free-basis in kJ/kg.[4]

3.2.5 Proton Induced X-ray Emission (PIXE)

Inorganic elemental (non-CHNO content) of algae lot# 2011 was analyzed and quantified through PIXE performed by Elemental Analysis, Inc. (Lexington, KY).

3.2.6 Inductively Coupled Plasma- Optical Emission Spectroscopy (ICP-OES)

ICP-OES (Agilent) was used for analysis during algae lot# 2013. The elements of: (Al, Ba, Ca, Fe, K, Mg, Na, P, S)- group “A”, (B, La, Mn, Ni, Zn) –group “B”, and (As, Co, Cu, Pb, Sr) group- “C”, were quantified in samples of the wastewater effluent, growth media in each

open ponds in series, the algae biomass, and the resultant HTL solid product. One standard stock solution was created by and purchased from Inorganic Ventures (Christiansburg, VA) with concentrations of 1000 ppm, 100 ppm, and 10 ppm, for group A, B, and C, respectively. Standard solutions were prepared and used at 5 vol% nitric acid (Fisher; trace metal grade) and concentrations of 0.5, 1, 2, 5, and 10 ppm with respect to group A, leaving group(s) B and C at their respective concentration magnitudes. Standard curves were created using the five concentrations and a blank with a quality control check at 3 ppm with respect to group A. When performing analysis a new standard curve was created every 10 samples. Samples were adjusted to 5 vol% nitric acid and filtered through a 0.2 µm filter before analysis. Solid samples (algae biomass and HTL solid product) were digested by standard acid microwave digestion.

3.3 Hydrothermal Liquefaction (HTL)

3.3.1 Reaction, Product Separation, and Yield Determination

All reactions were performed in a 450 mL 4560 series mini bentchtop reactor (Parr; Moline, IL) attached to a 4848 model controller (Parr) and used 50 mL of MilliQ water at a particular solids concentration. Once contents were sealed inside the reactor, oxygen was purged from the headspace by flowing nitrogen multiple times. Reactor temperatures were performed at 350 ± 5 °C with a reaction time of 1 hr and a stir rate of 150 rpm. Post reaction, the reactor was cooled using a water bath to quench the reaction and the contents were allowed to equilibrate overnight, upon which product recovery and characterizations were commenced. At least three identical experiments were performed to obtain standard deviations for each algae lot (except for macro lot# 2011; only duplicate reactions were performed due to the availability of algae

biomass). Between each experiment the reactor was thoroughly cleaned by hand, solvent cleaned with 50 mL of hot acetone (60°C, 600+ rpm, 30 min), and finally reactor walls were exposed to subcritical water by conditioning at 350°C for 30 min using 50 mL of water. Different methodologies for product handling and characterizations were for used for each lot of algae and are described separately as followed;

Algae lot# 2011:

3 g of ground freeze-dried algae were used at a specific solids concentration of 5.7 wt%. The product recovery follows the flow diagram presented in Figure 3-2. After overnight equilibration, 50 mL of decane (99+%; Fisher) was introduced to the reactor and the temperature was increased to 70 °C for 30 min while stirring at 150 rpm to allow for clumps of solid product to be loosened, maximizing solvent exposure and biocrude recovery. The reactor contents were collected in pre-weighed centrifuge tubes and were centrifuged at 1730 rcf for several minutes, resulting in four layers [from top to bottom: solvent containing biocrude, solid product, aqueous co-product (ACP), and solid product] shown in Figure 3-2b. The top organic layer (solvent containing biocrude) was removed by pipet, and the volume was recorded. A total of 30 mL of this fraction was separated and dried under nitrogen gas flow at 30 °C until the mass was constant to determine the biocrude concentration and, thus, overall mass of biocrude. A second solvent recovery step was employed to remove any other contents still residing in the reactor, mainly biocrude and solid product adhering to the reactor walls. The second recovery step involved adding 50 mL of decane to the reactor and stirring at 600+ rpm with no heat for 30 min. The contents were collected, measured, and processed in the same manner as the previous recovery step. Significant biocrude and solid product were collected during the second recovery.

The reactor was then cleaned with 50 mL of acetone at 200 °C for 30 min, where significant biocrude could be collected from fittings of the reactor head, but this mass was not added to the overall yield of the process.

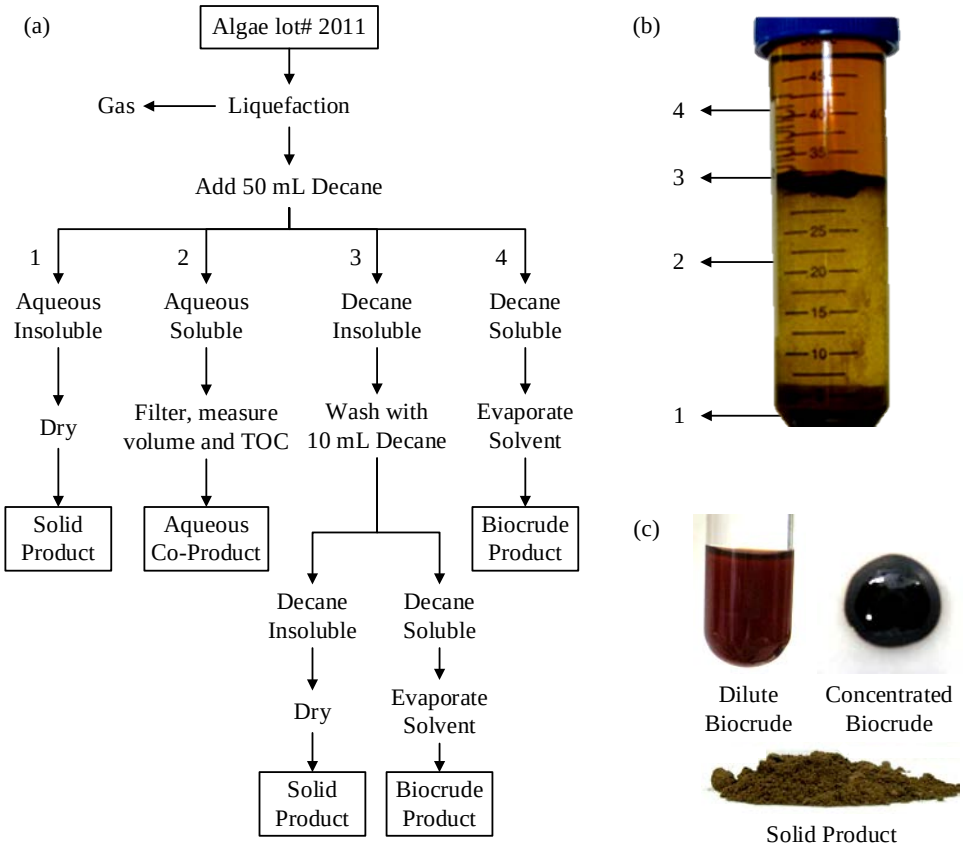

Figure 3-2. Product handling and recovery for Algae lot# 2011. (a) Flow diagram of product handling, (b) Phase separation of HTL products: 1- solids, 2- ACP, 3- solids, 4- dilute biocrude, and (c) pictures of main HTL products.

After centrifugation the solvent was completely pipetted from the solid pellet and dried in the same manner. Significant biocrude mass was extracted from this solid product fraction and added to the overall biocrude yield. The ACP was filtered through pre-rinsed Whatman GF/F glass-fiber filters, and the volume was recorded. A portion of ACP was diluted with milliQ

water [40:1; water: ACP] and analyzed for total organic carbon (TOC) and total nitrogen (TN) using a Torch Combustion TOC/TN Analyzer. All solids were dried under N_2 flow at 30 °C, and the weights of each were combined for a total solid product mass. The energy content (HHV) and elemental analysis of the solid product and biocrude were determined in the same manner as the starting algae. A photograph of the biocrude (dilute and concentrated) and solid product are shown in Figure 3-2c. A control experiment was performed using the same lot and amount of algae and water. Using the same reactor, the algae/ water suspension was agitated at 150 rpm for 1 hr at room temperature. The solvent recovery method described above was employed without addition of heat at any point. Both recovery steps were implemented, and oil mass determination methods were consistent for both HTL and control experiments.

Yields of each product fraction were equated from the following equations:

$$Biocrude\ yield = \frac{\sum mBiocrude}{mAlgae_{organics}} x\ 100 \quad (3.1)$$

$$ACP\ yield = \frac{[TOC] * Aq_{vol}}{mC_{algae}} x\ 100 \quad (3.2)$$

$$Solids\ yield = \frac{mSolids - mAsh_{algae}}{mAlgae_{organics}} x\ 100 \quad (3.3)$$

$$Gas\ yield = 100 - (3.1) - (3.2) - (3.3) \quad (3.4)$$

where, $\sum mBiocrude$ is the summation of all calculated masses of biocrude from each fraction, $mAlgae_{organics}$ is the mass of freeze dried algae * (100 – ash% - moisture%), [*TOC*] is the concentration of measured total organic carbon, Aq_{vol} is the measured filtered ACP volume, mC_{algae} is the mass of carbon (afdw%) in algae, *mSolids* is the mass of dried solid product, and $mAsh_{algae}$ is the mass of ash in starting algae. Dry weight (dw%) solid product yield was

calculated by relating the total dry weight of product to the dry weight of algae used in the reaction.

Algae lot# 2013:

5.56 g of ground freeze-dried algae were used resulting in 10.0 wt% solids for each reaction. Product recovery and isolation used dichloromethane (DCM) (high performance liquid chromatography grade, Fisher) and followed the flow diagram shown in Figure 3-2.

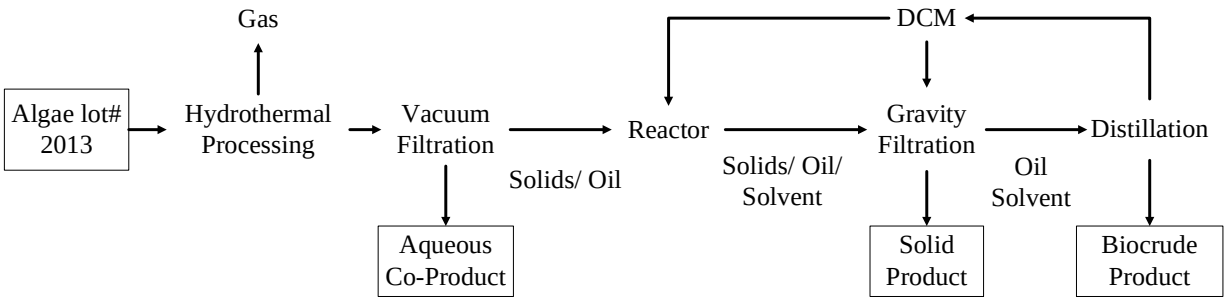

Figure 3-3. Schematic of product handling and isolation for algae lot# 2013.

Once the reactor contents had equilibrated, the gasses formed were vented and the contents were vacuum filtered separating the aqueous co-product (ACP) and solids/ oil mixture. The solids/ oil mixture was placed back into the reactor vessel with the addition of 50 mL DCM and heated to 40 °C with stir rate of 600+ rpm for 30 min. Upon cooling the vessel again in a water bath, the contents were gravity filtered and washed with additional DCM via slow pipette until no additional oil was extracted from the solids. The solid product was dried and the oil/ solvent mixture was distilled to remove solvent and obtain biocrude product.

Commencing product analysis directly after separations is critical for obtaining reliable yields, particularly for the biocrude fraction. After the majority of the DCM solvent was distilled off, a vacuum was applied to lower solvent content to <10 wt%. The weight of the biocrude was recorded in the tarred flask and immediately placed an ice bath. Simulated distillation (see section 3.4.4) and ultimate analysis (see section 3.4.2) was immediately performed on the biocrude using the same TGA instrument and CHN analyzer as used for the proximate and ultimate analysis of the algae biomass, respectively. Yield and ultimate analysis (using known molecular weight, carbon, and hydrogen content of DCM) are adjusted by the corresponding amount of residual solvent for each experiment individually.

The dried solid product was weighed and analyzed for proximate (TGA: see section 3.4.1) and ultimate (CHN: see section 3.4.2) contents, functional groups (FTIR: see section 3.4.6), and crystallography (XRD: see section 3.4.5), along with bulk and trace metal compositions (ICP-OES: see section 3.2.5). Yield of the solids was determined on a dry weight (dw) and an ash free dry weight (afdw) basis. Portions (~100 mg) of the solid product were calcined in 100 mL min^{-1} air flow in a homemade quartz tube furnace with a ramp rate of 2 °C min^{-1} to specified temperature (500, 600, 700, 800, 900 °C) for 8 hrs. Each calcination temperature was analyzed for FTIR (see section 3.4.6) and XRD (see section 3.4.5).

The aqueous co-product (ACP) underwent analysis of total organic carbon (TOC) and total nitrogen (TN). The TOC and TN were simultaneously measured by Torch TOC/TN analyzer. The measured volume of ACP and corresponding TOC were used for determining the afdw% yield. Any gasses that were formed during HTL were not analyzed and the yield was determined by a difference and/or using the ideal gas law assuming all CO_2, headspace volume,

and recorded post-reaction temperature and pressure, similar to algae lot# 2011. Post analysis of the elemental balance for carbon, hydrogen, nitrogen, and phosphorus for the feedstock and products were performed. The equations used for determining afdw% product yields are as followed:

$$Biocrude\ yield\ = \frac{wt_{biocrude}\,(1-\%DCM)}{algae_{afdw}} * 100 \quad (3.5)$$

$$Solids\ yield = \frac{wt_{solids}(1-\%ash_{solids})}{algae_{afdw}} * 100 \quad (3.6)$$

$$ACP\ yield = \frac{vol_{ACP} * TOC}{algae_{afdw} * \%\ carbon_{afdw}} * 100 \quad (3.7)$$

$$Gas\ yield = 100 - (3.5) - (3.6) - (3.7) \quad (3.8)$$

Where, $algae_{afdw}$ is the weight of algae used in the reactor minus the amount of moisture and ash determined by TGA, $wt_{biocrude}$ is the measured weight after distillation, %DCM is the fraction of solvent remaining found with SimDist, wt_{solids} is the measured weight of the solids fraction after gravity filtration, $\%ash_{solids}$ is the ash content of the solid product measured from TGA, vol_{ACP} is the measured volume of the ACP after vacuum filtration, TOC is the measured concentration of organic carbon in the ACP, and % $carbon_{afdw}$ is the amount of carbon in the algae normalized to the organic fraction of biomass.

3.4 Product Characterizations

3.4.1 Proximate Analysis

The solid product from algae lot# 2011 was not specifically evaluated for proximate analysis. The solids product from algae lot# 2013 was evaluated for proximate analysis in the same manner as the algae biomass of the corresponding algae lot# 2013 (see section 3.2.1).

3.4.2 Ultimate analysis

The ultimate analysis for both the biocrude and solid product of each algae lot was determined in the same manner as its respective algae biomass (see section 3.2.2).

3.4.3 Gas Chromatography-Mass Spectroscopy (GC-MS)

Algae lot# 2011:

GC-MS analysis of biocrude produced from algae lot# 2011 was performed using an Agilent 6890 Series GC-FID System with 5973 Network Mass Selective Detector equipped with a HP-5MS column (5% Phenyl Methyl Siloxane mobile phase; 30.0 m length, 250 µm diameter, 0.25 µm thickness). The method used an injection volume of 1.0 µL with a split ratio of 20:1, initial temp of 40 °C, ramp of 8 °C min^{-1} to 250 °C, holding for 5 min followed by a 20 °C min^{-1} ramp to 300 °C, holding for 1 min. Samples were prepared for the GC-MS analysis in two ways: 1) a derivatized sample of concentrated biocrude and 2) a non-derivatized sample of dilute biocrude in the decane solvent. The derivatized sample was prepared using 10.0 mg of concentrated biocrude, weighed in a GC vial, with 100 µL MSTFA (n-Methyl-n-(trimethylsilyl)trifluoroacetamide; derivatizing agent supplied by Agilent) and 100 µL pyridine (HPLC grade 99.5+%, Alfa Aesar) added and diluted with 800 µL n-heptane (99+%, Sigma).

Analysis of the biocrude in the concentrated derivatized sample revealed that residual decane was present, even though the oil had been dried until a consistent weight was reached. A 5-point (in triplicate) calibration curve was produced using known masses of decane in chloroform [high-performance liquid chromatography (HPLC); Fisher] to quantify residual decane in the concentrated biocrude and control experiment. The calibration curve had an R^2 value of 0.988. Four points of the calibration curve was obtained by creating a stock solution of 3.84 mg (5.0 µL) of decane diluted to 1 mL in chloroform and performing subsequent serial dilutions. The serial dilutions used 10, 20, 30, and 40 µL of stock solution and diluting to 1 mL again with chloroform. The fifth point used 1.0 µL of decane (0.72 mg) and 99.0 µL of chloroform.

Algae lot# 2013:

GC-MS analysis of the biocrude produced from algae lot# 2013 was performed using an Agilent 6890 Series GC−FID system with a 5973 network mass selective detector equipped with a Varian CP8956 column (5% phenyl methyl siloxane mobile phase; 30.0 m length; 320 µm diameter; and 0.50 µm thickness). The method used an injection volume of 1.0 µL with a split ratio of 1:1, an initial temperature of 40 °C with a holding time of 15 min, ramp of 10 °C min^{-1} to 100 °C, holding for 1 min, followed by a 1 °C min^{-1} ramp to 200 °C, with 15 min holds at 150 °C and 200 °C, followed by a 5 °C min^{-1} ramp to 270 °C, and final hold for 5 min. Samples were prepared for the GC-MS analysis in two ways: 1) 10.0 mg of biocrude in 1.0 mL of DCM and 2) 10.0 mg of biocrude derivatized with MSTFA (n-methyl-n-(trimethylsilyl)trifluoroacetamide; Agilent). The derivatized sample was prepared using 10.0 mg of biocrude, weighed in a GC vial, with 100.0 µL of MSTFA and 100.0 µL of pyridine [high-performance liquid chromatography

(HPLC) grade, 99.5+%, Alfa Aesar] added, and diluted with 800.0 μL of n-heptane (99+%, Sigma).

3.4.4 Simulated Distillation (SimDist)

SimDist was performed on the biocrude produced from algae lot# 2013 by thermogravimetric analysis (TGA) on a TA Instruments SDT 600. The method used was created to obtain accurate values of residual solvent (DCM) content in the biocrude after removal by distillation (see section 3.3.1). The method performed is as followed: Under a 10 mL min^{-1} flow of nitrogen gas a sample of biocrude (5-10 mg) was heated at a rate of 10 °C min^{-1} until 35 °C, where it entered a stepwise function (described in section 3.2.1) until 45 °C, to determine the precise amount of DCM in the biocrude same. The method then reverts back to a 10 °C min^{-1} until 800 °C. Determination of each distillate fraction within the sample followed the following equations, where wt%S is the weight percent of the sample.

Wt % DCM:	100 – wt%S [at the end of the step-wise]
Heavy Naphtha:	wt%S [at the end of the step-wise] – wt%S [at 193 °C]
Kerosene:	wt%S [at 193 °C] - wt%S [at 271 °C]
Gas Oil:	wt%S [at 271 °C] - wt%S [at 343 °C]
Vacuum Gas Oil:	wt%S [at 343 °C] - wt%S [at 538 °C]
Vacuum Gas Residual:	wt%S [at 538 °C] - wt%S [at 800 °C]
Ash:	wt%S remaining after 800 °C

3.4.5 X-ray Diffraction (XRD)

XRD patterns of the algae lot# 2013 combustion ash (see section 3.2.2), HTL solid product from algae lot# 2013, including each of its calcination temperatures (see section 3.3.1) were collected using monochromated CuKα radiation (λ= 1.54178 Å) on a Bruker Proteum Diffraction System equipped with Helios multilayer optics, an APEX II CCD detector and a Bruker MicroStar microfocus rotating anode x-ray source operating at 45 kV and 60 mA. Sample preparation included mixing powder with Paratone N oil and placing it in a <0.5 mm nylon loop mounted on a goniometer head. A Bruker Apex2 V2010.3-0 software package was used to collect and merge three, 60 sec. 180° φ-scans with the detector at 2θ = 30º, 60º and 90º using a sample-to-detector distance of 50.0 mm. The raw data was processed with Bruker EVA powder diffraction software.

3.4.6 Fourier-Transform Inferred Spectroscopy (FTIR)

FTIR spectrums of the algae lot# 2013 combustion ash (see section 3.2.2) and HTL solid product from algae lot# 2013, including each of its calcination temperatures (see section 3.3.1), were collected on a Varian 600 series FTIR equipped with a GladiATR^{TM} (PIKE Technologies) at a constant temperature of 105 °C. Absorbance spectra were averaged over 254 scans, collected from 4000 to 500 cm^{-1} with resolution and sensitivity of 4 cm^{-1} and 8 cm^{-1}, respectively.

3.4.7 Scanning Electron Microscopy -Energy Dispersive X-ray Spectroscopy (SEM-EDS) and Transmission Electron Microscopy (TEM)

All imaging of algae lot# 2013 solid products were performed by the University of Kansas Microscopy and Analytical Imaging (MAI) Laboratory, on a Carl Zeiss Leo 1550 field

emission scanning electron microscope (High Vacuum with a Schottky field emitter Operating Voltages from 200 V to 30kV) and a FEI Tecnai F20 XT transmission electron microscope (200kV electron source- Schottky field emitter, with high tension values of 20, 40, 80, 120, 160, and 200 kV).

3.4.8 Cell Culturing and Live/Dead Assay

Tissue-culture treated 24-well plates were coated, via aqueous suspension, with HTL solid product calcined at 600 °C. The plates were dried at 42 °C overnight and subsequently sterilized with ethylene oxide. Human umbilical cord Wharton's jelly cells (hWJCs) were trypsinized with 0.05% trypsin and seeded on plates at 6 $x10^4 \pm 2$ $x10^4$ hWJCs per well. hWJCs were cultured with Dulbecco's Minimal Essential Medium (DMEM) suspensions with 10% mesenchymal stem cell qualified fetal bovine serum (FBS) and 1% penicillin/streptomycin at 37^{o}C with 5% CO_2. hWJCs were isolated from Wharton's jelly of a human umbilical cord (#157) obtained from Lawrence Memorial Hospital (LMH) (LMH IRB approval #LMH 08-2). The umbilical cord came from a male born at full term under normal conditions. Growth medium was changed every 2 days. After 10 days, a viability assay was performed using LIVE/DEAD® Viability/Cytotoxicity Kit (Molecular Probes® LIVE/DEAD assay; from Invitrogen) and analyzed through fluorescence microscopy (Zeiss AX10). Images were processed using ZEN lite 2012 (blue edition) software.

3.5 References

1. Sturm, B. S. M.; Lamer, S. L., An energy evaluation of coupling nutrient removal from wastewater with algal biomass production. *Applied Energy* **2011,** *88*, (10), 3499-3506.

2. Sturm, B. S. M.; Peltier, E.; Smith, V.; deNoyelles, F., Controls of microalgal biomass and lipid production in municipal wastewater-fed bioreactors. *Environmental Progress & Sustainable Energy* **2012,** *31*, (1), 10-16.
3. Huang, H.; Yuan, X.; Zeng, G.; Zhu, H.; Li, H.; Liu, Z.; Jiang, H.; Leng, L.; Bi, W., Quantitative evaluation of heavy metals' pollution hazards in liquefaction residues of sewage sludge. *Bioresource Technology* **2011,** *102*, (22), 10346-10351.
4. Phichai, K.; Pragrobpondee, P.; Khumpart, T.; Hirunpraditkoon, S., Prediction Heating Values of Lignocellulosics from Biomass Characteristics.

4 Demonstrating Sustainability through Wastewater-Cultivated Algae

The purpose of algae lot# 2011 was to demonstrate the feasibility of a sustainable cultivation strategy [algae cultivated with effluent from an operating wastewater treatment plant (WWTP) as sole provider of both water and nutrients] integrated to an algae-to-biocrude process to produce renewable fuels and chemicals. The work presented in this chapter contains data collected from both a mixed-culture microalgae (see Table 3.1), cited in *Energy & Fuels* (2013) and previously presented data (American Institute of Chemical Engineers 2012 Annual Meeting) on a species of macroalgae (*Cladophora sp*.) which were co-harvested from the same growth ponds and will be commonly referred to as simply micro- and macro- algae, respectively, throughout the entirety of this chapter. This work (at the time of publication) represents the first of its kind to incorporate the hydrothermal liquefaction of algal biomass cultivated at an operating wastewater treatment facility. The biomass was cultivated at the pilot-scale using wastewater effluent as the sole provider of both water and nutrients. In addition, the data also represented the first to perform liquefaction on a mixed species algae culture. The main hypothesis was that using the sustainable strategy of wastewater cultivation would still provide comparable biocrude yields to those found in the literature (see section 2.2) and be a viable option for both advanced wastewater treatment and a renewable source of crude oil production, regardless of minimal lipid accumulation within the algae cells.

4.1 Algae Growth and Characterization

The average water quality and nutrient concentrations in the wastewater effluent feed and algal ponds can be found in Table 4-1, producing average biomass production rate[1] of 12 g m^{-2} day^{-1}. The average TN concentration of the wastewater effluent feed was 29.3 ± 4.8 mg L^{-1} and the average TP concentration was 2.65 ± 0.10 mg L^{-1}. During operation of the pond reactors in the previous year (2010), the average TN of the wastewater effluent was 19.5 ± 4.5 mg L^{-1} and the average TP was 3.21 ± 0.93 mg L^{-1}.[1] The measured concentrations over these two periods of operation are similar to the textbook TN concentration for wastewater effluent (20 mg L^{-1}), while the TP concentrations are slightly lower than the textbook TP concentration (10 mg L^{-1}).[2] Similar to the majority of WWTPs in the United States, the Lawrence WWTP does not perform biological nutrient removal (no phosphorus removal or denitrification). Only 206 of the more than 12,000 municipal WWTPs in the country reported use of denitrification or phosphorus removal technologies in the EPA 2008 Clean Watersheds Needs Survey.[3] Thus, the Lawrence WWTP effluent is representative of average municipal wastewater effluent characteristics in the United States.

Table 4-1. Average water quality of algal growth tanks at Lawrence WWTP.

Water quality parameter	Average measured value		Analysis method
	Wastewater Effluent Feed	Growth Ponds	
Total nitrogen (TN; mg L^{-1})	29.3 ± 4.8	27.0 ± 4.9	Standard Method 4500-N C[a]
Total dissolved nitrogen (TDN; mg L^{-1})	28.9 ± 5.2	22.4 ± 5.8	Standard Method 4500-N C[a]
Total phosphorus (TP; mg L^{-1})	2.65 ± 0.10	3.41 ± 0.67	Standard Method 4500-P E[a]
Total dissolved phosphorus (TDP; mg L^{-1})	2.52 ± 0.12	2.75 ± 1.1	Standard Method 4500-P E[a]
Total suspended solids (TSS; mg L^{-1})	13.3 ± 7.5	85.5 ± 22	Standard Method 2540 D[a]
pH	6.89 ± 0.31	7.44 ± 0.87	Field meter[b]
Temperature (°C)	25.7 ± 0.65	28.1 ± 2.2	Field meter[b]
Dissolved oxygen (DO; mg L^{-1})	2.71 ± 2.0	7.45 ± 0.51	Field meter[b]

[a]Standard methods can be found in Eaton et al.[4]
[b]YSI 556, Yello Springs, OH

The wastewater-cultured algae had high intercellular ash (non-combustible material) content of 29.0 dw% and 24.4 dw% for micro- and macro-algae, respectively. Compared to other reports of monoculture microalgae with ash contents as low as 5% and up to 25%.[5, 6] The majority, ~70%, of this non-combustible material is calcium and silica and calcium for the microalgae where potassium and calcium dominate in the macroalgae. These levels are directly related to the municipal wastewater effluent growth media. The high levels of silica can be ascribed to the presence of diatoms as confirmed by the species listed in Table 3-1. The high calcium is attributed to the municipal water source having an average water hardness of 40-120

mg L^{-1} as $CaCO_3$, with calcium concentrations of 24-43 mg L^{-1}.[7] High ash content is also normally found in marine macroalgae due to high levels of inorganics which incorporate into their cell wall.[8] Because the algae produced for this study had a high inorganic composition, the product yields were subsequently based on an ash free dry weight (afdw%) basis to understand the degree of organic conversion.

The organic and inorganic elemental analysis of the algae can be found in Table 4-2. The measured carbon content of the microalgae was 34.7 dw%, similar to other wastewater-cultivated algae (30-37 dw%)[9], or 48.9 afdw%, which is lower than 51.3-57.8 afdw% of commercially grown microalgae reported in the literature.[6] Since significant amount of the HTL studies reported in the literature use algae provided by companies, it is difficult to directly compare algal growth conditions between studies. Adding CO_2 to the algal tanks may increase the carbon content of microalgae, but this was not performed in the wastewater pilot. Although the algae have lower carbon content, it has a high oxygen content of 37.5 afdw%. This oxygen content is 5% to 15% higher than what has been reported for microalgae used in previous HTL studies.[5, 6, 8, 10-16] The combination of the low carbon and the high oxygen content directly affects the HHV of the algal biomass, which was measured at 15.1 and 14.1 MJ kg^{-1} for micro- and macro- algae, respectively. Ross et al.[5] reported HHV for *Spirulina sp.* and *Chlorella vulgaris* to be 21.2 and 23.2 MJ kg^{-1}, respectively. However, the carbon content for both species was near 54 afdw%, while the oxygen content was closer to 27 afdw%. These results indicate that microalgae grown using municipal wastewater effluent are unique compared to fertilized monoculture algae that are typically studied for HTL processing.

Table 4-2. Algae lot #2011 characterization data.

Algae Characteristics		
	Micro	Macro
C	48.9	45.5
H	7.1	6.8
N	8.4	5.9
O	37.5	41.8
Lipid	14.0	13.0
HHV (MJ kg^{-1})	15.1	14.1
Ash (wt%)	29.0	24.4
Moisture (wt%)	4.7	4.8

Inorganic Composition*		
	Micro	Macro
Si	35.6	8.3
Ca	34.0	32.0
P	16.4	8.7
S	5.0	9.2
K	2.7	28.0
Mg	1.7	1.6
Fe	1.7	0.4
Al	0.8	-
Na	0.7	1.2
Cl	0.7	9.8
others	0.7	0.8

*Normalized to ash content

4.2 Algae lot# 2011 HTL Product Yields

Results comparing the initial lipid content, control, and biocrude produced through HTL of the microalgae are found in Table 4-3. Good agreement was found between the Bligh-Dyer method and the solvent extraction/oil recovery method used for the control experiment for the microalgae at 14.0 afdw% and 13.95 afdw%, respectively. Therefore, it is assumed the macroalgae would perform in the same manner, and no control for macroalgae was performed in order to complete duplicate HTL experiments, due to limited amount of biomass collected. HTL of cultivated microalgae yielded 45 afdw% biocrude, 31% more than the initial lipid content. This biocrude yield is on the high end compared to HTL studies on fertilized monoculture algae, typically reported from 19% to 46.5%, corresponding to yields 6% - 30% above the initial lipid content.[5, 6, 8, 10-12, 14-18]

Table 4-3. Oil Yields from microalgae.

Oil Yields (afdw%)		
Lipid Content[a]	Control	Biocrude
14.0	13.95	45

[a]Measured by Bligh-Dyer method[19]

The product yields from HTL of both micro- and macro-algae are shown in Figure 4-1 on an afdw% basis. The main product was the biocrude at 45 ± 5%, followed by 21 ± 9% solid product, 18 ± 5% aqueous product, and 16 ± 8% gas. The gas is reported by difference; however, it was also verified using an ideal gal law calculation, assuming all the gas is CO_2 with equilibrated temperature (18 °C), pressure (4 psig), and a reactor head space volume of 400 mL. The macroalgae yielded similar afdw% results with the average of two experiments resulting in 43%, 22%, 15%, and 20% for biocrude, solids, aqueous, and gas, respectively. The two experiments performing HTL on the macroalgae had similar spread as the microalgae and is believed would have obtained very similar standard deviations had there been enough biomass to perform three reactions.

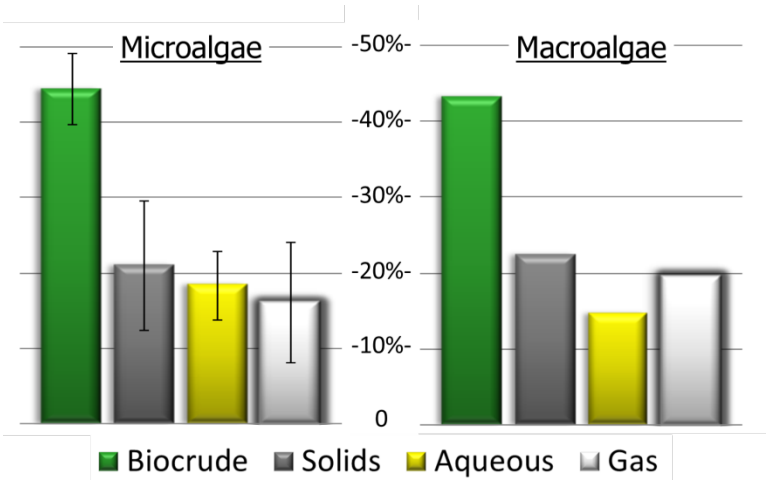

Figure 4-1. HTL yields from algae lot# 2011; reported on an afdw%. Error bars indicate standard deviations, which could not be calculated for macroalgae due to limited available biomass and restricting HTL experiments to two.

4.3 Algae lot# 2011 Biocrude Molecular Profile

Detailed chromatogram(s) of the biocrude obtained from the microalgae are shown in Figure 4-2. Peaks identified with the NIST library at a 90% confidence level and above are labeled and reported. A complete list of identified peaks, retention times, and structures are shown in Table 4-4. Many of these compounds are consistent with previous studies reporting the components of biocrude from HTL on monoculture algae.[5, 12] Two different sample preparations were employed for GC-MS analysis to allow for more complete compound identification. The first sample preparation was a derivatized sample of concentrated biocrude providing better separation and identification of functional groups; Figure 4-2a. Derivatizing with MSTFA alters compounds containing -OH, -NH, -SH by replacing the hydrogen atoms with $Si(CH_3)$ to give -X-$Si(CH_3)$, where X is either the oxygen, nitrogen, or sulfur atom. The second sample preparation, dilute biocrude in decane, was used to determine if any compounds were being lost during

drying/concentration; Figure 4-2b. Certain molecules were identified in the derivatized sample including hydrogen sulfide, methyl amine, phenols, and free fatty acids; overall the biocrude consisted of aliphatics, phenols, fatty acids, ketones, and indoles, including the presence of pyrrole, pyridine and phthalate. Both sample preparations indicate the presence of a phthalate, which is a common plasticizer, and was suspected to have been contamination from various centrifuge tubes and/or pipette tips. However, GC-MS analysis of the solvent, in this case decane, exposed to all types of lab ware used indicated there was no phthalate stripped from the plastics involved.

(a)

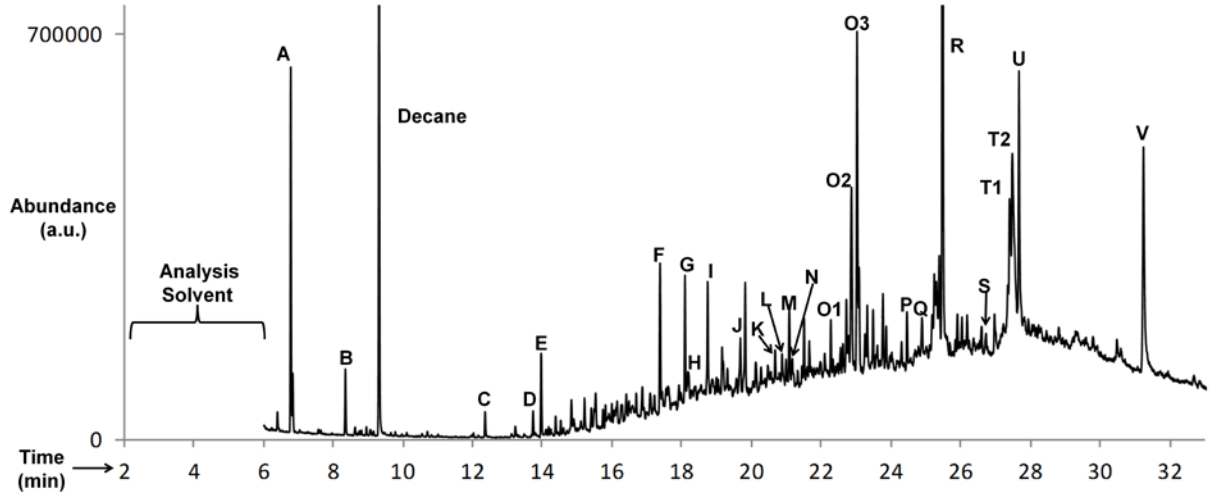

(b)

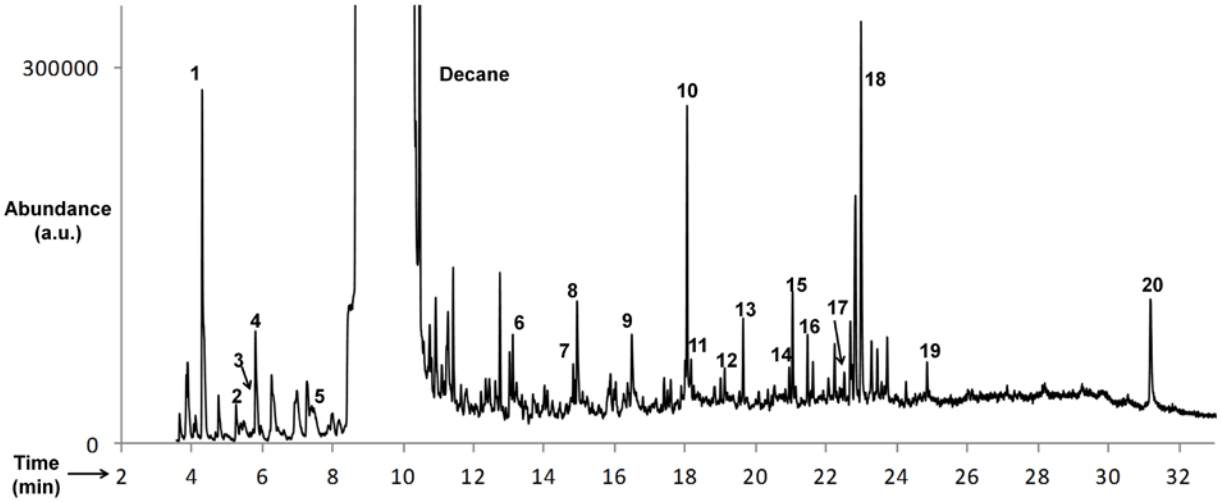

Figure 4-2. GC-MS chromatograms for biocrude produced from microalgae from samples (a) concentrated and derizatized with MSTFA and (b) dilute biocrude in decane obtained as is from extraction procedure.

Table 4-4. Identified compounds using GC-MS of (a) concentrated derivatized biocrude and (b) biocrude diluted in decane straight from the reactor.

(a)

Peaks as Labeled in Figure 4-2a	Retention Time (min)	Compound	Structure
A	6.77	Methyl amine	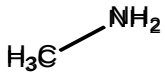
B	8.33	Hydrogen sulfide	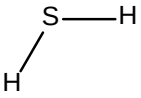
C	12.34	Methyl phenol	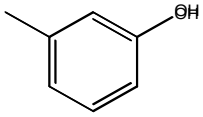
D	13.72	2,6-Dimethyl phenol	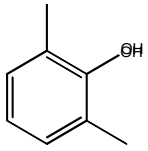
E	13.95	3,5-Dimethyl phenol	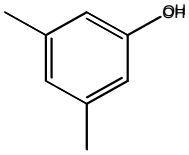
F	17.36	Indole	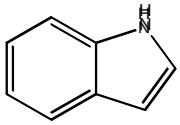
G	18.07	1-Pentadecene	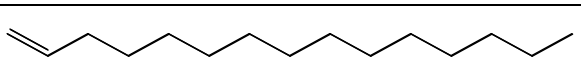

H	18.17	1H-Indole, 2,5-dimethyl-	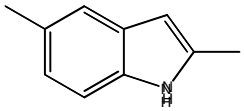
I	18.72	1H-Indole, 3-methyl-	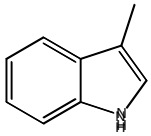
J	19.66	Hexadecane	
K	20.45	Dodecanoic acid	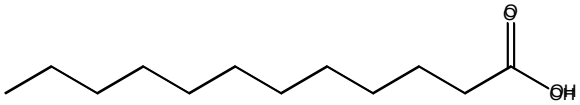
L	20.66	1,7-Trimethylene-2,3-dimethylindole	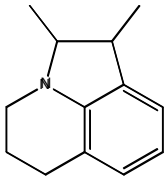
M	20.97	1-Heptadecene	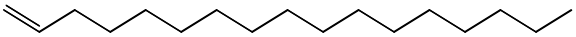
N	21.07	Heptadecane	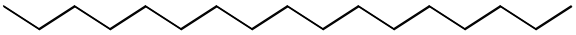
O1	22.26	2-Phytene Isomer	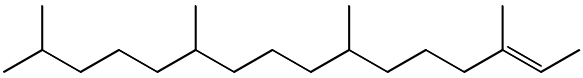
O2	22.85		
O3	23.01		
P	24.44	Hexadecanol	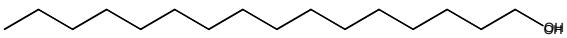
Q	24.87	Eicosane	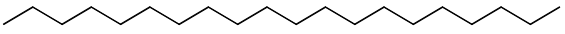

R	25.46	Palmitic acid	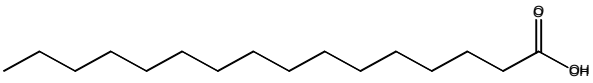
S	26.58	Heptadecanoic acid	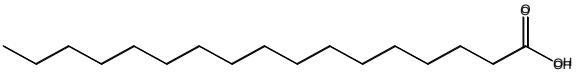
T1	27.38	Oleic acid	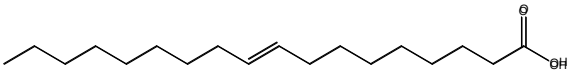
T2	27.46		
U	27.65	Stearic acid	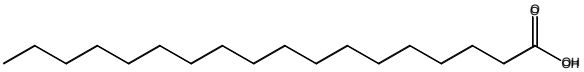
V	31.22	Bis(2-ethylhexyl) phthalate	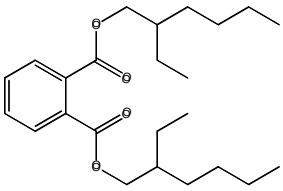

(b)

Peaks as Labeled in Figure 4-2b	Retention Time (min)	Compound	Structure
1	4.32	Toluene	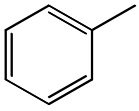
2	5.28	1-Ethyl-1H-Pyrrole	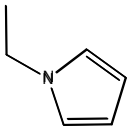
3	5.41	2-Methyl pyridine	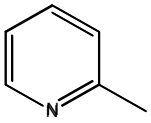
4	5.83	2-Methyl cyclopentanone	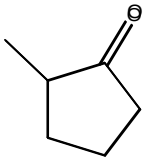
5	7.29	2-Methyl-2-cyclopenten-1-one	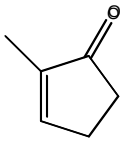
6	13.13	2-Decanone	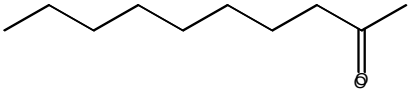
7	14.84	1-Tridecene	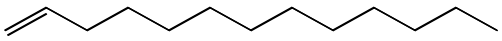
8	14.96	5H-1-pyridine	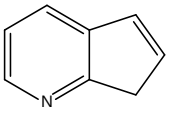

9	16.50	5-Methyl-1H-Indole	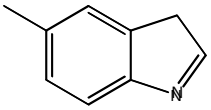
10	18.07	1-Pentadecene	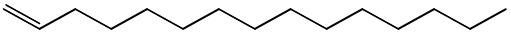
11	18.18	Pentadecane	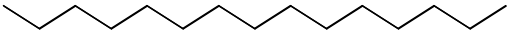
12	19.02	Cyclododecane	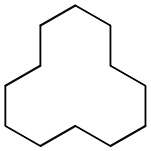
13	19.66	Hexadecane	
14	20.97	1-Heptadecene	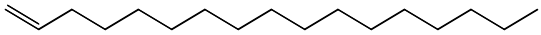
15	21.07	Heptadecane	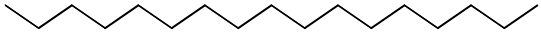
16	21.49	1-Nonadecene	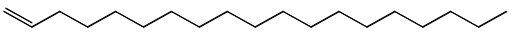
17	22.46	4-Methyl-dodec-3-en-1-ol	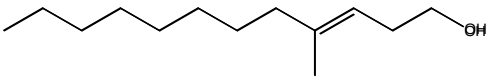
18	23.00	2-Phytene Isomer	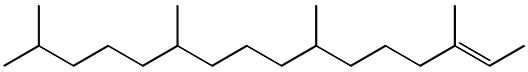
19	24.88	Eicosane	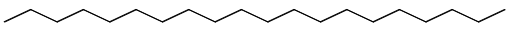
20	31.22	Bis(2-ethylhexyl) phthalate	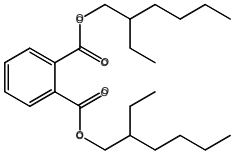

Comparison of the chromatograms indicates that compounds evaporated with the decane solvent. There are fewer peaks eluting under 15 minutes in the concentrated than the dilute biocrude. Specifically, 2-Methyl-2-cyclopenten-1-one (7.29 min), 2-Decanone (13.13 min), 1-Tridecene (14.84 min), and 5H-1-pyridine (14.96 min) are absent in Figure 4-2a. These compounds would not be altered from derivatization, and if present, would elute at the same time in Figure 4-2a. Other compounds were identified in the dilute biocrude but not the concentrated biocrude. These are listed as followed with their corresponding identification confidence level: cyclopentanone (65%), ethylbenzene (87%), p-xylene (76%), styrene (64%), dimethyl pyrazine (86%), dimethyl pyridine (68%), and dodecane (86%). It is likely that these compounds have been lost during solvent evaporation as has been previously suggested by Brown et al.[11] The macroalgae was analyzed using similar sample preparations. The chromatogram from the dilute (in decane) non-derivatized biocrude produced from macroalgae is shown in Figure 4-3, with corresponding identification of compounds in Table 4-5. Significant differences between the biocrude from the micro- and macro-algae are the abundances of lighter compounds present in the macro- biocrude produced, including derivatives of propane, butane, and pentanes. The macro- biocrude also lacks heavier compounds found within the micro- biocrude including variances among the fatty acid content. Comparison of the concentrated derivatized biocrude from each respective algae biomass is shown in Figure 4-4. Biocrude from the micro- algae mainly resulted in $C_{16\text{-}18}$ fatty acids while the macro- biocrude contained a wider range of $C_{14\text{-}24}$.

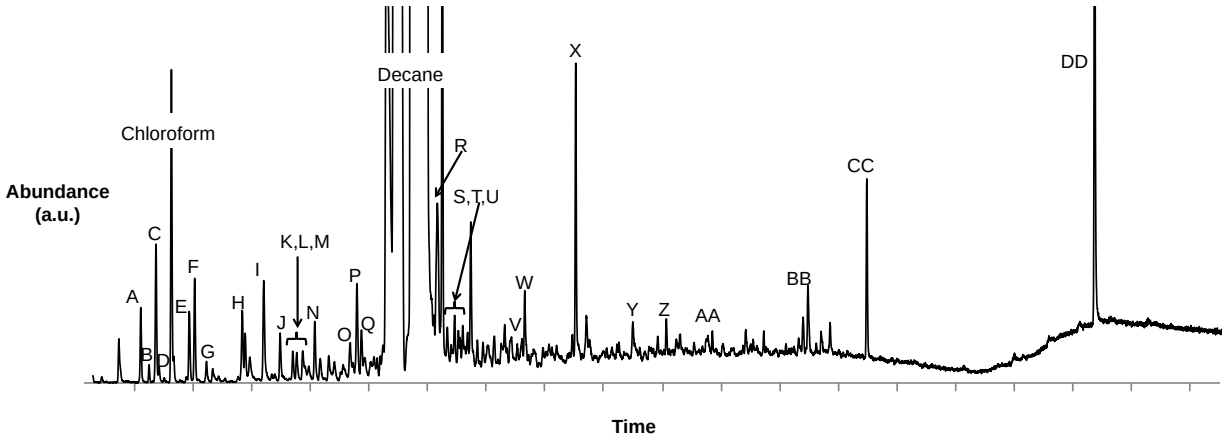

Figure 4-3. GC-MS chromatogram of dilute (in decane) biocrude from macro lot# 2011.

Table 4-5. Compound identification of biocrude from macro lot# 2011.

Compound Identification from Figure 4-3			
A	Propanal, 2-methyl-	P	Cyclopentanone, 2-methyl-
B	Pentane, 3-methyl-	Q	2-Cyclopenten-1-one, 2-methyl-
C	Hexane	R	Pyridine, 2-ethyl-5-methyl-
D	Furan, 2-methyl-	S	Cyclopentane, pentyl-
E	Butanal, 3-methyl-	T	Phenol, 3-methyl-
F	2-methyl butanal	U	Phenol, 4-methyl-
G	2-Pentanone	V	1H-Pyrrole, 2-ethyl-3,4,5-trimethyl-
H	1H-Pyrrole, 1-methyl-	W	Dodecane
I	Toluene	X	Tridecane
J	Cyclopentanone	Y	1H-Indole, 4-methyl-
K	1H-Pyrrole, 2-ethyl-	Z	1-Pentadecene
L	Pyridine, 2-methyl-	AA	Hexadecane
M	Pyrazine, methyl-	BB	2-Hexadecene, tetramethyl-
N	Cyclopentanone, 2-methyl-	CC	Eicosane
O	Styrene	DD	Bis(2-ethylhexyl) phthalate

(a)

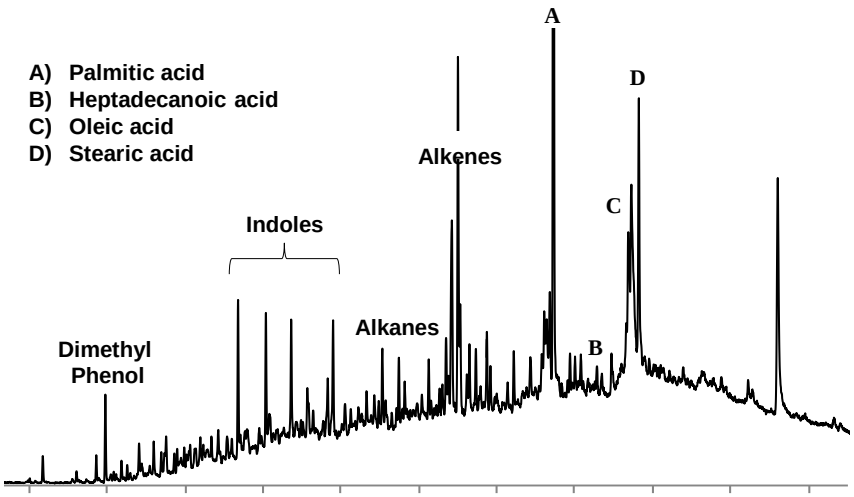

(b)

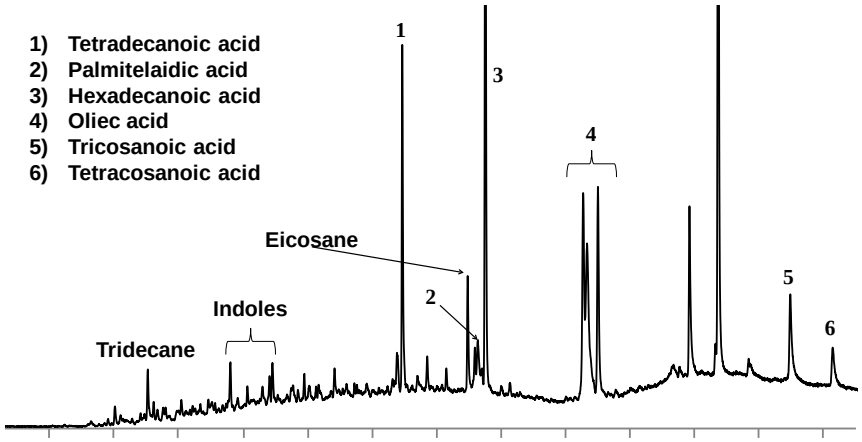

Figure 4-4. GC-MS of derivatized concentrated biocrude from (a) microalgae and (b) macroalgae.

These combined differences of molecular profiles provided varying viscosities, which were not directly measured, but are demonstrated in a simple pictograph of droplets of each biocrude placed on an elevated weigh tray, shown in Figure 4-5.

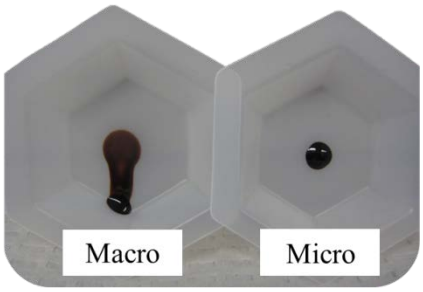

Figure 4-5. Effect of gravity and surface tension, demonstrating relative viscosity, on droplets of each biocrude produced.

4.4 Biocrude Energy and Heteroatom Content

Using the wastewater cultivation strategy and HTL conversion, a biocrude was obtained with similar properties to petroleum crude and significant benefits over biocrude produced from fertilized, monoculture microalgae. The elemental analysis of the biocrude is shown in Table 4-6. The carbon content of the micro- biocrude was 78.7 wt% compared to others reported in the literature ranging from 68-76 wt% carbon.[5, 6, 11, 12, 17, 18] The high carbon content is especially significant given the relatively low carbon content of the feedstock algae. The hydrogen content of biocrude was measured at 10.1 wt%, which is comparable to previous studies.[17] The heteroatom (N & O) content of biocrude is the major difference compared to petroleum crude (typically 0.1-2.0 wt% N and 0.1-1.5 wt% O)[10, 11, 20], and is important to analyze for upgrading

purposes. The micro- biocrude produced had a nitrogen content of 4.4 wt% and an oxygen content of 5.5 wt%. In contrast, the oxygen content is typically 10-30 wt%[21, 22] and 10-20 wt%[10,6] for pyrolysis-produced algal oils and HTL biocrude from fertilized-monoculture microalgae, respectively.

Table 4-6. Ultimate analysis and HHV of micro- and macro- biocrude and micro- solid product.

	Elemental Composition				
	C	H	N	O	HHV (MJ kg^{-1})
Micro-Biocrude (wt%)	78.7	10.1	4.4	5.5	39
Micro-Solids (dw%)	20.4	2.0	1.8	10.8	8-10
Macro-Biocrude (wt%)	76.9	9.6	4.8	7.4	42

When comparing the heteroatom content of biocrude produced in this study to most HTL studies (see Table 2-3), nitrogen is comparable while oxygen is lower, better resembling heavy petroleum crude.[17] One study has reported an oxygen content of HTL-produced biocrude near 5 wt%[17] for *Nannochloropsis sp.*, but a reaction temperature of 500 °C was used. This increase in temperature decreased oxygen but sacrificed hydrogen (7.1 wt%) and the overall biocrude yield (16 wt%). The micro- biocrude produced here had low oxygen content, did not sacrifice hydrogen, and maintained high organic conversion to biocrude. One other study which showed a

high carbon, low oxygen, and high hydrogen biocrude; Sapphire Energy reported HTL-produced biocrude (reaction temperature of 260 °C) from *Nannochloropsis sp*. with 77.7 wt%, 11.7 wt%, and 5.7 wt% for carbon, hydrogen, and oxygen, respectively.[23] However, a very different procedure was used for oil recovery (variable heating after reducing pH with H_3PO_4), and no information was provided on algal growth conditions or the elemental analysis of the feedstock algae, so a direct comparison is not possible. The macro- biocrude had slightly different heteroatom content compared to the micro- biocrude, even though they had been harvested from the same growth ponds. The macro- biocrude had slightly lower carbon and hydrogen, 76.9% and 9.6%, respectively, with higher nitrogen and oxygen, 4.8% and 7.4%, respectively.

As discussed in Chapter 2, the relationship between the H/C ratio and the O/C ratio, and the trade-off between maximizing H/C while minimizing O/C, can be seen in a van Krevelen diagram. Higher H/C atomic ratios and lower O/C atomic ratios indicate that the energy content of the substance (feedstock, crude, or fuel) is high with less need for extensive upgrading. The data collected with algae lot# 2011 has been applied to the van Krevelen diagram in Chapter 2 (Figure 2-2) and is shown in Figure 4-6. Both the micro- and macro- biocrude produced are both favorable (closest to petroleum crude) compared the majority of the literature values, and the O/C ratio for the micro- biocrude is the lowest (farthest left on the x-axis) while still maintaining a high H/C ratio, which suggests that the least amount of heteroatom upgrading would be needed for biocrude produced under comparable HTL conditions.

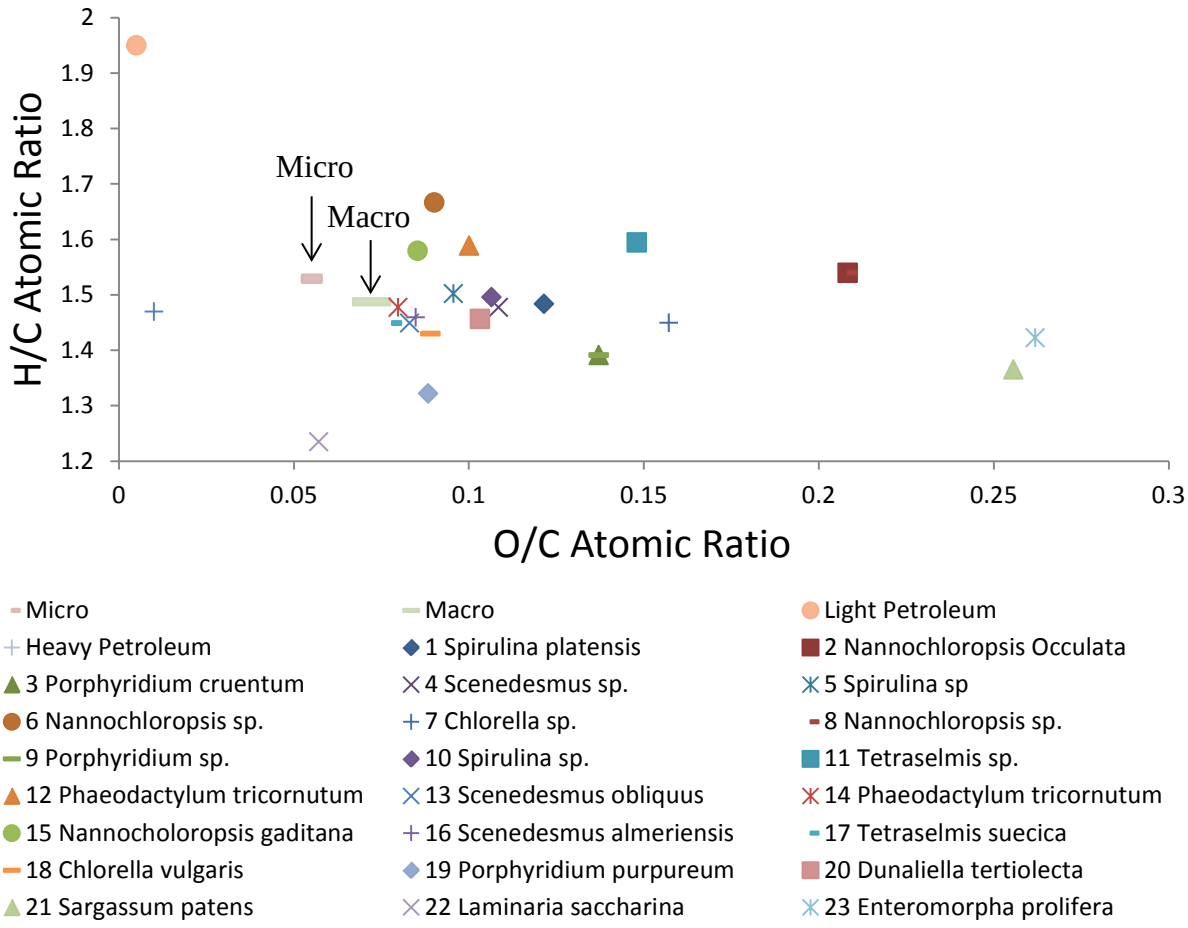

Figure 4-6. Van Krevelen diagram from Figure 2-2 including data from algae lot# 2011.

The measured HHV of the micro- and macro- biocrude was 39 and 42 MJ kg^{-1}, respectively, compared to the petroleum crude HHV of 41-43 MJ kg^{-1}. The large HHV of the micro- biocrude is attributed to the high C and H and low O contents of the biocrude. Interestingly, the even higher measured HHV of the macro- biocrude, with lower C & H and higher N & O content compared to the micro-, can be explained when re-evaluating the molecular profile described in the previous section. It could be expect that the macro- biocrude would have a higher octane

number based off the degree of branching associated with identified compounds within the as well as the increased number of lower boiling point molecules. This concludes that the macro-algae produced a biocrude containing a higher fraction of direct fuels but with higher heteroatom content, which would need to be removed, compared to biocrude produced from the micro-algae.

Both the micro- and macro- algae have favorable energy densities and heteroatom content, clearly depicted by the van Krevelen diagram in Figure 4-6. Previous studies on *Spirulina sp.* and *Chorella vulgaris* have shown that adding alkali catalysts to HTL reactors results in lower oxygen and larger HHV when compared to adding organic acids.[5] Furthermore, studies have shown that alkali catalysts are detrimental to oil formation when algae has a high starting initial lipid content, but are advantageous when algae is high in carbohydrates.[6] Based on the elemental distribution of the inorganic composition of the cultivated algae, alkali species are present during the HTL reaction. At the time of data collection for this demonstration study, it was unclear of the exact role of these alkali species; however the hypothesis was that catalyzed reactions were proceeding to reduce the overall oxygen content of the biocrude within the HTL reactor. Further findings (see Chapter 5 & 6) will indicate this hypothesis to be true and is discussed in detail within subsequent chapters. Thus, the higher inorganic fraction of wastewater-fed algae has found to be advantageous for producing a biocrude with lower oxygen and larger HHV.

4.5 HTL Co-Products

The HTL conversion of the cultivated microalgae resulted in an aqueous co-product (ACP) containing ~50% of the algae's cellular nitrogen with a fraction of the cellular

phosphorus. The concentrations of carbon (TOC), nitrogen (TN), and phosphorus (TP) in the ACP derived from the microalgae were measured at 4550 ± 460 mg L^{-1}, 1640 ± 250 mg L^{-1}, and 3.5 mg L^{-1}, respectively; the macroalgae derived ACP resulted in slightly lower compared to the micro- derived ACP with TOC and TN at 3130 and 1250 mg L^{-1}, respectively. It is speculated that the bulk of the algal phosphorus resides in the solid product. The macronutrient concentrations in the ACP compared to the wastewater effluent feed was 56:1 for TN and 1:1 for TP. The NRC report[24] has specifically listed the availability of N & P as a "high importance" concern for algal biofuel sustainability. Fortier and Sturm[25] have shown that wastewater treatment facilities alone would not supply adequate levels of nutrients to meet high demands of fuel consumption. The ability to capture N and P from HTL co-products and recycle them for algal cultivation would increase the potential of algal fuel production. Few studies to date have supplemented algal culture media with ACP from HTL processing. Jena et al.[26] reported an optimal recycle fraction of 0.2 vol% ACP diluted with deionized water achieving an algal growth rate of 0.035 g L^{-1} day^{-1} compared to a rate of 0.07 g L^{-1} day^{-1} for algae cultivated in BG 11 growth media. Zhou et al.[27] showed that recycling higher amounts of ACP from two HTL feedstocks (swine manure and *Spirulina sp.*) had inhibitory effects on algal growth. When diluting the ACP with F/2 medium, they determined that algal growth was inhibited when supplemented with greater than 5 vol% swine manure ACP and 1 vol% *Spirulina sp.* ACP. Previous studies on *Spirulina sp.* and *Chorella vulgaris* used TOC analysis to show that a significant amount of the organic products are water soluble.[5] Acetic acid, glycerol, and 3-pyridinol have been identified as the primary water soluble organics in the ACP produced during HTL of *Enteromorpha prolifera* macroalgae.[8] Depending on the organics identified, it may be

possible through separation to produce value-added organics and allow higher levels of the ACP to be recycled for algae growth. Overall, further research is necessary to determine the recycle potential and value of the ACP produced from HTL.

Another major co-product of HTL conversion is solid product. On a dry weight basis, 45.0 ± 5.9 dw% of biomass is retained in the form of solid product (from microalgae) due to high amounts of non-combustible intercellular material. Most of the solid product is comprised of the inorganic content of the algae shown in Table 4-2. The solid product was found to contain 35 wt% organic material, containing 20.4 dw% carbon. This is reported as a weighted average of the two fractions of solid product produced, shown in Figure 3-2, where the ultimate analysis differed by <2 wt% between fractions. The measured HHV of the solid product was 8-10 MJ kg^{-1}, depending on which fraction of solids were evaluated. Beyond burning the solid product for energy recovery, it could be used for soil amendments[28], absorbents[29], and catalysts.[30] Further research into the solid product produced from wastewater-cultivated algae has revealed exciting and encouraging results for applications into value-added products and is the main area of discussion of Chapter 5: Increasing Value-Added Product Streams and Chapter 6: Hydroxyapatite Synergies and its Potential Applications.

4.6 Conclusions

The described algal cultivation strategy (open pond, wastewater-fed, naturally inoculated mixed culture) and hydrothermal liquefaction conversion (whole, wet biomass to produce a drop-in crude replacement and co-products) were successfully demonstrated. Micro- and macro-algae cultivated in same growth ponds yields comparable results for individual product yields;

obtaining 45 and 43 afdw% biocrude yield for micro- and macro- algae, respectively. Significant differences were found within the biocrude properties in terms of heteroatom content, energy density, and molecular profile. Microalgae resulted in a biocrude with low oxygen content, 5.5 wt%, high amounts of straight chain aliphatics $>C_{16}$, and an energy density of 39 MJ kg^{-1}. Macroalgae derived biocrude had 7.4 wt% oxygen, large number of low boiling point compounds including branched aliphatics which resulted in a low visual viscosity and high energy density, 42 MJ kg^{-1}. Overall macro- derived biocrude potentially creates a higher fraction of direct fuel distillates but may require more heteroatom removal then compared to micro-derived biocrude.

The main hypothesis of the study was confirmed to be true; algae cultivated using treated wastewater (prior to discharge) would yield significant biocrude yields once exposed to subcritical water reaction media, resulting in 31% organic conversion above the solvent extractible lipid fraction. However, unexpected results showed a superior quality biocrude was produced with very large production of solid product compared to fertilized monoculture algae typically studied in the literature. This developed new hypotheses which speculated the formation of the solid product, particularly the inorganic content established from wastewater-cultivated algae, was contributing to the desirable properties biocrude and potentially leading to catalytic effects. These hypotheses drove further investigations into understanding both the composition of the solid product and what role it may be playing in reducing the oxygen content of the biocrude. The remainder of this dissertation describes the composition of the solid product, the effects of the solid product formation on the biocrude *in-situ*, and its applications as a value-added product within the scope of algal biofuels.

4.7 References

1. Sturm, B. S. M.; Lamer, S. L., An energy evaluation of coupling nutrient removal from wastewater with algal biomass production. *Applied Energy* **2011,** *88*, (10), 3499-3506.
2. National Research Council Committee on the Use of Treated Municipal Wastewater Effluents Sludge in the Production of Crops for Human Consumption, *Use of reclaimed water and sludge in food crop production*. National Academy Press: 1996.
3. United States Environmental Protection Agency (US EPA), Clean Watersheds Needs Survey 2008 Report to Congress. In US EPA, Office of Water Management: Washington, D.C., 2008.
4. Eaton, A. D.; Clesceri, L. S.; Rice, E. W.; Greenberg, A. E., *Standard methods for the examination of water & wastewater*. 21 ed.; American Public Health Association: 2005.
5. Ross, A. B.; Biller, P.; Kubacki, M. L.; Li, H.; Lea-Langton, A.; Jones, J. M., Hydrothermal processing of microalgae using alkali and organic acids. *Fuel* **2010,** *89*, (9), 2234-2243.
6. Biller, P.; Ross, A. B., Potential yields and properties of oil from the hydrothermal liquefaction of microalgae with different biochemical content. *Bioresource Technology* **2011,** *102*, (1), 215-225.
7. Huang, H.; Yuan, X.; Zeng, G.; Wang, J.; Li, H.; Zhou, C.; Pei, X.; You, Q.; Chen, L., Thermochemical liquefaction characteristics of microalgae in sub- and supercritical ethanol. *Fuel Processing Technology* **2011,** *92*, (1), 147-153.
8. Zhou, D.; Zhang, L.; Zhang, S.; Fu, H.; Chen, J., Hydrothermal Liquefaction of Macroalgae Enteromorpha prolifera to Bio-oil. *Energy & Fuels* **2010,** *24*, (7), 4054-4061.
9. Griffiths, E. W. Removal and Utilization of Wastewater Nutrients for Algae Biomass and Biofuels. Utah State University, 2009.
10. Jena, U.; Das, K. C.; Kastner, J. R., Effect of operating conditions of thermochemical liquefaction on biocrude production from Spirulina platensis. *Bioresource Technology* **2011,** *102*, (10), 6221-6229.
11. Brown, T. M.; Duan, P.; Savage, P. E., Hydrothermal Liquefaction and Gasification of Nannochloropsis sp. *Energy & Fuels* **2010,** *24*, (6), 3639-3646.
12. Valdez, P. J.; Dickinson, J. G.; Savage, P. E., Characterization of Product Fractions from Hydrothermal Liquefaction ofNannochloropsissp. and the Influence of Solvents. *Energy & Fuels* **2011,** *25*, (7), 3235-3243.
13. Demirbas, M. F., Biofuels from algae for sustainable development. *Applied Energy* **2011,** *88*, (10), 3473-3480.
14. Anastasakis, K.; Ross, A. B., Hydrothermal liquefaction of the brown macro-alga Laminaria Saccharina: Effect of reaction conditions on product distribution and composition. *Bioresource Technology* **2011,** *102*, (7), 4876-4883.
15. Shuping, Z.; Yulong, W.; Mingde, Y.; Kaleem, I.; Chun, L.; Tong, J., Production and characterization of bio-oil from hydrothermal liquefaction of microalgae Dunaliella tertiolecta cake. *Energy* **2010,** *35*, (12), 5406-5411.

16. Minowa, T.; Yokoyama, S.-y.; Kishimoto, M.; Okakura, T., Oil production from algal cells of Dunaliella tertiolecta by direct thermochemical liquefaction. *Fuel* **1995,** *74*, (12), 1735-1738.
17. Garcia Alba, L.; Torri, C.; Samorì, C.; van der Spek, J.; Fabbri, D.; Kersten, S. R. A.; Brilman, D. W. F., Hydrothermal Treatment (HTT) of Microalgae: Evaluation of the Process As Conversion Method in an Algae Biorefinery Concept. *Energy & Fuels* **2011**, 111201165948002.
18. Vardon, D. R.; Sharma, B. K.; Scott, J.; Yu, G.; Wang, Z.; Schideman, L.; Zhang, Y.; Strathmann, T. J., Chemical properties of biocrude oil from the hydrothermal liquefaction of Spirulina algae, swine manure, and digested anaerobic sludge. *Bioresource Technology* **2011,** *102*, (17), 8295-8303.
19. Bligh, E. G.; Dyer, W. J., A rapid method of total lipid extraction and purification. *Canadian Journal of Biochemistry and Physiology* **1959,** *37*, (8), 911-917.
20. Matar, S.; Hatch, L. F., *Chemistry of petrochemical processes*. Gulf Professional Publishing: 2001.
21. Pan, P.; Hu, C.; Yang, W.; Li, Y.; Dong, L.; Zhu, L.; Tong, D.; Qing, R.; Fan, Y., The direct pyrolysis and catalytic pyrolysis of Nannochloropsis sp. residue for renewable bio-oils. *Bioresource Technology* **2010,** *101*, (12), 4593-4599.
22. Vardon, D. R.; Sharma, B. K.; Blazina, G. V.; Rajagopalan, K.; Strathmann, T. J., Thermochemical conversion of raw and defatted algal biomass via hydrothermal liquefaction and slow pyrolysis. *Bioresource Technology* **2012,** *109*, 178-187.
23. Roussis, S. G.; Cranford, R.; Sytkovetskiy, N., Thermal Treatment of Crude Algae Oils Prepared Under Hydrothermal Extraction Conditions. *Energy & Fuels* **2012,** *26*, (8), 5294-5299.
24. Council, N. R., Sustainable Development of Algal Biofuels in the United States. In Academies, N. R. C. o. t. N., Ed. National Academy Press: Committee on the Sustainable Development of Algal Biofuels, 2012.
25. Fortier, M.-O. P.; Sturm, B. S. M., Geographic Analysis of the Feasibility of Collocating Algal Biomass Production with Wastewater Treatment Plants. *Environmental Science & Technology* **2012,** *46*, (20), 11426-11434.
26. Jena, U.; Vaidyanathan, N.; Chinnasamy, S.; Das, K. C., Evaluation of microalgae cultivation using recovered aqueous co-product from thermochemical liquefaction of algal biomass. *Bioresource Technology* **2011,** *102*, (3), 3380-3387.
27. Zhou, Y.; Schideman, L.; Zhang, Y.; Yu, G.; Wang, Z.; Pham, M., Resolving Bottlenecks in Current Algal Wastewater Treatment Paradigms: A Synergistic combination of Low-Lipid algal Wastewater Treatment and Hydrothermal Liquefaction for Large-Scale Biofuels Production. *Energy and Water* **2011**, 347-361.
28. Singh, B.; Singh, B. P.; Cowie, A. L., Characterisation and evaluation of biochars for their application as a soil amendment. *Australian Journal of Soil Research* **2010,** *48*, 516-525.
29. Park, J. H.; Lamb, D.; Paneerselvam, P.; Choppala, G.; Bolan, N.; Chung, J.-W., Role of organic amendments on enhanced bioremediation of heavy metal(loid) contaminated soils. *Journal of Hazardous Materials* **2011,** *185*, (2-3), 549-574.

30. Muradov, N.; Fidalgo, B.; Gujar, A. C.; Garceau, N.; T-Raissi, A., Production and characterization of Lemna minor bio-char and its catalytic application for biogas reforming. *Biomass and Bioenergy* **2012,** *42*, 123-131.

5 Increasing Value-Added Product Streams

The data presented in this chapter was obtained entirely from algae lot# 2013. The main goals of the studies performed for algae lot# 2013 were to answer hypotheses formulated when evaluating the results from algae lot# 2011 described in Chapter 4. The main hypotheses, post evaluation of algae lot# 2011, was that the majority of the phosphorus resided in the solid product and that the inorganics were paying significant (catalytic) role in producing higher quality biocrude, particularly reducing the oxygen content. Therefore, it was imperative to understand and determine the composition of the solid product. In order to do so, it was hypothesized that thorough understanding of the nutrient uptake by the algal biomass from wastewater effluent and the fate of those nutrients post liquefaction would provide the basic fundamentals of which elements are retained in the solid product. Once the elemental composition of the solid product was known, exploratory characterization could then be guided to determine both the structure of the solid product and functionality within the HTL reactor. This chapter is subcategorized into three main bodies; 1) the characterization of algae lot# 2013 and the bulk HTL yields, 2) nutrient mining effects of wastewater-cultivated algae and HTL process, and 3) the novel discovery of higher-value products co-produced during the HTL of wastewater-cultivated algae. The majority of the work presented in this chapter is published in *Green Chemistry* (2015), **17**, 2560.

5.1 Algae lot# 2013 Characterization and HTL Bulk Yields

The algae biomass cultivated and collected obtained similar characteristics to that of algae lot# 2011 with slight decrease in ash, hydrogen, and oxygen content(s) and an increase in carbon and nitrogen. The novel method developed, described in section 3.2.1, for obtaining a full proximate analysis was used in evaluating algae lot# 2013 and its finding are shown in Figure 5-1 alongside the ultimate analysis of the biomass. Undergoing the TGA method for proximate analysis we clearly see three distinct temperatures for pyrolysis (Py) decomposition of the algal biomass around 310, 375, and 450 °C, presumed to be the decomposition of macromolecular components such as carbohydrates, proteins, and lipids.[1] During the post pyrolysis combustion (PPyC) stage the majority of the fixed carbon decomposes at 400 °C with the remaining residual decomposing at 600 °C, representing bulk fixed carbon and coke, respectively.

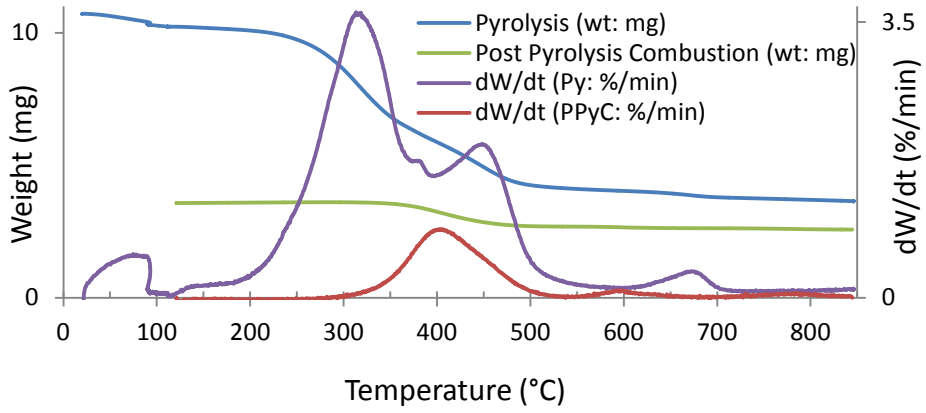

Proximate Analysis (wt %)		Ultimate Analysis (afdw %)	
Moisture	4.4	Carbon	55.6
Volatiles	61.6	Hydrogen	6.2
Combustibles	9.9	Nitrogen	7.6
Ash	24.1	Oxygen*	30.6

*oxygen calculated by difference after normalized to the ash: O (afdw%) = C - H - N [afdw%].

Figure 5-1. Proximate (TGA) and ultimate (CHN Analyzer) analysis of algae lot# 2013. TGA plot indicates pyrolysis weight change (blue) and post pyrolysis combustion (green) and corresponding derivative weight change, (purple) and (red), respectively. Ultimate analysis is provided on a ash free dry weight percent (afdw%).

Similarly to the algae lot# 2011, the main product yields from algae lot# 2013 were the solid product and biocrude fractions. Again, the ash free dry weight yields represent a significant difference in compared to the dry weight yields, due to the relatively high ash content of both the starting biomass and the solid product fraction. Figure 5-2 details the bulk product yields and organic elemental composition. The partitioning of carbon and nitrogen was evaluated for each product; the biocrude product contained 50% and 23% of the algal carbon and

nitrogen, respectively, where the ACP contained 13% and 44% of the algal carbon and nitrogen, respectively. Half of the carbon is recovered into the desired product fraction where 20% is lost as gas, presumably as CO_2.[2] The carbon recovery is similar to another reported low-lipid algae[3] and much lower compared to biocrude produced with extremely fast reaction times which result in substantially higher heteroatom content.[4] Therefore, biocrude carbon recovery has been linked to reaction times and process temperature, typically acquiring heteroatom removal at the expense of carbon efficiency. Close to 75% of the nitrogen is accounted for in the three main product fractions, majorly in the aqueous phase, comparable to other reports.[2] The significant nitrogen in the aqueous product could potentially be available to future nutrient use for continuing algal cultivation,[5] specifically when added with essential micronutrients.[6]

	Biocrude (wt%)	Solids (wt%)
Yield	27.3	29.5
C	76.9 ± 1.6	24.2 ± 1.6
H	10.1 ± 0.4	2.6 ± 0.05
N	4.7 ± 0.2	1.1 ± 0.04
O*	6.7 ± 2.0	-
Ash	1.6	67.6

Aqueous Co-Product ($g\ L^{-1}$)	
TOC	6.6
TN	3.1

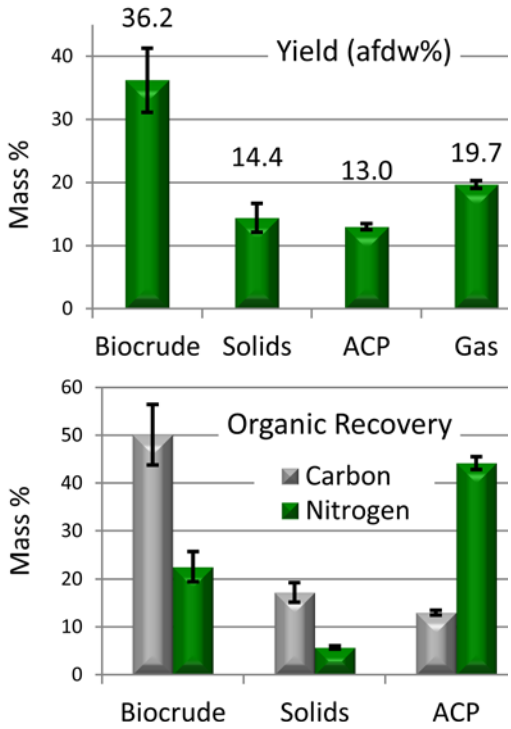

Figure 5-2. Product Yields, and respective organic elemental content, from the HTL of algae lot#2013. The organic recovery represents the fate of algal carbon and nitrogen toward each perspective product fraction. *oxygen calculated by difference; O = 100- C- H- N- ash [wt%]

5.2 Wastewater Nutrient Removal

The cultivation strategy used for algae lot# 2013 provided interesting evaluation of the effectiveness of wastewater algal polishing. Using the algal growth ponds in series (as seen in Figure 3-1) it was possible to evaluate nutrients and minerals from the wastewater effluent (ww-effluent), each algal cultivation pond, resultant algal biomass, and HTL solid product. This evaluation determines which components are mined by the algae and ultimately stay within the

solid product, post HTL. Table 5-1 shows the ICP-OES data collected from each stage throughout the process. The production of each element represents a theoretical maximum and was calculated using the data collected and following assumtions: all of the wastewater was processed through algae cultivation and all the phosphorus was used to form algae. The following formula was used;

$$\text{Production day}^{-1} = (\text{ww-effluent flow})^* (\text{X-concentration of ww-effluent})^* (\text{measured \%-X of algae})^* (\%\ \text{HTL solid yield})^* (\text{measured \%-X solid product})$$

Where, X represents a specific element of interest and daily production represents total theoretical mass incorporated into a solid product removed from the ww-effluent.

Table 5-1. Bio-mining effects from algae cultivation and hydrothermal liquefaction.

	Ca	P	Mg	S	Fe	K	Al	Na	Ba	Sr	Mn	Zn
WW-Effluent (ppm)	82.8	5.1	10.2	24.3	0.05	17.2	0.07	19.8	0.05	0.3	0.02	0.08
Pond 1 (ppm)	85.7	5.1	10.8	24.9	0.03	17.0	0.02	20.3	0.02	0.3	0.002	0.03
Pond 2 (ppm)	78.5	3.1	12.8	29.2	0.01	16.2	-	23.2	0.01	0.3	-	0.02
Algae (wt%)	5.7	2.3	0.4	0.8	0.1	0.4	0.06	0.06	0.01	0.02	0.01	0.02
Solid Product (wt%)	17.1	7.4	1.4	0.5	0.4	0.3	0.16	0.09	0.07	0.06	0.05	0.03
Recovery in Solid Product (%)	89	95	100	19	84	24	79	44	(206)	89	(147)	59
Production (kg day^{-1})	508	220	43	16	11	9	5	3	2	2	1.5	1

Most of the elements show a progressive decrease from the ww-effluent to each cultivation pond with that element accumulating in the algae biomass, which would be expected. However, some elements indicate increases through the progression which is not necessarily unexpected and can be explained by one of two mechanisms. First, the extremely dynamic nature of wastewater creates constant fluxes within a short time frame and the algal growth ponds (running at an HRT of 10 days each) may not have responded to a particular flux within that time frame of sample collection. Second, biomass die-off could cause a slight increase in a particular element; continuous cultivation with dynamic inputs could cause algae to enter into various sinusoidal stages of their growth cycle, i.e., lag phase, exponential growth phase, stationary phase, and death phase. The elements of Ba and Mn were found to be much higher concentrations in the solid product then were even present in the starting biomass (indicated in parenthesis). Potentially, this could be attributed to analysis interference with some of the larger amounts of calcium and magnesium, which have been reported.[7] The main findings of the data indicate that significant mining of minerals and phosphorus within a solid product can occur during algae cultivation and hydrothermal liquefaction. In addition, certain elements which accumulate into algal cells are recovered or retained with higher affinity to the solid HTL product. Element such as Ca, P, Mg, Fe, Al, and Sr all prefer to retain within the HTL solid product where most others such as, S, K, and Na do not.

5.3 *In-situ* Crystallization of Substituted Hydroxyapatite during HTL of Municipal Wastewater-Cultivated Algae

Hydroxyapatite (HA) preparation typically proceeds through a well-controlled synthesis combining reagents from individual phosphorus and calcium sources. Synthesis procedures follow co-precipitation, hydrothermal, or various wet and dry methods resulting in a variety of morphologies and ionic substitutions.[8-11] Certain marine algae (*Corallina officinalis* and *Amphiroa ephedrathe*) have be used as a calcium source for HA crystallization, but only after prior removal of organics and using an external phosphorus source.[12, 13] This section will detail the crystallization of HA *in-situ*, using algae lot# 2013 as both the calcium and phosphorus source without pre-treatment.

Calcium hydroxide, or lime, is added by the wastewater treatment facility in significant quantities daily (2000 lbs day^{-1}) as a buffering agent to raise alkalinity and pH as activated sludge, or bacteria, performs nitrification in the water column. The effects of this addition are shown both in Table 5-1 and the elemental characterization of algae lot# 2011 discussed in previous chapter.

In the growth ponds, calcium, phosphorous, magnesium, sulfur, potassium, and sodium had the highest observable concentrations; silicon, although not measured by ICP due to analytical limitations, is expected from the presence of diatoms in the mixed algal cultures (as seen by algae lot#2011 inorganic composition). The retention of certain elements (Ca, P, Mg, Fe, and Al) within HTL solid product is significantly interesting since literature suggests algae that have higher sodium and potassium and lower calcium concentrations produce less solids during HTL and retain more inorganics in the aqueous product.[14-16]

The general HA structure, $Ca_{10}(PO_4)_6(OH)_2$, allows both cationic and anionic substitutions, including magnesium, silicon, and carbonate substitutions, which have been shown to improve HA performance as biomaterials.[17-20] Analysis of the HTL solids from algae lot# 2013 with XRD determines the crystallographic structure is monophasic HA, according to JCPDS# 73-0293, and is confirmed by FTIR. Additional information from the FTIR spectrum indicates residual organics remain from HTL processing, B-type (PO_4) carbonate substitutions occur, and significant hydroxyl deficiencies and phosphorus bound hydroxyls are present. To confirm that the HA was not formed via precipitation during the cultivation process, but rather from the HTL reaction, comparison of the XRD and FTIR patterns from the solid product and the combustion ash produced from algae lot# 2013 were performed. The ash was solely tricalcium phosphate (TCP) and calcium oxide. A previous study[21] demonstrated combustion of calcium and phosphorus sources results in an amorphous material which, upon calcination at 600 °C, crystallizes to form TCP. However, the combustion process at 600 °C is not sufficient for significant transformation of HA to TCP.[22, 23] Thus, significant HA formation does not occur during algae cultivation and is formed during the HTL of wastewater-cultivated algae. Figure 5-3 shows XRD and FTIR analysis from the HTL solid product and algae lot#2013 combustion ash.

(a)

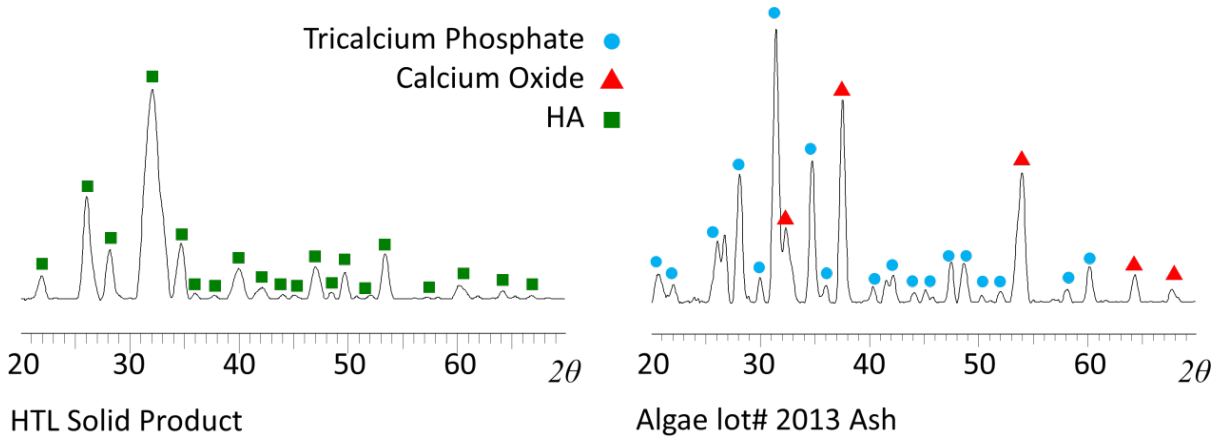

(b)

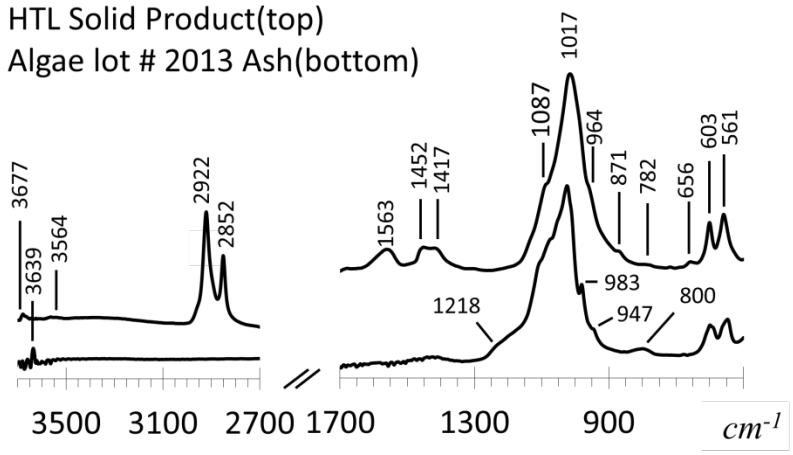

Figure 5-3. (a) Integration of powder XRD of HTL solid product and combustion-produced algal ash at a 2θ range of 20° to 70°; peaks for HA (green square), calcium oxide (red triangle) and TCP (blue circle), JCPDS# 70-2005, are identified. (b) FTIR spectrum of HTL solid product and algae ash; all peaks present in the range from 500-3700 cm^{-1} are shown.

Peak identification for the FTIR spectrums present in Figure 5-3b are as followed:

The solid HTL product exhibit distinct absorption bands for HA; including PO_4^{3-} vibrations, v_1 (964 cm^{-1}), v_3 (1087 and 1017 cm^{-1}), v_4 (603 and 561 cm^{-1}), hydroxide stretching (3564 cm^{-1} and 3677 cm^{-1}; lattice -OH and P-OH, respectively), CO_3^{2-} (1417 and 1452 cm^{-1}; carbonate B-Type substitution), and either HPO_4^{2-} or CO_3^{2-} (871 cm^{-1}). Residual organics from HTL processing show bands for C-O (1563 cm^{-1}) and C-H (2852 and 2922 cm^{-1}) groups. Algae lot# 2013 ash exhibit FTIR vibration bands for PO_4^{3-} (947 and 983 cm^{-1}; as TCP), $P_2O_7^{4-}$ (1218 cm^{-1}) and surface hydroxyl (3639 cm^{-1}; from calcium oxide).

Commercial production of HA gives significant effort to generating calcium orthophosphates with both controlled nanoparticle rod and hierarchical morphologies.[11] Previous studies have demonstrated that HA nanorods can aggregate into bundles and, through Oswald ripening, form sheets and hierarchical flower structures.[24, 25] To facilitate nanoparticle rod and hierarchical morphologies, surfactants have been incorporated during commercial HA crystallization, including an array of molecules such as fatty acids[26], amino acids[27, 28], and a variety of organic polymers.[11, 25] The hydrothermal synthesis of HA has also been demonstrated utilizing a biogenic phosphate source (adenosine 5'-triphosphate or ATP) as both morphological control and a phosphorus source using an external calcium source.[29] Algae contain phosphorus in many biomolecules within the cell, including DNA, RNA, ATP, and phospholipids. Since the wastewater-cultivated algae also contains significant calcium (Table 5-1), there are biomolecules present that can contribute to hierarchical structures without the addition of an external calcium sources.

Morphology and hierarchical structures are shown through transmission electron (TEM) and scanning electron micrographs (SEM) of the HA product directly after HTL formation presented in Figure 5-4. Hexagonal nanocrystals (Figure 5-4a,b) are present up to 1 micron in length along the *c*-axis and 15 nm about the *a* and *b*-axis; these crystals then form into bundles along the *c*-axis, Figure 5-4b. Each bundle can then form hierarchical sheets and flower-like structures, Figure 5-4c. Unlike literature studies, which have suggested homogenous formation of the nanoparticles and hierarchical morphologies in the presence of a single surfactant, the *in-situ* crystallization of HA during HTL of algae lot# 2013 results in heterogeneous morphologies. The heterogeneity of the material could be due to the short reaction times compared to conventional HA synthesis techniques, or the presence of variable growth mechanisms due to localized biomolecules (i.e., fatty acids, amino acids, phospholipids) being present at different concentrations during the HTL processing.

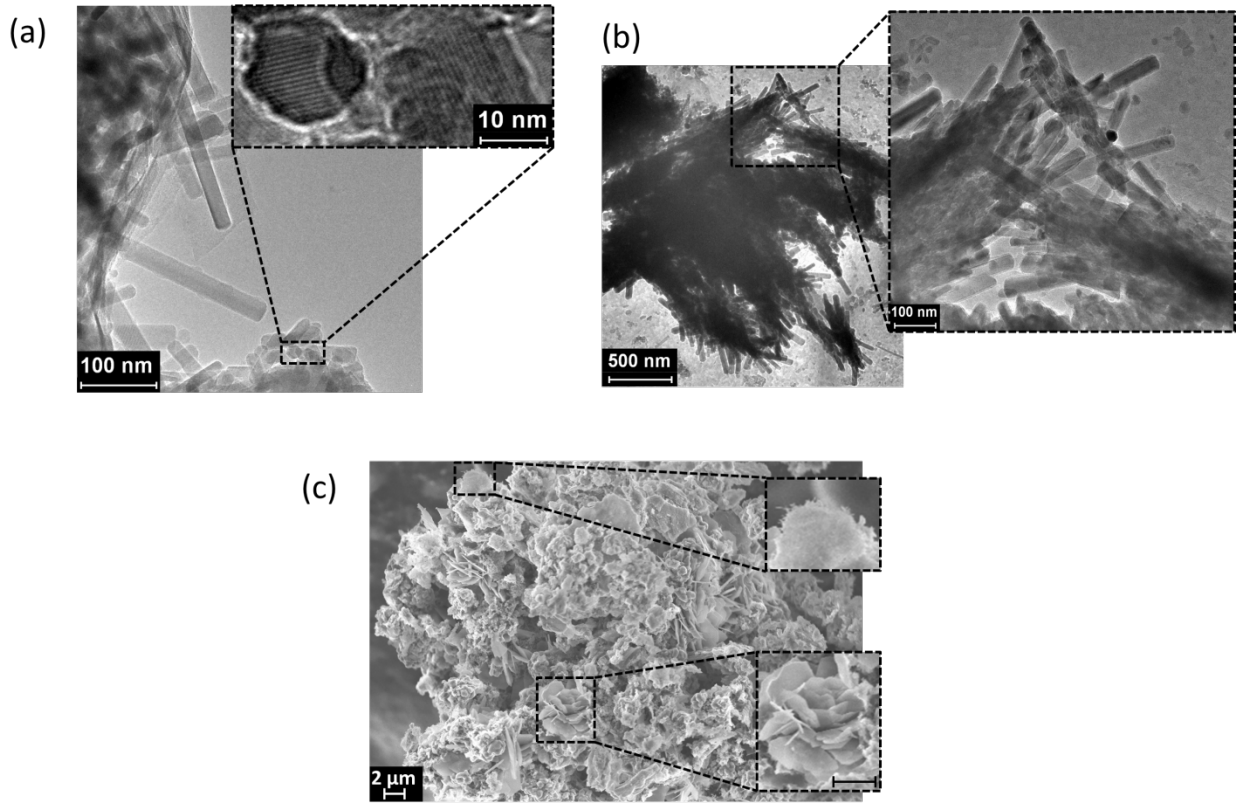

Figure 5-4. HA product consists of hexagonal nanorods, which assemble into hierarchal structures from bundles to sheets to flowers. TEM images of (a) well-defined hexagonal nanocrystals which (b), aggregate to bundles along the *c*-axis. SEM images of (c), ~40 µm particle with sheet and flower-like hierarchical morphologies

Algae lot# 2013, as the biogenic source for HA production, provides elements that favor ionic substitutions during calcium orthophosphates crystallization. In addition to the carbonate B-type substitution shown in the FTIR (Figure 5-3b), other dominate substitutions in the HA product are shown by scanning electron microscopy-energy dispersive x-ray spectroscopy (SEM-EDS), Figure 5-5, which include Mg and Si for Ca and P, respectively. Additional elements preferentially retained (Table 5-1) in the HA product would be present as minor substitutions and show relatively small peaks on the EDS spectrum. FTIR confirmation of these elemental substitutions was also found (Figure 5-3b); Mg substitution is indicated by the hydroxyl shift from the typical 3572 cm^{-1} to the observed 3564 cm^{-1}. Previously, this was seen when x = 2 in Mg substituted HA of the form $Ca_{10-x}Mg_x(PO_4)_6(OH)_2$.[30] Mg results in lower IR absorbance of lattice -OH[17, 18], consistent with Figure 5-3b. The presence of silicate can be confirmed by the FTIR bands at 656 and 782 cm^{-1} (Si in HA) in the HA product.[18]

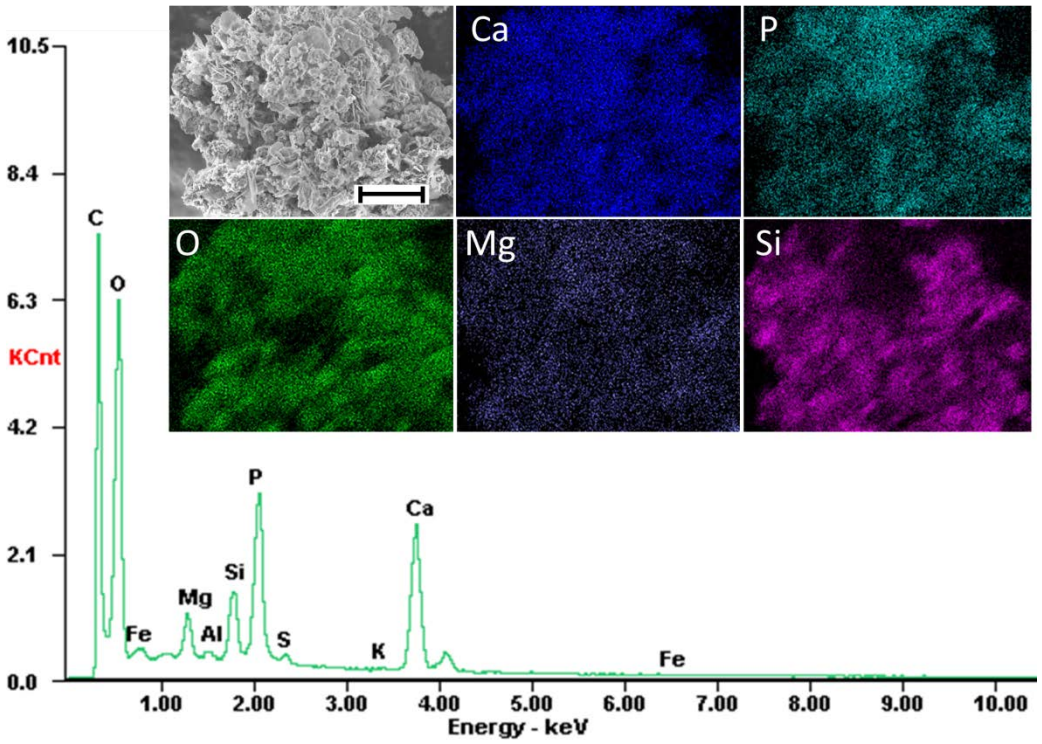

Figure 5-5. SEM-EDS imaging and spectrum of a single particle of solid HTL product, scale bar equals 10 µm, with elemental mapping of calcium, phosphorus, oxygen, magnesium, and silicon.

5.4 Conclusions

The fundamental scientific method employed within this chapter, step-wise determination of elemental content and fundamental solid characterizations, led to the novel discovery that the hydrothermal liquefaction of wastewater-cultivated algae can result in not only significant organic conversion to biocrude oil but also large quantities of highly substituted (carbonate, magnesium, and silicon) pure phase hydroxyapatite. This novel process is the first hydroxyapatite synthesis procedure to use both calcium and phosphorus from the same biogenic

source, which also provided biological crystallization directing agents (resulting in hierarchical micro structures produced from hexagonal nano-rods), and the source for the significant elemental substitutions present.

In conclusion, it is possible to mine municipal wastewater, through algae cultivation and hydrothermal processing, into value-added products, including a low oxygen content biocrude and significant amounts of highly substituted hydroxyapatite. Hydroxyapatite has applications in use of fertilizers, heterogeneous catalysts, and tissue engineering scaffold materials; each with an increased value proportional to the quality control of a commercial scale production. The next chapter of this dissertation will evaluate further *in-situ* synergies between the biocrude and hydroxyapatite as well as describe the potential tuning of the hydroxyapatite product by creating a secondary tricalcium phosphate phase.

5.5 References

1. Marcilla, A.; Gómez-Siurana, A.; Gomis, C.; Chápuli, E.; Catalá, M. C.; Valdés, F. J., Characterization of microalgal species through TGA/FTIR analysis: Application to nannochloropsis sp. *Thermochimica Acta* **2009,** *484*, (1-2), 41-47.
2. Elliott, D. C.; Hart, T. R.; Schmidt, A. J.; Neuenschwander, G. G.; Rotness, L. J.; Olarte, M. V.; Zacher, A. H.; Albrecht, K. O.; Hallen, R. T.; Holladay, J. E., Process development for hydrothermal liquefaction of algae feedstocks in a continuous-flow reactor. *Algal Research* **2013,** *2*, (4), 445-454.
3. Yu, G.; Zhang, Y.; Schideman, L.; Funk, T.; Wang, Z., Distributions of carbon and nitrogen in the products from hydrothermal liquefaction of low-lipid microalgae. *Energy & Environmental Science* **2011,** *4*, (11), 4587.
4. Faeth, J. L.; Valdez, P. J.; Savage, P. E., Fast Hydrothermal Liquefaction of Nannochloropsis sp. To Produce Biocrude. *Energy & Fuels* **2013,** *27*, (3), 1391-1398.
5. Biller, P.; Ross, A. B.; Skill, S. C.; Lea-Langton, A.; Balasundaram, B.; Hall, C.; Riley, R.; Llewellyn, C. A., Nutrient recycling of aqueous phase for microalgae cultivation from the hydrothermal liquefaction process. *Algal Research* **2012,** *1*, (1), 70-76.
6. Garcia Alba, L.; Torri, C.; Fabbri, D.; Kersten, S. R. A.; Brilman, D. W. F., Microalgae growth on the aqueous phase from Hydrothermal Liquefaction of the same microalgae. *Chemical Engineering Journal* **2013,** *228*, 214-223.

7. Boevski, I.; Daskalova, N.; Havezov, I., Determination of barium, chromium, cadmium, manganese, lead and zinc in atmospheric particulate matter by inductively coupled plasma atomic emission spectrometry (ICP-AES). *Spectrochimica Acta Part B: Atomic Spectroscopy* **2000,** *55*, (11), 1643-1657.
8. Silvester, L.; Lamonier, J.-F.; Vannier, R.-N.; Lamonier, C.; Capron, M.; Mamede, A.-S.; Pourpoint, F.; Gervasini, A.; Dumeignil, F. Y., Structural, textural and acid-base properties of carbonates-containing hydroxyapatites. *Journal of Materials Chemistry A* **2014**.
9. Tsuchida, T.; Kubo, J.; Yoshioka, T.; Sakuma, S.; Takeguchi, T.; Ueda, W., Reaction of ethanol over hydroxyapatite affected by Ca/P ratio of catalyst. *Journal of Catalysis* **2008,** *259*, (2), 183-189.
10. Matsuura, Y.; Onda, A.; Yanagisawa, K., Selective conversion of lactic acid into acrylic acid over hydroxyapatite catalysts. *Catalysis Communications* **2014,** *48*, 5-10.
11. Sadat-Shojai, M.; Khorasani, M. T.; Dinpanah-Khoshdargi, E.; Jamshidi, A., Synthesis methods for nanosized hydroxyapatite with diverse structures. *Acta biomaterialia* **2013,** *9*, (8), 7591-621.
12. Walsh, P. J.; Walker, G. M.; Maggs, C. A.; Buchanan, F. J., Thermal preparation of highly porous calcium phosphate bone filler derived from marine algae. *Journal of materials science. Materials in medicine* **2010,** *21*, (8), 2281-6.
13. Spassova, E.; Gintenreiter, S.; Halwax, E.; Moser, D.; Schopper, C.; Ewers, R., Chemistry, ultrastructure and porosity of monophasic and biphasic bone forming materials derived from marine algae. *Materialwissenschaft und Werkstofftechnik* **2007,** *38*, (12), 1027-1034.
14. Elliott, D. C.; Hart, T. R.; Schmidt, A. J.; Neuenschwander, G. G.; Rotness, L. J.; Olarte, M. V.; Zacher, A. H.; Albrecht, K. O.; Hallen, R. T.; Holladay, J. E., Process development for hydrothermal liquefaction of algae feedstocks in a continuous-flow reactor. *Algal Research* **2013**.
15. Valdez, P. J.; Dickinson, J. G.; Savage, P. E., Characterization of Product Fractions from Hydrothermal Liquefaction ofNannochloropsissp. and the Influence of Solvents. *Energy & Fuels* **2011,** *25*, (7), 3235-3243.
16. Valdez, P. J.; Nelson, M. C.; Wang, H. Y.; Lin, X. N.; Savage, P. E., Hydrothermal liquefaction of Nannochloropsis sp.: Systematic study of process variables and analysis of the product fractions. *Biomass and Bioenergy* **2012,** *46*, 317-331.
17. Huang, T.; Xiao, Y.; Wang, S.; Huang, Y.; Liu, X.; Wu, F.; Gu, Z., Nanostructured Si, Mg, CO3 2− Substituted Hydroxyapatite Coatings Deposited by Liquid Precursor Plasma Spraying: Synthesis and Characterization. *Journal of Thermal Spray Technology* **2011,** *20*, (4), 829-836.
18. Marchat, D.; Zymelka, M.; Coelho, C.; Gremillard, L.; Joly-Pottuz, L.; Babonneau, F.; Esnouf, C.; Chevalier, J.; Bernache-Assollant, D., Accurate characterization of pure silicon-substituted hydroxyapatite powders synthesized by a new precipitation route. *Acta biomaterialia* **2013,** *9*, (6), 6992-7004.
19. Mostafa, N. Y.; Hassan, H. M.; Abd Elkader, O. H., Preparation and Characterization of Na+, SiO44−, and CO32−Co-Substituted Hydroxyapatite. *Journal of the American Ceramic Society* **2011,** *94*, (5), 1584-1590.

20. Pietak, A. M.; Reid, J. W.; Stott, M. J.; Sayer, M., Silicon substitution in the calcium phosphate bioceramics. *Biomaterials* **2007,** *28*, (28), 4023-32.
21. Loher, S.; Stark, W. J.; Maciejewski, M.; Baiker, A.; Pratsinis, S. E.; Reichardt, D.; Maspero, F.; Krumeich, F.; Günther, D., Fluoro-apatite and Calcium Phosphate Nanoparticles by Flame Synthesis. *Chemistry of Materials* **2004,** *17*, (1), 36-42.
22. Zorn, K.; Gbureck, U.; Mitró, D.; Müller, F. A.; Vorndran, E., Hydrothermal synthesis of calcium-deficient hydroxyapatite whiskers and their thermal transformation to polycrystalline β-tricalcium phosphate short fibers. *Bioinspired, Biomimetic and Nanobiomaterials* **2013,** *2*, (1), 11-19.
23. Fathi, M. H.; Hanifi, A.; Mortazavi, V., Preparation and bioactivity evaluation of bone-like hydroxyapatite nanopowder. *Journal of Materials Processing Technology* **2008,** *202*, (1-3), 536-542.
24. Ma, M. G., Hierarchically nanostructured hydroxyapatite: hydrothermal synthesis, morphology control, growth mechanism, and biological activity. *International journal of nanomedicine* **2012,** *7*, 1781-91.
25. Nathanael, A. J.; Han, S. S.; Oh, T. H., Polymer-Assisted Hydrothermal Synthesis of Hierarchically Arranged Hydroxyapatite Nanoceramic. *Journal of Nanomaterials* **2013,** *2013*, 1-8.
26. Wang, X.; Zhuang, J.; Peng, Q.; Li, Y. D., Liquid–Solid–Solution Synthesis of Biomedical Hydroxyapatite Nanorods. *Advanced Materials* **2006,** *18*, (15), 2031-2034.
27. Boanini, E.; Fini, M.; Gazzano, M.; Bigi, A., Hydroxyapatite Nanocrystals Modified with Acidic Amino Acids. *European Journal of Inorganic Chemistry* **2006,** *2006*, (23), 4821-4826.
28. Cui, H.; Liu, H.; Qin, J.; Li, Y.; Tang, H.; Yang, X., Hydrothermal synthesis and characterisation of glutamine-modified rod-like hydroxyapatite nanoparticles. *Micro & Nano Letters* **2012,** *7*, (12), 1292-1295.
29. Qi, C.; Tang, Q.-L.; Zhu, Y.-J.; Zhao, X.-Y.; Chen, F., Microwave-assisted hydrothermal rapid synthesis of hydroxyapatite nanowires using adenosine 5'-triphosphate disodium salt as phosphorus source. *Materials Letters* **2012,** *85*, 71-73.
30. Diallo-Garcia, S.; Laurencin, D.; Krafft, J.-M.; Casale, S.; Smith, M. E.; Lauron-Pernot, H.; Costentin, G., Influence of Magnesium Substitution on the Basic Properties of Hydroxyapatites. *The Journal of Physical Chemistry C* **2011,** *115*, (49), 24317-24327.

6 Hydroxyapatite Synergies and its Potential Applications

The work in this chapter is used to confirm the hypothesis formulated at the end of Chapter 4: Demonstrating Sustainability through Wastewater-Cultivated Algae, that inorganics formed within the HTL solid product [now known to be hydroxyapatite(HA)] are performing catalytic roles in obtaining a biocrude with low oxygen content. Evaluation of this hypothesis included obtaining both a detailed distillate and molecular profile for comparison with literature sources which have performed HTL on algae and subsequent thermal and catalytic treatment of the resultant biocrude. In addition, since this work represents the first to create a HA material during the HTL of algae significant potential remains to understand how the material can be used as a higher-value product. Two main hypotheses which were formulated based of the full characterization of the substitutions included: 1) the material could be altered to a secondary tricalcium phosphate phase through heat treatments and 2) since the material contains more bone-like substitutions it would be well suited for bioactivity as a tissue engineering scaffold material. In order to evaluate each hypotheses the HA product was 1) calcined at variable temperatures and evaluated for structure and functionality and 2) used as an *in-vitro* growth substrate for human Wharton's jelly cells and evaluated with a live/dead assay. The work presented in this chapter was collected in conjunction with Chapter 5 using algae lot# 2013 and has been published in *Green Chemistry* (2015), **17**, 2560.

6.1 *In-situ* Catalytic Upgrading of the Biocrude from Hydroxyapatite Crystallization

HA is increasingly studied for its acid-base catalytic capabilities. Typical catalytic applications of HA include dehydration (acid catalyzed) and dehydrogenation (base catalyzed)[1, 2], Guerbet coupling reactions[3], and use as active metal support materials.[4] While biocrude oil can be generated from a variety of feedstocks, it typically needs to be upgraded, or further processed for lower heteroatom content and more desired distillate fractions, in order to be easily integrated into current infrastructure for refining and transportation. Therefore, creating a biocrude with lower oxygen and nitrogen, while increasing amount of lower boiling point distillate fractions, is of significant interest. The HA produced by HTL of wastewater-cultivated algae provides *in-situ* upgrading in both accounts. Complete analysis of molecular profile, resulting from the non-derivatized and MSTFA-derivatized samples are found in Figure 6-1 and Figure 6-2, respectively, with corresponding compound identification(s) found in Table 6-1 and Table 6-2, respectively. The SimDist TGA profile and corresponding distillate fractions are found in Figure 6-3. The biocrude product resulted in 80 wt% direct fuels and vacuum gas oil, and overall 96 wt% of the biocrude could be distilled below 600 °C. GC-MS analysis on the biocrude indicates the direct fuels are highly aromatic with primary components including phenol, cresol isomers, dimethyl and ethyl phenols, and indoles, along with significant amounts of straight chain and branched aliphatics. The vacuum gas oil primarily consists of free fatty acids and $>C_{20}$ straight chain aliphatics. The free fatty acids and methyl amine are shown in the MSTFA-derivatized GC-MS chromatogram. Only one fatty acid amide was present, in small amounts, and no nitriles. Studies have shown both thermal[5] and catalytic[6] upgrading treatments to reduce fatty acid amides and nitriles while producing lower boiling point aromatics and

aliphatics. Roussis et al.[5] explains a thermal upgrading pathway from amides to nitriles to aliphatics and aromatics at thermal treatment above 400 °C. Within the biocrude produced from algae lot# 2013, small amounts of fatty acid amides, with no nitriles, and the presence of methyl amine suggests that HA product is catalyzing the dehydration pathway from amides to aliphatics and aromatics. The three main stages of this pathway include dehydration of the amides to nitriles (reducing oxygen content by water removal), deamination of nitriles to alkanes and olefins (producing methyl amine), followed by dehydrogenation producing olefin isomers and aromatics. Both the dehydration and deamination steps would be catalyzed by active acid sites while the dehydrogenation results from basic active sites. It is hypothesized that the dehydration step is the rate limiting step while deamination occurs relatively quickly, due to the fact that small amount of amides where still identified and no nitriles were present. Further evidence of HA catalysis can be found by comparing results to Bai et al. catalytically treated biocrude.[6] Their findings also included reduction of fatty acid amides and nitriles, and upon upgrading they began to form benzenamine and carbozole. Both of these compounds are found within the biocrude from algae lot# 2013 (Figure 6-1, peak 23: benzenamine and Figure 6-2, peak E`: carbozole). Additionally, Bai et al. determined catalytic treatment was required to achieve total distillation of >90 wt% at or below 600 °C, similar to the biocrude produced during HA crystallization.

The distillate fractions from the biocrude co-produced with HA, presented in Figure 6-3, more closely resemble Roussis et al. thermally-upgraded biocrude at 400 °C, especially in the lower boing point distillates. The amount of vacuum gas oil and residual are more similar to Roussis et al. 350 °C upgraded oil, however, this is misleading because vacuum gas residuals

(which boil much higher than 600 °C) are cracking which produce higher amounts of $>C_{20}$ aliphatics, leading to more vacuum gas oils and remaining vacuum gas residuals which boil below 600 °C. Overall, the distillate fractions, oxygen content, and molecular profile of the biocrude are affected by the catalytic dehydration pathway induced by HA.

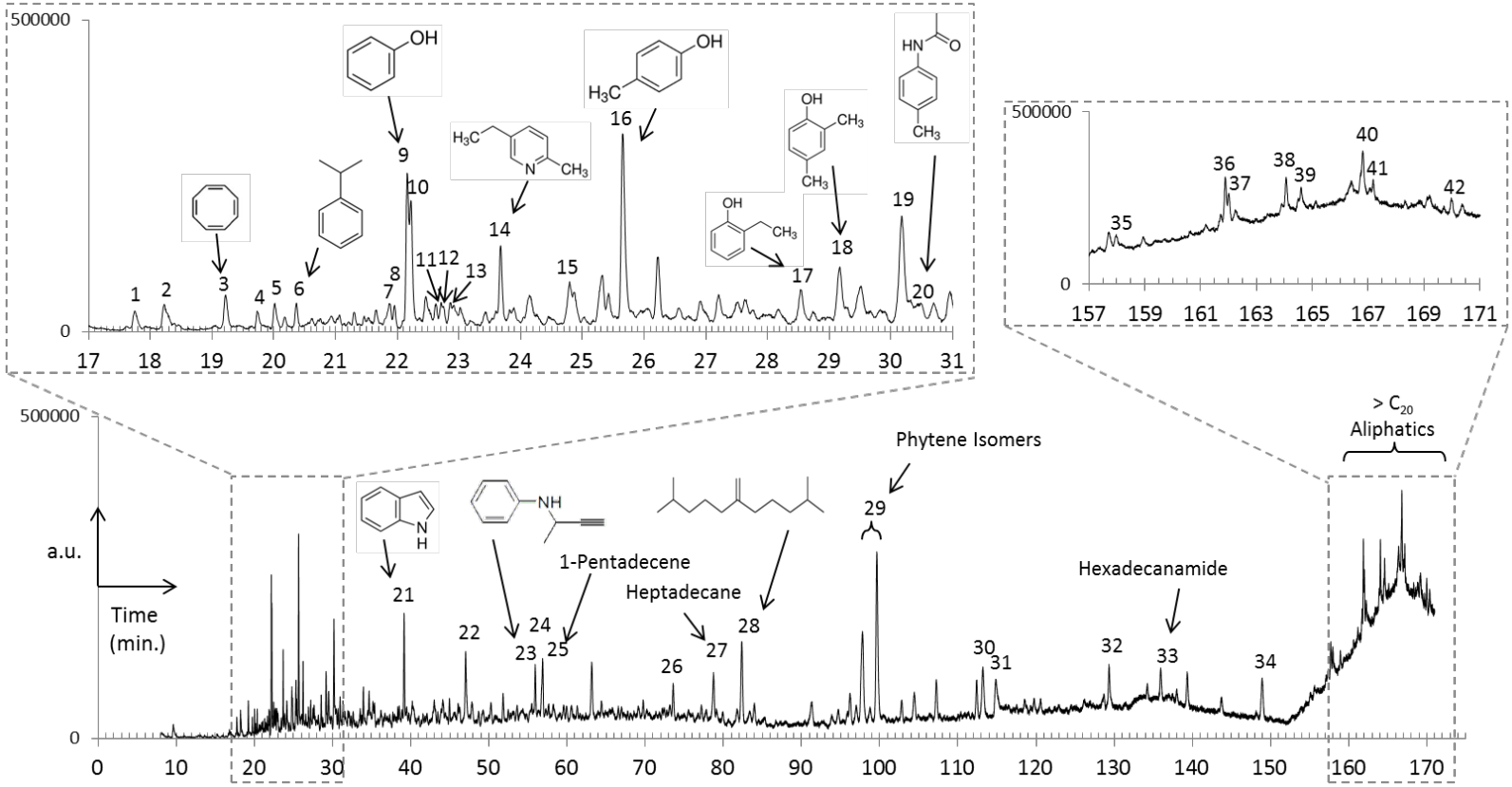

Figure 6-1. GC-MS chromatogram from the biocrude (non-derivatized) produced through HTL of algae lot#2013.

Table 6-1. Compound identification list from GC-MS analysis of biocrude from Figure 6-1; above 90% confidence as compared with NIST MS library.

	Retention Time	Compound Name		Retention Time	Compound Name
1	17.75	Ethylbenzene	23	55.93	N-(1-Methyl-2-propynyl)benzenamine
2	18.23	1,3-Dimethyl benzene	24	56.74	2,3-Dimethyl indole
3	19.20	1,3,5,7-Cyclooctatetraene	25	56.88	1-Pentadecene
4	19.73	2-Cyclopenten-1-one	26	73.58	1,7-Trimethylene-2,3-dimethyl indole
5	20.02	2,5-Dimethyl pyrazine	27	78.74	Heptadecane
6	20.36	1-Methylethyl benzene	28	82.33	2-Isohexyl-6-methyl-1-heptene
7	21.88	Dimethyl trisulfide	29	97.77	Phytene isomer
8	21.96	Cyclotetrasiloxane		99.62	Phytene isomer
9	22.18	Phenol	30	113.20	1-Methyl-9H-pyrido[3,4b]indole
10	22.23	Methyl styrene	31	114.76	9H-Pyrido[3,4-b]indole
11	22.70	2,3-Dimethyl-2-cyclopentene-1-one	32	129.35	Phytol
12	22.76	2-Ethyl-6-methyl pyrazine	33	135.95	Hexadecanamide
13	22.91	2-Ethyl-5-methyl pyrazine	34	148.94	Nonadecane
14	23.68	2-Ethyl-5-methyl pyridine	35	157.94	> C20 alkane
15	24.78	2-Methyl phenol	36	161.72	> C20 alkene
16	25.65	4-Methyl phenol	37	161.88	> C20 alkane
17	28.53	2-Ethyl phenol	38	164.06	1-(12-Methyltetradecanoyl) pyrrolidine
18	29.17	2,4-Dimethyl phenol	39	164.60	> C20 alkane
19	30.17	4-Ethyl phenol	40	166.80	> C20 alkene
20	30.53	4'-Methylacetanilide	41	167.18	2-Pentacosanone
21	39.15	Indole	42	169.97	Cholest-4-ene
22	47.00	3-Methyl indole			

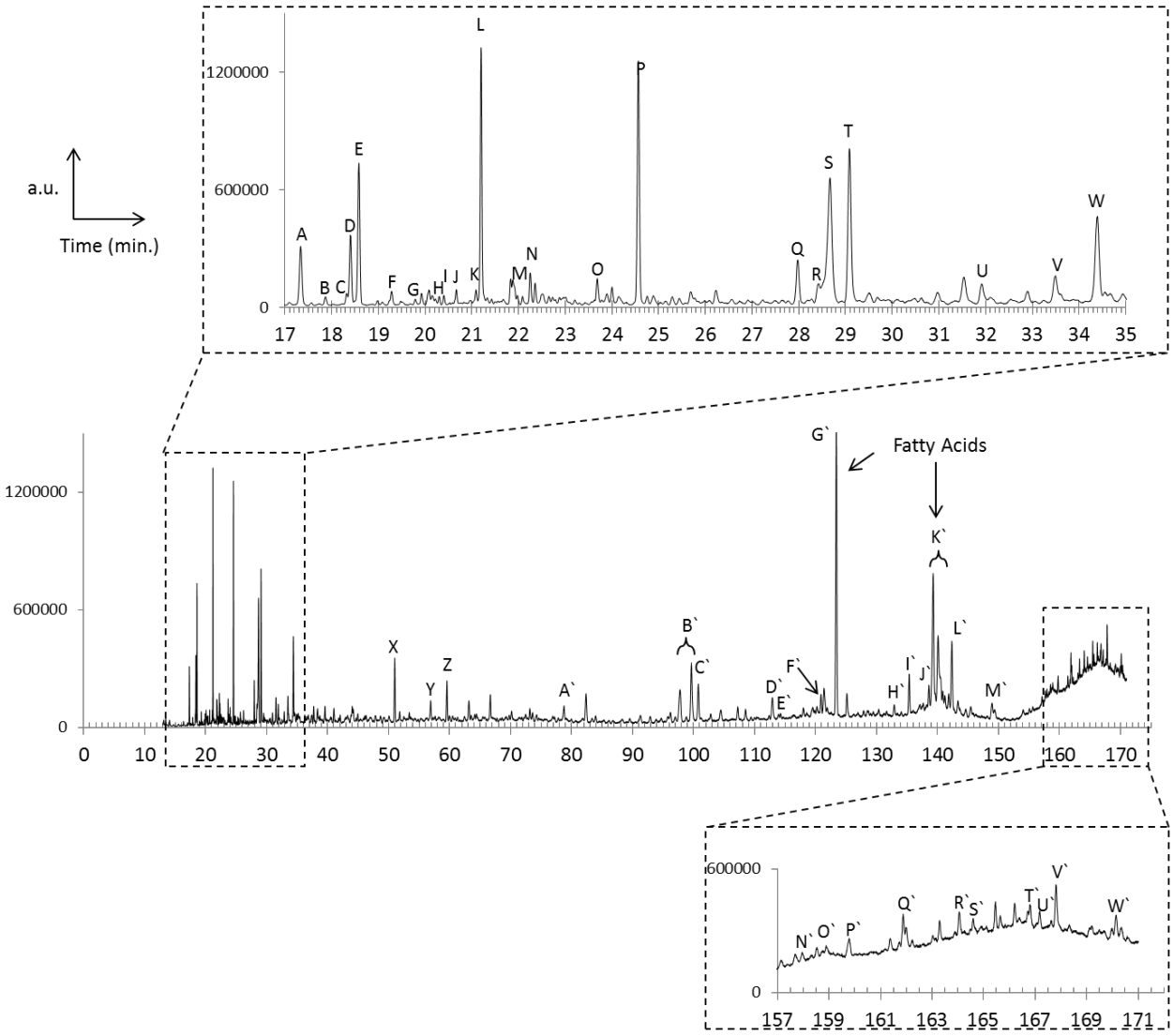

Figure 6-2. GC-MS chromatogram from the biocrude (derivatized) produced through HTL of algae lot#2013.

Table 6-2. Compound identification list from GC-MS analysis of biocrude from Figure 6-1; above 90% confidence as compared with NIST MS library.

	Retention Time	Compound Name		Retention Time	Compound Name
A	17.33	MSTFA	B`	97.68	Phytene isomer
B	17.86	Ethylbenzene		99.64	Phytene isomer
C	18.32	1,3-dimethylbenzene	C`	100.73	Tetradecanoic acid
D	18.40	Dihydroxy(dimethyl)silane	D`	112.96	1-Methyl-9H-pyrido[3,4-b]indole
E	18.59	Methylamine	E`	113.92	9H-Carbazole
F	19.29	1,3,5,7-Cyclooctatetraene	F`	120.95	9-Hexadecenoic acid
G	19.79	2-Methyl-2-cyclopenten-1-one	G`	123.40	Hexadecanoic acid
H	20.29	2-Methylbutyric acid	H`	132.94	Heptadecanoic acid
I	20.40	Cumene	I`	135.39	3,7,11,15-Tetramethyl-2-hexadecen-1-ol
J	20.68	3-Methylbutanoic acid	J`	138.58	9,12-Octadecanoic acid
K	21.08	Piperidine		139.30	Oliec acid isomer
L	21.19	Hydrogen sulfide		139.60	Oliec acid isomer
M	21.92	Dimethyl trisulfide	K`	140.10	Oliec acid isomer
N	22.25	Methyl styrene		140.50	Oliec acid isomer
O	23.69	2-Ethyl-5-methylpyridine		140.80	Oliec acid isomer
P	24.59	Phenol		141.20	Oliec acid isomer
Q	27.98	2-Methylphenol	L`	142.40	Octadecanoic Acid
R	28.42	Pyridine	M`	148.97	Nonadecane
S	28.08	4-Methylphenol	N`	157.98	> C20 alkane
T1	28.60	Piperdine (co-elute)	O`	158.90	11-Eicosenoic acid
T2	28.60	6-Propylquinoline (co-elute)	P`	159.79	Eicosanoic acid
U	31.91	3-Hydroxy-6-methylpyridine	Q`	161.70	> C20 alkene
V	33.48	2,4-Dimethylphenol	R`	164.04	1-(12-Methyltetradecanoyl)pyrrolidine
W	34.39	2,5-Dimethylphenol	S`	164.60	> C20 alkane
X	51.00	Indole	T`	166.70	> C20 alkene
Y	56.88	Pentadecene	U`	167.19	2-Pentacosanone
Z	59.58	3-Methyl indole	V`	167.80	Tricosanoic acid
A`	78.76	Heptadecane	W`	170.13	Tetracosanoic acid

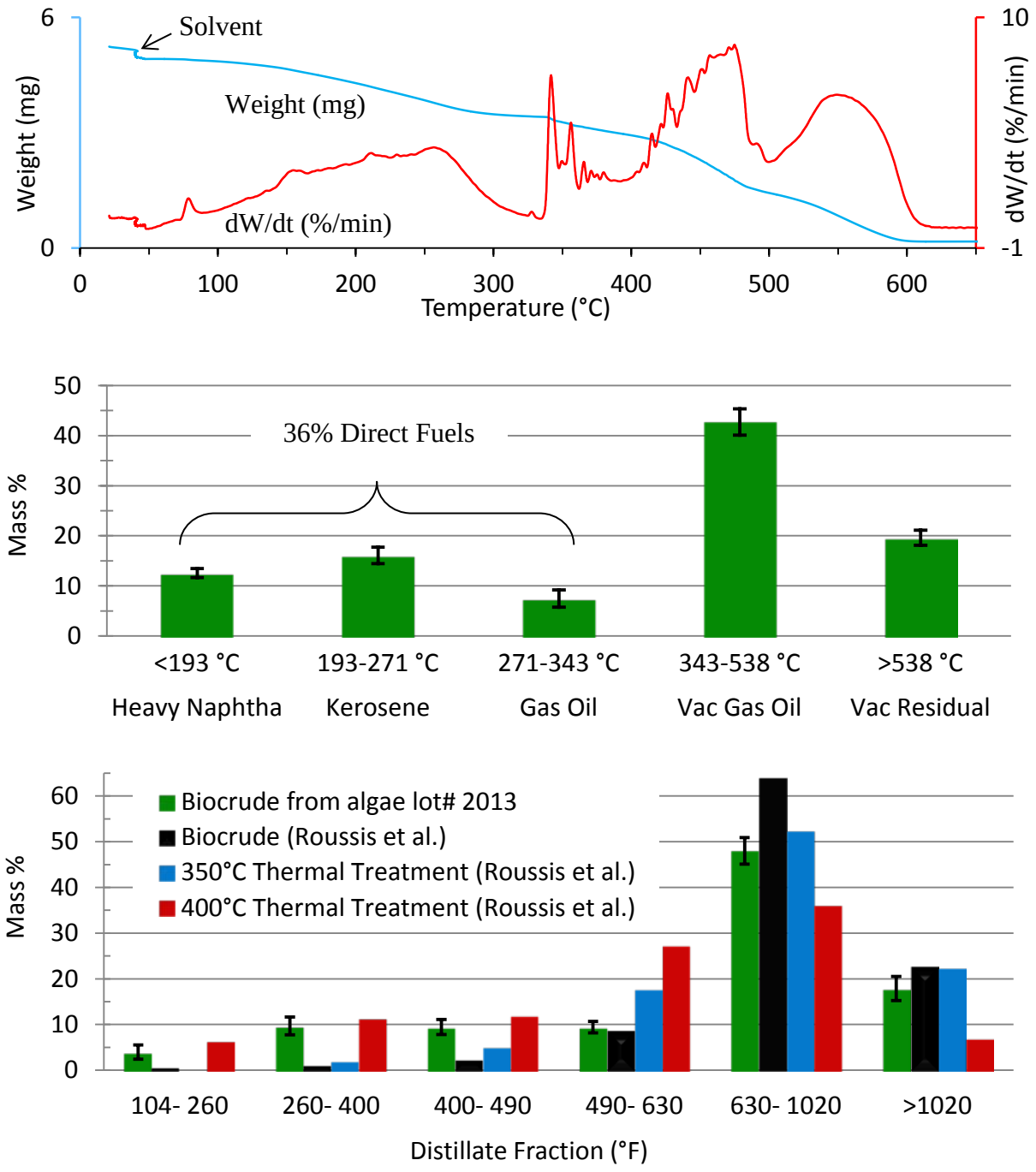

Figure 6-3. Simulated distillation via TGA of the biocrude and corresponding distillate fractions found in the biocrude produced in the presence of HA crystallization.

6.2 Phase Tuning of Hydroxyapatite

Ionic substitutions in HA can promote thermal transformation to tricalcium phosphate (TCP) at temperatures above 600 °C.[7-9] Multiphasic calcium orthophosphates (mixtures of HA and TCP) as biomaterials are known to have high osteogenicity and osteoinductive properties[7], particularly in achieving an optimum balance between the more stable HA and more soluble TCP.[10] Thermal treatment of the HA product steadily transforms the material to TCP with intermediate temperatures giving variable biphasic mixtures. XRD and FTIR analysis of thermally treated HA product in 100 °C increments from 500 °C to 900 °C are depicted in Figure 6-4. Residual organics from HTL processing are removed at 500 °C, as observed by the disappearance of the C-O peak at 1563 cm^{-1} and the C-H bands at 2852 & 2922 cm^{-1} (not shown) in the FTIR spectra. However, the XRD spectrum indicates that thermal treatment at 500 °C does not alter the HA structure. The FTIR at 500 °C retains significant carbonate peaks at 1417 & 1452 cm^{-1}, indicative of B-type, or PO_4, substitution. These ionic substitutions can distort the lattice and compensate charge by creating hydroxyl vacancies resulting in a reduction of FTIR stretching intensity[11], as seen with HA product (Figure 5-3 & Figure 6-4).

A clear decrease in the FTIR carbonate bands (1417 & 1452 cm^{-1}) is observed with increasing thermal treatment. The XRD spectra defines the onset of transition from HA to TCP at 600 °C and corresponds to the loss of carbonate bands, indicating that carbonate decomposition plays a role within phase transformation. The TGA for the ultimate analysis of the HA product, shown in Figure 6-5, indicates there are four main areas of decomposition between 600-850 °C. Loss of carbonate ions within the lattice of substituted HA is still an active area of research, trying to understand how relationships between lattice dimension, density, and

solubility variances as carbonate is liberated.[12, 13] The TGA plot (Figure 6-5) shows that 500 °C is sufficient to remove all residual organics remaining from HTL while still obtaining a pure phase HA material [XRD analysis (Figure 6-4)]. The amount of solid product leaving the HTL reactor, 68 wt% represents a refined substituted HA product.

Three regions in the XRD pattern can be used to monitor phase transformation from HA to TCP; indicated in Figure 6-4 by dashed red lines. First, the peak at $2\theta = 30.5°$ is unique to TCP, initially observed at 600 °C, and grows with increasing temperature. Second, the primary HA peak ($2\theta = 32.0°$) shifts to 31.5°, characteristic of TCP. Third, the peaks at $2\theta = 47°$ & 50° for HA shift closer together to 47.5° & 48.5°, indicative of the TCP structure. The transition from HA to TCP is nearly complete after thermal treatment at 900 °C, when comparing the XRD patterns with databases. [JCPDS #73-0293 (HA); JCPDS #70-2065 (TCP)]

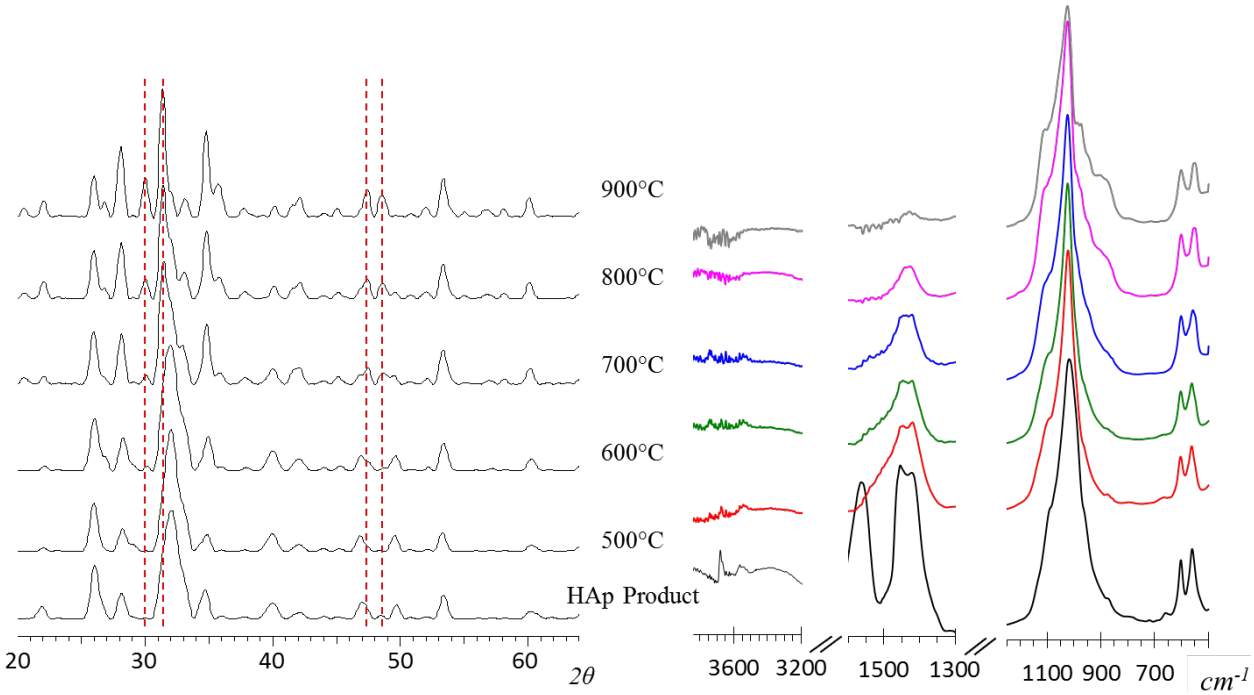

Figure 6-4. HA product transforms to tricalcium phosphate in stages up to 900 °C. Powder XRD integration of 2θ from 20° to 70°; TCP begins to form at 600 °C until it is the primary phase at 900 °C. Dashed red lines indicate characteristic peaks for TCP. FTIR spectrum(s) showing hydroxyl (3300- 3800 cm^{-1}), carbonate (1300-1600 cm^{-1}) and phosphate (500-1300 cm^{-1}) regions. TCP retains silica substitution dissimilar to the TCP form during combustion of algae lot# 2013 shown in Figure 5-3b.

Significant broadening of the phosphate shoulder peaks at 800- 1000 cm^{-1} in the FTIR patterns occur with increasing thermal treatment. Broad shoulders with multiple peaks are unlike typical FTIR patterns for TCP, which have a sharp peak near 983 cm^{-1} and small shoulder at 947 cm^{-1}, similar to algae lot# 2013 ash spectra shown in Figure 5-3b. These shoulders are attributed to SiO_4^{4-} substitution, which have been seen in pure Si-HA.[14] However, the XRD profiles suggest that the SiO_4^{4-} is actually within the TCP phase, suggesting the Si present in HA is retained during the transformation to TCP. If the Si was not integrated in the TCP structure, FTIR peaks for silicate or poly-silicate would expected to be observed, similar to the algae lot# 2013 ash, with increasing thermal treatment. However, no characteristic peak for amorphous silica is observed at 800 cm^{-1}.

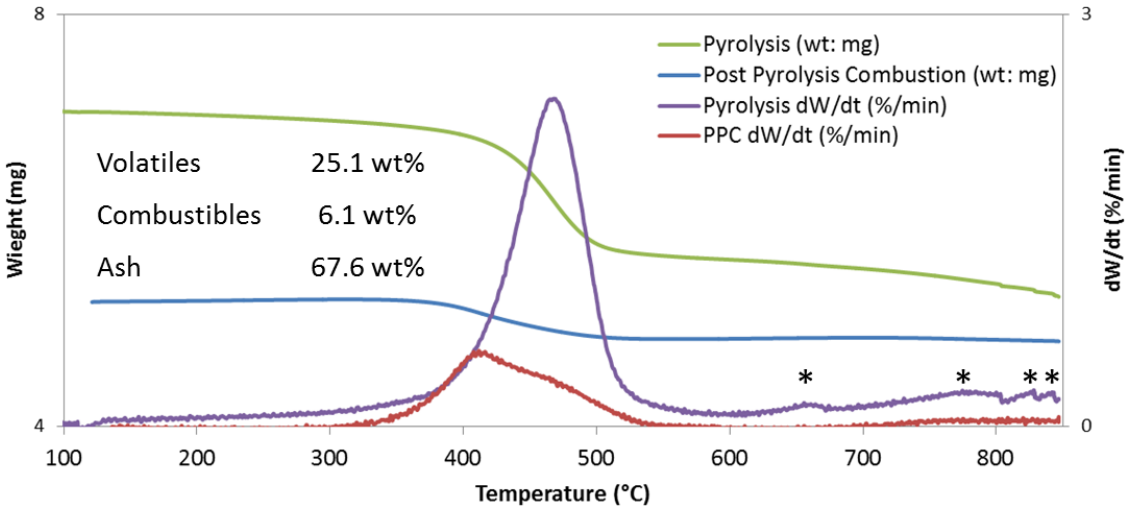

Figure 6-5. HA (HTL solid product) proximate analysis and corresponding TGA plot; carbonate loss associated with phase change are indicated with asterisk.

Transformation to the TCP phase induces globular morphological changes, as shown through SEM images in Figure 6-6. The combination of both phase and morphological changes that occur through simple heat treatments of the HA product allows tunability within each market, catalysis and/or biomedical.

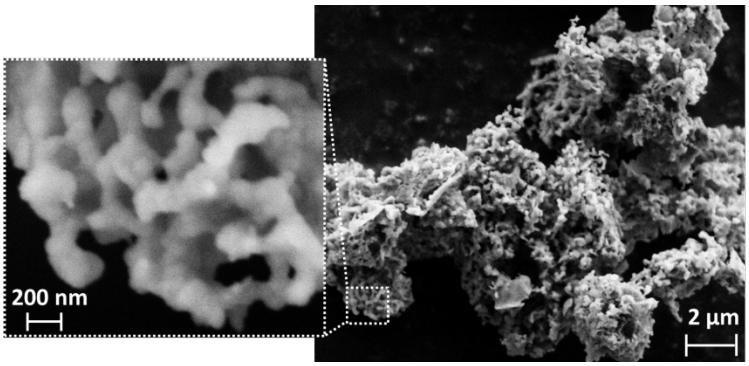

Figure 6-6. SEM image of HTL solid product from algae lot# 2013 after calcining in air at 900 °C; hexagonal nano-rods (shown in Figure 5-4) have sintered into a globular morphology indicative of TCP.

HA is primarily a non-porous crystal which exhibits acid-base activity on external crystal surfaces. The amount and strength of the active sites are a function of Ca/P ratio, substitutions, and crystal morphology; each altering which atoms are exposed on the crystal surface.[15-18] Silvester et al.[15] contribute P-OH as Brønsted acid sites and the Ca^{2+} and OH vacancies as Lewis acids. Yan et al.[1] describe when organics adsorb on the HA surface, a P-OH complex is formed and catalytically dehydrates lactic acid to acrylic acid. Once the molecule desorbs from the surface the $P\text{-}O^-$ is regenerated.

A closer view of the FTIR hydroxyl stretching area of the HA product in Figure 6-4 show two things; 1) the lattice hydroxyl peak is extremely small from considerable hydroxyl vacancies (or Lewis acids),[15, 16] and 2) the there is a pronounced P-OH complex peak.[16] Removal of organics at 500 °C results in no changes to lattice hydroxyls, however, the P-OH complex is lost suggesting the original $P\text{-}O^-$ is regenerated. These results demonstrate that regeneration can be achieved through minimal heat treatment and create a pure phase HA product stream after the *in-situ* synthesis of a HA catalyst which, compared to the evaluation of Silvester et al.[15] and Yan et al.[1] contains Brønsted and Lewis acid sites. Overall, the contribution of these active sites provide the means for *in-situ* catalytic upgrading of the biocrude produced, as previously discussed in section 6.1.

6.3 Cell Culturing on Hydroxyapatite Product

The substituted HA structure formed with HTL of algae lot# 2013 shows great promise for biomedical and bioengineering applications. Although natural bone is mainly Ca^{2+} and PO_4^{3-}, it also incorporates other ions of CO_3^{2-}, SiO_4^{4-}, and Mg^{2+}. These substitutions, and optimizing HA/TCP ratio through calcination, can help HA behave more like natural apatite in human bone and increase bioactivity to allow steady bone regeneration over an extended period of time.[9, 19] The first stage chosen to evaluate efficacy for bone scaffolds or regenerative materials was to determine whether human Wharton's jelly cells (hWJCs) will attach to the material. It was observed within 1 day of seeding hWJCs on the HA product calcined at 600 °C, cells began to attach and showed beginning stages of morphological changes. After 10 day incubation, a live/dead assay was performed; the images in Figure 6-6 show living cells which are clearly

attached to the HA product through extended filopodia. These promising results strongly warrant further investigation to understand if the HA product will promote a genetic response toward an osteogenic lineage. If so, this process could provide a cheap and effective alternative to producing bone-like apatite, greatly contributing to higher-value product streams for the HTL of algae.

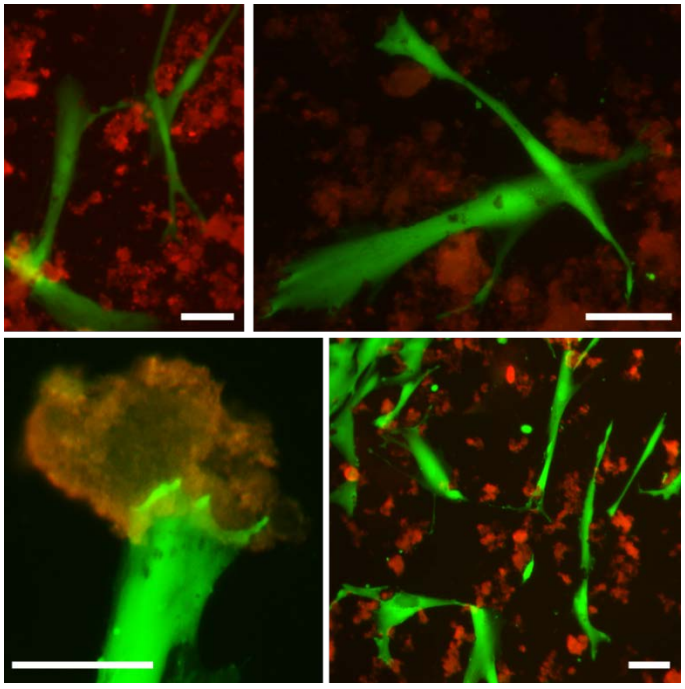

Figure 6-7. Human Wharton's jelly cells attached to HA product. Live/ dead assay micrograph after 10 day incubation on HA product calcined at 600 °C. Live cells fluoresce in green, dead cells fluoresce in red. The HA product interacted with the florescent components to induce auto fluorescence, primarily in the red. Scale bars are 100 µm.

6.4 Conclusions

The work in this chapter confirmed the overall hypothesis that crystallizing hydroxyapatite within the reactor for the HTL of wastewater-cultivated algae resulted in catalytic upgrading of the biocrude product. Particularly, in the dehydration of fatty acid amides to alkenes and aromatics, overall reducing the amount of oxygen content of the resultant biocrude and producing an increased amount of (desired) lower boiling point distillate fractions. The biocrude was found to achieve >90 wt% distillation below 600 °C, where previously had only been reported when thermally or catalytically treated.

In addition, both hypotheses formulated to evaluate the hydroxyapatite product for higher-value applications were confirmed. There existed gradual phase tunability with a secondary tricalcium phosphate phase, utilizing a simple calcination procedure. Steady increases in calcination temperature decomposed carbonate substitutions within the hydroxyapatite, resulting in increased degree of tricalcium phosphate phase, up to 900 °C, where primarily tricalcium phosphate was present. Once the material was in the tricalcium phosphate phase, it was determined silicon substitution remained and induction of globular morphologies occurred. Phase tunability of the hydroxyapatite product could greatly enhance functionality within it respective markets, controlling factors such as catalytically active sites and solubility for either a fertilizer or biomedical material. The preliminary cell culturing study indicated attachment and morphological changes occurred with the growth of Wharton's jelly cells after 10 day incubation *in-vitro*.

This work represents the first of its kind to produce a catalyst and utilize active sites *in-situ* during the HTL of algae. Further, the catalytic active sites can be regenerated and

potentially tuned with a simple heat treatment, potentially making the overall HTL of wastewater-cultivated algae process a high-value catalysts producer with a by-product of high quality renewable crude oil. This work also represents novel formulation of potential biomedical materials; linking the traditionally separate fields of study including environmental remediation, energy, and medicine.

6.5 References

1. Yan, B.; Tao, L.-Z.; Liang, Y.; Xu, B.-Q., Sustainable Production of Acrylic Acid: Catalytic Performance of Hydroxyapatites for Gas-Phase Dehydration of Lactic Acid. *ACS Catalysis* **2014**, 1931-1943.
2. Rahmanian, A.; Ghaziaskar, H. S., Continuous dehydration of ethanol to diethyl ether over aluminum phosphate–hydroxyapatite catalyst under sub and supercritical condition. *The Journal of Supercritical Fluids* **2013,** *78*, 34-41.
3. Kozlowski, J. T.; Davis, R. J., Heterogeneous Catalysts for the Guerbet Coupling of Alcohols. *ACS Catalysis* **2013,** *3*, (7), 1588-1600.
4. Indra, A.; Gopinath, C. S.; Bhaduri, S.; Kumar Lahiri, G., Hydroxyapatite supported palladium catalysts for Suzuki–Miyaura cross-coupling reaction in aqueous medium. *Catalysis Science & Technology* **2013,** *3*, (6), 1625.
5. Roussis, S. G.; Cranford, R.; Sytkovetskiy, N., Thermal Treatment of Crude Algae Oils Prepared Under Hydrothermal Extraction Conditions. *Energy & Fuels* **2012,** *26*, (8), 5294-5299.
6. Bai, X.; Duan, P.; Xu, Y.; Zhang, A.; Savage, P. E., Hydrothermal catalytic processing of pretreated algal oil: A catalyst screening study. *Fuel* **2014,** *120*, 141-149.
7. Dorozhkin, S. V., Biphasic, triphasic and multiphasic calcium orthophosphates. *Acta biomaterialia* **2012,** *8*, (3), 963-77.
8. Zorn, K.; Gbureck, U.; Mitró, D.; Müller, F. A.; Vorndran, E., Hydrothermal synthesis of calcium-deficient hydroxyapatite whiskers and their thermal transformation to polycrystalline β-tricalcium phosphate short fibers. *Bioinspired, Biomimetic and Nanobiomaterials* **2013,** *2*, (1), 11-19.
9. Fathi, M. H.; Hanifi, A.; Mortazavi, V., Preparation and bioactivity evaluation of bone-like hydroxyapatite nanopowder. *Journal of Materials Processing Technology* **2008,** *202*, (1-3), 536-542.
10. Daculsi, G., Biphasic calcium phosphate concept applied to artificial bone, implant coating and injectable bone substitute. *Biomaterials* **1998,** *19*, (16), 1473-1478.
11. Huang, T.; Xiao, Y.; Wang, S.; Huang, Y.; Liu, X.; Wu, F.; Gu, Z., Nanostructured Si, Mg, CO3 2− Substituted Hydroxyapatite Coatings Deposited by Liquid Precursor Plasma

Spraying: Synthesis and Characterization. *Journal of Thermal Spray Technology* **2011,** *20*, (4), 829-836.
12. Gamelas, J.; Martins, A., Surface properties of carbonated and non-carbonated hydroxyapatite obtained after bone calcination at different temperatures. *Colloids and Surfaces A: Physicochemical and Engineering Aspects* **2015**.
13. Liu, Q.; Matinlinna, J. P.; Chen, Z.; Ning, C.; Ni, G.; Pan, H.; Darvell, B. W., Effect of thermal treatment on carbonated hydroxyapatite: Morphology, composition, crystal characteristics and solubility. *Ceramics International* **2015,** *41*, (5), 6149-6157.
14. Marchat, D.; Zymelka, M.; Coelho, C.; Gremillard, L.; Joly-Pottuz, L.; Babonneau, F.; Esnouf, C.; Chevalier, J.; Bernache-Assollant, D., Accurate characterization of pure silicon-substituted hydroxyapatite powders synthesized by a new precipitation route. *Acta biomaterialia* **2013,** *9*, (6), 6992-7004.
15. Silvester, L.; Lamonier, J.-F.; Vannier, R.-N.; Lamonier, C.; Capron, M.; Mamede, A.-S.; Pourpoint, F.; Gervasini, A.; Dumeignil, F. Y., Structural, textural and acid-base properties of carbonates-containing hydroxyapatites. *Journal of Materials Chemistry A* **2014**.
16. Diallo-Garcia, S.; Laurencin, D.; Krafft, J.-M.; Casale, S.; Smith, M. E.; Lauron-Pernot, H.; Costentin, G., Influence of Magnesium Substitution on the Basic Properties of Hydroxyapatites. *The Journal of Physical Chemistry C* **2011,** *115*, (49), 24317-24327.
17. Matsuura, Y.; Onda, A.; Ogo, S.; Yanagisawa, K., Acrylic acid synthesis from lactic acid over hydroxyapatite catalysts with various cations and anions. *Catalysis Today* **2014,** *226*, 192-197.
18. Tsuchida, T.; Kubo, J.; Yoshioka, T.; Sakuma, S.; Takeguchi, T.; Ueda, W., Reaction of ethanol over hydroxyapatite affected by Ca/P ratio of catalyst. *Journal of Catalysis* **2008,** *259*, (2), 183-189.
19. Khan, A. F.; Saleem, M.; Afzal, A.; Ali, A.; Khan, A.; Khan, A. R., Bioactive behavior of silicon substituted calcium phosphate based bioceramics for bone regeneration. *Materials science & engineering. C, Materials for biological applications* **2014,** *35*, 245-52.

7 Future Directions

This chapter details future studies (as it pertains to the findings of this dissertation and the incorporation of hydrothermal liquefaction of algae) that have been deemed most significant to advance current knowledge and data found within the field for creating increased sustainability and end-use applications. Three main areas of focus to be discussed include liquefaction studies, post catalytic studies for the hydroxyapatite product, and bioactivity of the hydroxyapatite product for medical use.

7.1 Furthering Liquefaction Studies

7.1.1 Increasing Biocrude Productivity through Activated Municipal Sludge

The data presented in this dissertation and among collaborating researchers[1-4] have shown that municipal wastewater contributes a fraction of a local population's fuel demands; therefore increasing liquid fuel production from a sustainable pathway can have greater long-term significance for contributing to end-use biofuels. The proposed investigation to further the biocrude productivity of a wastewater treatment plant includes the co-liquefaction of discarded activated municipal sludge (AMS) and algae.

Few studies have presented data on the liquefaction of AMS[5-7] and bacteria[8], where most interest with the hydrothermal conversion has been at lower temperature carbonization[9-11] for producing a coal supplement/ substitute or a soil conditioner.[11] Typically, the biocrude produced from the liquefaction from AMS has slightly lower yields, lower carbon and higher oxygen

content then compared to algae.[5, 7, 8] However, addition of calcium oxide has shown to facilitate hydrolysis and deamination processes.[7]

The present hypothesis is that co-liquefaction of wastewater-cultivated algae, similar to those evaluated in this dissertation, and AMS will perform the following: 1) addition of more total biomass for higher overall biocrude return, 2) AMS has the potential to also crystallize hydroxyapatite *in-situ*, if not, the algae can facilitate crystallization while AMS can contribute more carbon, calcium, and phosphorus to the process, and 3) *in-situ* upgrading of biocrude produced from co-liquefaction of algae and AMS will result in lower overall oxygen content similarly to HTL of algae alone.

The suggested study involves a simple experimental plan well suited for the current research group and its collaborators, which includes the following: Once the AMS is obtained from the Lawrence Wastewater Treatment Plant and characterized (similarly to algae biomass in this dissertation), perform HTL experiments on the AMS alone, as a baseline, and mixed with wastewater-cultivated algae. The evaluation of hydroxyapatite crystallization should be performed after each HTL experiment as well as all relevant HTL product characterizations.

This study has the potential to utilize valuable nitrogen and phosphorus in a responsible manner and "recycle" carbon into usable fuels and chemicals, overall, increasing productivity and sustainability of algae-based biofuels and chemicals

7.1.2 Fraction Distillation of Biocrude for Complete End-Use Characterization

Growing interest within hydrothermal liquefaction (of algae) and the promise it has for commercial scale production warrants insight into end-use applications and scope of downstream processing. To date, insufficient characterization(s) of the whole biocrude has been reported,

particularly limited to those presented in this dissertation (GC-MS, simulated distillations, and elemental content(s)). Recently, techniques such as two dimensional nuclear magnetic resonance (2D-NMR) and Fourier transform ion cyclotron resonance mass spectrometry (FT-ICR MS) have been employed to understand relationship between molecules which have heteroatoms (O & N) within a particular carbon number.[12-14] These techniques begin to evaluate molecules of the biocrude product which are out of the range for GC-MS which contribute to the understanding of the complexity of the biocrude but fundamentally lack insight into creating an end-use product.

Moving toward commercial use of biocrude (in place of petroleum) will require efforts for end-use application studies and characterizations. Therefore, it is believed the first step in this direction is to obtain significant quantities of biocrude and perform fraction distillation prior to characterization and upgrading. Evaluating individual distillate fractions will aid in determining optimal upgrading techniques to employ, or targeted markets for an increased return. This type of study has not been demonstrated in the literature and could provide insightful advantages or disadvantages to HTL biocrude. The current research group has existing equipment that could be used to perform necessary studies. Currently housing a 4.8 L reaction vessel capable of safely operating in the supercritical water regime which can be used for obtaining significant quantities of biocrude, and a vacuum distillation apparatus which is design for specific ASTM methods for biodiesel, which could be slightly altered to acquire fractionation. It is believed that once individual fractions are obtained of various distillates thorough characterizations (GC-MS and ultimate analysis) will reveal individual distillate fractions contain various commodity chemicals and heteroatom content(s). Once identified,

further research could be performed into purification and upgrading strategies to optimize higher-value product streams.

7.1.3 Continuous HTL Operation with Regenerative Recycle

In reference to the data presented and conclusive findings of this dissertation, a completely novel approach to hydrothermal liquefaction of algae is suggested. A common and well-studied unit operation in chemical engineering is the fluidized catalytic cracking (FCC) unit. Since the HTL of wastewater-cultivated algae has resulted in the synthesis of a beneficial heterogeneous catalyst, which has shown regenerative capabilities through simple heat treatment, a FFC unit could be used as the reactor/ catalyst regenerator/ recycle to fully utilize the catalytic potential of hydroxyapatite in dehydration reactions further reducing overall oxygen content of the biocrude produced. Thoughtful in the design of the FCC unit, the purging of (typically spent) catalyst would actually become a high-value product stream of the refined hydroxyapatite.

This type of operation would benefit HTL of algae in multiple ways, including: valuable heat integration from flue gasses from the regenerator, optimizing usability of acid-base catalytic power of hydroxyapatite by ensuring available active sites at all times of operation, potentially obtaining a superior hydroxyapatite product by removing unwanted impurities as the material continuously alters through crystal growth and regenerative sintering, and minimizing overall operational cost by maximizing catalytic efficiency.

7.2 Continuing Catalytic Studies of Hydroxyapatite Product

As an acid-base catalyst, HA is has been used to catalyze a number of reactions including dehydration and dehydrogenation reactions[15-20], Guerbet alcohol coupling[21-25], and Michael

addition.[26] Two reactants of particular interest include both ethanol and lactic acid, both produced through conventional fermentation of biomass and its components. Therefore, it is of great interest to find efficient and environmentally friendly reaction pathways to transform these chemicals to commodities and value-added products. HA has proven to be a suitable catalyst for the conversion of either reactant because acid-base properties can be tuned by altering HA synthesis procedure and changing the Ca/P molar ratio resulting in higher acid or basic sites, resulting in variable selectivity to dehydration or dehydrogenation products, respectively. Stoichiometric HA, $Ca_{10}(PO_4)_6(OH)_2$, has the Ca/P ratio of 1.67, higher acid or basic sites are found at Ca/P < 1.67 and ≥1.67, respectively. The HA produced through the liquefaction of wastewater-cultivated algae shows the phase can be slowly altered through increasing calcination temperature to more basic tricalcium phosphate (TCP), $Ca_3(PO_4)_2$, thus, it is proposed that acid-base properties of the HA product can be easily tuned for desired reactions and selectivities without altering the synthesis procedures and only employing variable calcination temperatures resulting in different ratios of HA and TCP.

Acid-base properties of HA with various Ca/P ratios have been reported to achieve total conversion of dehydration lactic acid where highest selectivity (60%) to acrylic acid using the lowest Ca/P ratio and thus highest number of acid sites.[27] Alcohol coupling or Guerbet alcohols were found to have the highest selectivity with HA with increasing Ca/P ratios with higher basic sites[25], where TCP showed higher alcohol coupling rate compared to HA.[24] The HA produced in this dissertation should lead to interesting acid-base properties, where it is unknown how the multitude of substitutions will affect the overall acid-base properties of the material. Recent studies have begun to identify some substitution effects on catalytic sites, including CO_3/ Na,[28]

Mg,[29] and Sr/ Pb/ VO_4.[30] In the case of CO_3 and Na, acid site density were found in the order of Ca-deficient > stoichiometric > carbonate-HA > Na/CO_3-HA > CO_3 rich-HA > Na/CO_3 rich-HA which directly correlated to the selectivity of propylene from isopropyl alcohol (90% - 5%). In contrast, catalytic basicity (selectivity of acetone from isopropyl alcohol) had the exact opposite trend (5% - 70%). The degree at which the HA produced in this dissertation is substituted, both anionic and cationic, primarily with CO_3^{2-}, SiO_4^{4-}, Mg^{2+} would give significant quantities of both acid and base active sites. It is believed the HA product will contain more acid than basic sites and as the calcination temperature increases, changing the phase toward TCP, the basic sites will increase due to more exposed PO_4 ion in the TCP structure because of changing morphology (as shown in Figure 5-4 and Figure 6-6). However, the biphasic intermediate temperatures could potentially form interesting ratios and strengths of both acid and base sites and therefore each temperature should be carefully considered for future catalytic reactions.

There have been an increasing number of research articles, published in the current year (2015),[31-42] incorporating and understanding hydroxyapatite's catalytic ability which have demonstrated extreme versatility as an effective green catalyst in a variety of reactions including hydrogenation, oxidation, hydrocracking, and photocatalytic degradation and have also shown that hydroxyapatite can be used as-is or as support material for gold, ruthenium, cesium, rhodium, and lanthanum. Therefore, there is a strong urge to demonstrate the activity (and versatility) of the hydroxyapatite co-produced with biocrude from algae. The suggested starting point is the full characterizations of acid-base active sites through temperature programmed desorption of both ammonia (for acid sites) and CO_2 (for basic sites) at each calcination temperature presented in section 6.2, followed by a simple and straight forward reaction study

converting isopropyl alcohol to either acetone or propylene utilizing current set-up in conjunction with the Unit Operations laboratory for undergraduate coursework at the University of Kansas. Other suggested studies are to follow similar studies to that of Tsuchida et al.[23] and Ghantani et al.[27] for conversion of ethanol and lactic acid, respectively.

7.3 Bioactivity and Genealogical Promotion Studies of Hydroxyapatite Product

Differentiating stem cells toward an osteogenic lineage has been a top area of interest in regenerative medicine for bone reconstruction and tissue engineering for over two decades.[43] One component of bone is natural apatite material; therefore, hydroxyapatite (HA) was a likely candidate for regenerative bone engineering and proved itself for scaffolding materials many years ago.[44] Synthetic HA has demonstrated bone-like bioresorption,[45] biocapatability,[44] and genealogical lineage differentiation (the ability to promote stem cells toward a specific phenotype; in this case osteocytes).[46] Multiple studies have shown silicon substituted HA can increase the efficacy of for bone regeneration.[47]

Natural bone is mainly Ca^{2+} and PO_4^{3-}, it also incorporates other ions of CO_3^{2-}, SiO_4^{4-}, and Mg^{2+}. As these substitutions are found in the HA product in this work, in conjunction with optimizing HA/TCP ratio through calcination, it is believed this HA will behave more like natural apatite in human bone and increase bioactivity to allow steady bone regeneration over an extended period of time.[45, 47]

Continuing bioactivity efforts will strengthen higher-value market targeting for commercial use of these products. Suggested studies include evaluating genealogical lineage similar to Guo et al.[44] or Cameron et al.[46] using simple disk pellets as a scaffold from a HA

materials and evaluated *in-vitro* culturing mesenchymal stem cells (MSCs). Evaluation of the gene expression is suggested to be conducted similarly to the study by Cameron et al.[46] evaluating gene markers endoglin (CD105), runt related transcription factor 2 (RUNX2), parathyroid hormone recepot 1 (PTH1R), collagen type 1 (Col1a1), osteocalcin (BGLAP), and dentin matrix acidic phophoprotein 1 (DMP1). A simple description of each gene is provided in Table 7-1.

Table 7-1. Genes and their descriptions expressed through the osteogenic lineage from mesenchymal stem cells (MSCs).[46]

Gene	Description
CD105	cell surface receptor commonly associated with MSCs, and decreases in expression as these cells differentiate
RUNX2	a key role in osteoblast differentiation, indicating onset
PTH1R	expression is associated with endochondral ossification and plays a vital role in calcium homeostasis in bone
Col1a1	early marker of osteoblast differentiation and a reporter of osteoblast activity
BGLAP	late marker of osteoblast differentiation, expressed at the onset of mineralization
DMP1	Expressed by terminally differentiated osteocytes

It is suggested to create pressed disks of the hydroxyapatite material to perform *in-vitro* studies. Two methods could be used when pressing the disks, 1) calcine the powder HA material directly from the reactor and use a circular die (roughly 14 mm diameter and 1 mm thick)[46] using a hydraulic or mechanical press (pressures may need to be experimented with to obtain a

mechanically stable disk) and 2) press the HA material directly from the reactor and then calcine the material. The latter may form a macro-porous disk from the removal of the organics which could create higher surface area for increased cell attachment. Once the scaffolds are created MSCs should be cultured in an osteogenic medium including 50 μM ascorbic acid phosphate, 10 mM β-glycerophosphate, and 100 nM dexamethasone, replacing media three times every 7 days.[46] Post cell culturing, total RNA extraction and RT-PCR performed to evaluate gene expression for those listed in Table 7-1 following protocol from Cameron et al.[46] Advantages may arise between the variable phase mixtures (HA/TCP) produced through increased calcination temperatures and therefore, it is suggested each temperature is to be carefully considered for optimum performance in osteogenic differentiation. Further studies may also be considered for protein drug delivery applications, following similar studies to that of Zhao et al.[48] which has shown promising results based off of flower-like morphologies of HA materials similar to those found with the HTL of wastewater-cultivated algae.

7.4 References

1. Roberts, G. W.; Fortier, M.-O. P.; Sturm, B. S. M.; Stagg-Williams, S. M., Promising Pathway for Algal Biofuels through Wastewater Cultivation and Hydrothermal Conversion. *Energy & Fuels* **2013,** *27*, (2), 857-867.
2. Roberts, G. W.; Sturm, B. S. M.; Hamdeh, U.; Stanton, G. E.; Rocha, A.; Kinsella, T. L.; Fortier, M.-O. P.; Sazdar, S.; Detamore, M. S.; Stagg-Williams, S. M., Promoting catalysis and high-value product streams by in situ hydroxyapatite crystallization during hydrothermal liquefaction of microalgae cultivated with reclaimed nutrients. *Green Chem.* **2015**.
3. Fortier, M.-O. P.; Sturm, B. S. M., Geographic Analysis of the Feasibility of Collocating Algal Biomass Production with Wastewater Treatment Plants. *Environmental Science & Technology* **2012,** *46*, (20), 11426-11434.
4. Fortier, M.-O. P.; Roberts, G. W.; Stagg-Williams, S. M.; Sturm, B. S., Life cycle assessment of bio-jet fuel from hydrothermal liquefaction of microalgae. *Applied Energy* **2014,** *122*, 73-82.

5. Vardon, D. R.; Sharma, B. K.; Scott, J.; Yu, G.; Wang, Z.; Schideman, L.; Zhang, Y.; Strathmann, T. J., Chemical properties of biocrude oil from the hydrothermal liquefaction of Spirulina algae, swine manure, and digested anaerobic sludge. *Bioresource Technology* **2011,** *102*, (17), 8295-8303.
6. Huang, H.-j.; Yuan, X.-z.; Zhu, H.-n.; Li, H.; Liu, Y.; Wang, X.-l.; Zeng, G.-m., Comparative studies of thermochemical liquefaction characteristics of microalgae, lignocellulosic biomass and sewage sludge. *Energy* **2013,** *56*, 52-60.
7. Malins, K.; Kampars, V.; Brinks, J.; Neibolte, I.; Murnieks, R.; Kampare, R., Bio-oil from thermo-chemical hydro-liquefaction of wet sewage sludge. *Bioresour Technol* **2015,** *187*, 23-29.
8. Valdez, P. J.; Nelson, M. C.; Faeth, J. L.; Wang, H. Y.; Lin, X. N.; Savage, P. E., Hydrothermal liquefaction of bacteria and yeast monocultures. *Energy & Fuels* **2013,** *28*, (1), 67-75.
9. Lu, X.; Jordan, B.; Berge, N. D., Thermal conversion of municipal solid waste via hydrothermal carbonization: comparison of carbonization products to products from current waste management techniques. *Waste Manag* **2012,** *32*, (7), 1353-65.
10. He, C.; Giannis, A.; Wang, J.-Y., Conversion of sewage sludge to clean solid fuel using hydrothermal carbonization: Hydrochar fuel characteristics and combustion behavior. *Applied Energy* **2013,** *111*, 257-266.
11. Zhang, J.-h.; Lin, Q.-m.; Zhao, X.-r., The Hydrochar Characters of Municipal Sewage Sludge Under Different Hydrothermal Temperatures and Durations. *Journal of Integrative Agriculture* **2014,** *13*, (3), 471-482.
12. Sudasinghe, N.; Dungan, B.; Lammers, P.; Albrecht, K.; Elliott, D.; Hallen, R.; Schaub, T., High resolution FT-ICR mass spectral analysis of bio-oil and residual water soluble organics produced by hydrothermal liquefaction of the marine microalga Nannochloropsis salina. *Fuel* **2014,** *119*, 47-56.
13. Sudasinghe, N.; Cort, J. R.; Hallen, R.; Olarte, M.; Schmidt, A.; Schaub, T., Hydrothermal liquefaction oil and hydrotreated product from pine feedstock characterized by heteronuclear two-dimensional NMR spectroscopy and FT-ICR mass spectrometry. *Fuel* **2014,** *137*, 60-69.
14. Sanguineti, M. M.; Hourani, N.; Witt, M.; Sarathy, S. M.; Thomsen, L.; Kuhnert, N., Analysis of impact of temperature and saltwater on Nannochloropsis salina bio-oil production by ultra high resolution APCI FT-ICR MS. *Algal Research* **2015,** *9*, 227-235.
15. Yan, B.; Tao, L.-Z.; Liang, Y.; Xu, B.-Q., Sustainable Production of Acrylic Acid: Catalytic Performance of Hydroxyapatites for Gas-Phase Dehydration of Lactic Acid. *ACS Catalysis* **2014**, 1931-1943.
16. Stošić, D.; Bennici, S.; Sirotin, S.; Calais, C.; Couturier, J.-L.; Dubois, J.-L.; Travert, A.; Auroux, A., Glycerol dehydration over calcium phosphate catalysts: Effect of acidic–basic features on catalytic performance. *Applied Catalysis A: General* **2012,** *447-448*, 124-134.
17. Maki-Arvela, P.; Simakova, I. L.; Salmi, T.; Murzin, D. Y., Production of lactic acid/lactates from biomass and their catalytic transformations to commodities. *Chemical reviews* **2014,** *114*, (3), 1909-71.

18. Blanco, E.; Delichere, P.; Millet, J. M. M.; Loridant, S., Gas phase dehydration of lactic acid to acrylic acid over alkaline-earth phosphates catalysts. *Catalysis Today* **2014,** *226*, 185-191.
19. Matsuura, Y.; Onda, A.; Yanagisawa, K., Selective conversion of lactic acid into acrylic acid over hydroxyapatite catalysts. *Catalysis Communications* **2014,** *48*, 5-10.
20. Tavan, Y.; Hosseini, S. H.; Ghavipour, M.; Khosravi Nikou, M. R.; Shariati, A., From laboratory experiments to simulation studies of methanol dehydration to produce dimethyl ether—Part I: Reaction kinetic study. *Chemical Engineering and Processing: Process Intensification* **2013,** *73*, 144-150.
21. Ozer, R.; Fagan, P. J.; Calvarese, T. G., Conversion of butanol to a reaction product comprising 2-ethylhexanol using hydroxyapatite catalysts. In Google Patents: 2013.
22. Fagan, P. J.; Calvarese, T. G.; Davis, R. J.; Ozer, R., Conversion of ethanol to a reaction product comprising 1-butanol using hydroxyapatite catalysts. In Google Patents: 2013.
23. Tsuchida, T.; Sakuma, S.; Takeguchi, T.; Ueda, W., Direct Synthesis ofn-Butanol from Ethanol over Nonstoichiometric Hydroxyapatite. *Industrial & Engineering Chemistry Research* **2006,** *45*, (25), 8634-8642.
24. Kozlowski, J. T.; Davis, R. J., Heterogeneous Catalysts for the Guerbet Coupling of Alcohols. *ACS Catalysis* **2013,** *3*, (7), 1588-1600.
25. Tsuchida, T.; Kubo, J.; Yoshioka, T.; Sakuma, S.; Takeguchi, T.; Ueda, W., Reaction of ethanol over hydroxyapatite affected by Ca/P ratio of catalyst. *Journal of Catalysis* **2008,** *259*, (2), 183-189.
26. Gruselle, M.; Kanger, T.; Thouvenot, R.; Flambard, A.; Kriis, K.; Mikli, V.; Traksmaa, R.; Maaten, B.; Tõnsuaadu, K., Calcium Hydroxyapatites as Efficient Catalysts for the Michael C–C Bond Formation. *ACS Catalysis* **2011,** *1*, (12), 1729-1733.
27. Ghantani, V. C.; Lomate, S. T.; Dongare, M. K.; Umbarkar, S. B., Catalytic dehydration of lactic acid to acrylic acid using calcium hydroxyapatite catalysts. *Green Chemistry* **2013,** *15*, (5), 1211.
28. Silvester, L.; Lamonier, J.-F.; Vannier, R.-N.; Lamonier, C.; Capron, M.; Mamede, A.-S.; Pourpoint, F.; Gervasini, A.; Dumeignil, F. Y., Structural, textural and acid-base properties of carbonates-containing hydroxyapatites. *Journal of Materials Chemistry A* **2014**.
29. Diallo-Garcia, S.; Laurencin, D.; Krafft, J.-M.; Casale, S.; Smith, M. E.; Lauron-Pernot, H.; Costentin, G., Influence of Magnesium Substitution on the Basic Properties of Hydroxyapatites. *The Journal of Physical Chemistry C* **2011,** *115*, (49), 24317-24327.
30. Matsuura, Y.; Onda, A.; Ogo, S.; Yanagisawa, K., Acrylic acid synthesis from lactic acid over hydroxyapatite catalysts with various cations and anions. *Catalysis Today* **2014,** *226*, 192-197.
31. Silvester, L.; Lamonier, J.-F.; Faye, J.; Capron, M.; Vannier, R.-N.; Lamonier, C.; Dubois, J.-l.; Couturier, J.-l.; Calais, C.; Dumeignil, F. Y., Reactivity of Ethanol over Hydroxyapatite-Based Ca-enriched Catalysts with Various Carbonate Contents. *Catalysis Science & Technology* **2015**.
32. Moeinpour, F.; Khojastehnezhad, A., Cesium carbonate supported on hydroxyapatite coated Ni 0.5 Zn 0.5 Fe 2 O 4 magnetic nanoparticles as an efficient and green catalyst for the synthesis of pyrano [2, 3-c] pyrazoles. *Chinese Chemical Letters* **2015**.

33. Saffar-Teluri, A., Bovine Bone Derived Natural Nanocrystalline Hydroxyapatite Supported Boron Trifluoride: An Efficient, Recyclable and Eco-friendly Heterogeneous Catalyst for Diastereoselective Formation of α-Hydroxy-β-methoxyketones. *Synthesis and Reactivity in Inorganic, Metal-Organic, and Nano-Metal Chemistry* **2015**, (just-accepted), 00-00.
34. Wang, Y.; Chen, B.-b.; Crocker, M.; Zhang, Y.-j.; Zhu, X.-b.; Shi, C., Understanding on the origins of hydroxyapatite stabilized gold nanoparticles as high-efficiency catalysts for formaldehyde and benzene oxidation. *Catalysis Communications* **2015,** *59*, 195-200.
35. Huang, C.; Ma, Z.; Xie, P.; Yue, Y.; Hua, W.; Gao, Z., Hydroxyapatite-supported rhodium catalysts for N 2 O decomposition. *Journal of Molecular Catalysis A: Chemical* **2015,** *400*, 90-94.
36. Oh, S. C. In *Oxidative Coupling of Methane over Hydroxyapatite Catalysts*, 24th North American Catalysis Society Meeting, 2015; Nam: 2015.
37. Wen, C.; Cui, Y.; Chen, X.; Zong, B.; Dai, W.-L., Reaction temperature controlled selective hydrogenation of dimethyl oxalate to methyl glycolate and ethylene glycol over copper-hydroxyapatite catalysts. *Applied Catalysis B: Environmental* **2015,** *162*, 483-493.
38. Kim, D.; Kim, Y.; Jung, K.; Choi, M. Y.; Park, M.; Lee, B. Y.; Kim, T. H.; Kwon, K. Y., Ruthenium-Incorporated Hydroxyapatites for the Oxidation of Alcohols and Amines Using Molecular Oxygen as an Oxidant. *Bulletin of the Korean Chemical Society* **2015,** *36*, (1), 1-2.
39. Farooq, M.; Ramli, A., Biodiesel production from low FFA waste cooking oil using heterogeneous catalyst derived from chicken bones. *Renewable Energy* **2015,** *76*, 362-368.
40. Liu, K. J.; Yu, H. G. In *Synthesis and Photocatalytic Activity of Silicon-Substituted Hydroxyapatite*, Key Engineering Materials, 2015; Trans Tech Publ: 2015; pp 115-117.
41. Fan, K.; Yang, X.; Liu, J.; Rong, L., Effect of reducing coke of catalyst by La loading in hydrocracking of Jatropha oil. *RSC Advances* **2015**.
42. Puértolas, B.; Mayoral, A.; Arenal, R.; Solsona, B.; Moragues, A. M.; Murcia-Mascaros, S.; Amoros, P.; Hungría, A. B.; Taylor, S. H.; Garcia, T., High Temperature Stable Gold Nanoparticle Catalysts for Application under Severe Conditions: The Role of TiO2 Nanodomains on Structure and Activity. *ACS Catalysis* **2015**.
43. Heng, B. C.; Cao, T.; Stanton, L. W.; Robson, P.; Olsen, B., Strategies for directing the differentiation of stem cells into the osteogenic lineage in vitro. *Journal of bone and mineral research : the official journal of the American Society for Bone and Mineral Research* **2004,** *19*, (9), 1379-94.
44. Guo, H.; Su, J.; Wei, J.; Kong, H.; Liu, C., Biocompatibility and osteogenicity of degradable Ca-deficient hydroxyapatite scaffolds from calcium phosphate cement for bone tissue engineering. *Acta biomaterialia* **2009,** *5*, (1), 268-78.
45. Fathi, M. H.; Hanifi, A.; Mortazavi, V., Preparation and bioactivity evaluation of bone-like hydroxyapatite nanopowder. *Journal of Materials Processing Technology* **2008,** *202*, (1-3), 536-542.
46. Cameron, K.; Travers, P.; Chander, C.; Buckland, T.; Campion, C.; Noble, B., Directed osteogenic differentiation of human mesenchymal stem/precursor cells on silicate

substituted calcium phosphate. *Journal of biomedical materials research. Part A* **2013,** *101*, (1), 13-22.
47. Khan, A. F.; Saleem, M.; Afzal, A.; Ali, A.; Khan, A.; Khan, A. R., Bioactive behavior of silicon substituted calcium phosphate based bioceramics for bone regeneration. *Materials science & engineering. C, Materials for biological applications* **2014,** *35*, 245-52.
48. Zhao, X.-Y.; Zhu, Y.-J.; Chen, F.; Lu, B.-Q.; Wu, J., Nanosheet-assembled hierarchical nanostructures of hydroxyapatite: surfactant-free microwave-hydrothermal rapid synthesis, protein/DNA adsorption and pH-controlled release. *CrystEngComm* **2013,** *15*, (1), 206-212.

8 Concluding Remarks

The hydrothermal liquefaction of wet algae biomass presents promising results for creating renewable fuels and chemicals to replace its petroleum counterparts, while reaching towards federal goals of producing 36 billion gallons of renewable fuels by 2022. The work presented in this dissertation substantially alleviates concerns for algae-based fuels and chemicals in terms of sustainability and economics. This dissertation demonstrates municipal wastewater is suitable for algae cultivation and provides multiple benefits, particularly achieving advanced wastewater treatment and environmental remediation while cheaply cultivating biomass. Combining hydrothermal liquefaction as part of the holistic strategy produces a carbon-rich crude oil, with relatively similar properties to that of petroleum, alongside solid and aqueous co-products. Algae cultivation with municipal wastewater results in relatively low (10 dw%) cellular oils and relatively large amounts of inorganic ash fraction (24-29 dw%) which is composed largely of calcium and silicon. Post liquefaction, half of the algal carbon is partitioned into the biocrude product, and the remainder is partitioned in a 20-20-10 (wt%) for solid, gas, and aqueous fractions, respectively. A significant portion of the algal nitrogen (45 wt%) resides in the aqueous product and almost all the algal phosphorus (95 wt%) accumulates into the solid product. In terms of nutrient recovery and re-use, these numbers hold great significance, and pose prospect in recovering future fertilizers from municipal wastewater.

The biocrude produced from hydrothermal liquefaction of wastewater-cultivated algae has superior quality compared to many previous studies using fertilized monocultures, in terms of heteroatoms (5-7 wt% oxygen) and energy content (39 MJ kg^{-1}), while resulting in significant

amounts of aliphatics (straight and branched) which can be used as direct fuels and lower order aromatics (phenolics). The biocrude was shown to be comprised of 36 wt% direct fuel distillate and have a higher limit distillate temperature of 600 °C, where 96 wt% of the biocrude boiled below 600 °C. Macro-algae derived biocrude, compared to biocrude derived from micro-algae, produced slightly less desirable oxygen content but much higher amounts of lower boiling point compounds and aromatics and, while not quantified, had a much lower viscosity. Overall, hydrothermal liquefaction of wastewater-cultivated macro-algae resulted in similar yields of biocrude but with higher fraction of direct fuel distillates which would require more heteroatom removal compared to micro-algae.

High production yields of solid product (29- 45 dw%) from the liquefaction of wastewater-cultivated algae warranted extensive investigation, which lead to the discovery of high-value product determination and a mechanistic understanding of the more desired biocrude properties as compared to previous studies throughout the literature. It was determined that the solid product consisted of highly substituted (silicon, magnesium, and carbonate) hydroxyapatite hexagonal nano-rods which underwent hierarchical micro structuring into bundles, sheets, and flower-like morphologies. The crystallization and presence of hydroxyapatite in the reactor provided effective means of catalytic dehydration of fatty acid amides into methyl amine and alkenes, while also providing necessary acid-base chemistries for cracking high boiling distillate fractions. The substitutions within the crystal lattice provides mean for phase tunability with tricalcium phosphate which can increase usability within the market place as either a primary acid or base catalyst as well as contribute to the bioactivity as a medical scaffolding material. Phase tunability studies indicated that residual organics within the hydroxyapatite are easily

removed and regenerate catalytically active intermediate Brønsted acid sites. Once the material was fully transitioned into the tricalcium phosphate phase it was determined silicon substitutions remained in the material.

Crystallization of hydroxyapatite directly from algae using hydrothermal liquefaction represents a new value stream for traditional algae biofuel production. It was found a reasonably small municipal wastewater treatment plant (serving population of ~80,000, with average flow of 12 million gallons per day) could produce up to 18 barrels of biocrude and 2000 kg of refined pure phase substituted hydroxyapatite per day, while simultaneously reclaiming nitrogen and phosphorous. Data suggests that a commercial scale hydrothermal liquefaction plant can now have the ability to synthesize a catalyst within the process, utilize its catalytic ability *in-situ* and upon regeneration, produce a high-value product stream.

This novel approach for creating high-value product streams from water reclamation sources can have significant impacts to tax payer dollars, creating profit for a traditionally regulatory industry while contributing to biofuels, green catalysis, and medicine. These findings provide the basis for new developments in algae-based fuels, chemicals, and bioproducts at both the fundamental and macro commercialization levels, where the full impacts into heterogeneous catalysis and tissue engineering applications are widely unknown.